

Neuromodulation of neocortical microcircuitry: a multi-scale framework to model the effects of cholinergic release

Présentée le 7 juillet 2022

A la Faculté des sciences de la vie
Projet Bluebrain
Programme doctoral en neurosciences

pour l'obtention du grade de Docteur ès Sciences

par

Cristina COLANGELO

Acceptée sur proposition du jury

Prof. K. Hess Bellwald, présidente du jury
Prof. H. Markram, Dr S. Ramaswamy, directeurs de thèse
Prof. A. Disney, rapporteuse
Prof. H. Mansvelder, rapporteur
Prof. G. Knott, rapporteur

To my parents, who sparked my love for knowledge.

"The only thing I know is that I know nothing"

The apology of Socrates, Plato

Acknowledgements

Despite having imagined this moment for years, I hadn't expected this task to feel so light and burdensome at the same time. Naturally, it is a great pleasure to wrap up five long years of work and have the occasion to thank all the lovely humans that have accompanied me in this path; but is also anxiety-provoking to think that I could somehow fail to acknowledge really important contributions to this thesis. It's been a long journey, made of joy and disappointment, laughter and tears, realizations, failures of expectations, and most importantly self-growth. I do not feel like I am the same person that I was when I arrived to EPFL; rather, I am a much more conscious and expanded version of myself, and for this amazing fact I have so many people to thank.

First things, first: this thesis could not have been done without the support of my supervisors, Henry Markram and Srikanth Ramaswamy. Thank you Henry, for giving me this opportunity, guiding me when I needed it and for teaching me to trust my intuitions and take the leading role in the evolution of my PhD experience.

Srikanth, there are so many things that you have taught me that listing them would not do them justice. I am glad to have been your first student. You have been a firm and solid presence throughout this whole journey, which is not something that many PhD students can say. I would like to thank you for your exceptional attention to details, for having pushed me in every conceivable way (from paper writing to abstract submissions and conference talks) out of my comfort zone, and for the really enjoyable discussions about the intricacies of neuromodulation. I can now say that I have read at least as many (neuromodulation) papers as you, which is, for whoever doesn't know Srikipedia, a truly remarkable accomplishment.

My thanks also go to Eilif Muller. Eilif, I can never forget the first time I met you and the discussion we had about the equations that make up the H-H model. It was the first time that I felt like I belonged in the theoretical neuroscience community. Thank you for seeing something in me, and for opening the doors to this incredible world made of simulations and abstract concepts, supercomputing resources and jargony HPC stuff. I am not sure how I lived without Python before. I guess I was sitting in my comfy chair :D

To all of my long-standing and newly acquired BBP and EPFL friends, in no particular order: Leda and Eleftherios, Hugo, Polina S., Polina L., Anil, Aleksandra, Kerem, Davide, Marwan, Francesco, Checco, Andras, Sirio,

James, Werner and Akiko, Joni, Dimitri, Daniela, Joe, Dan, Karin, Danny, Judit, Alina, Raquel, Dace, Tristan, Anna-K, Eugenia, Cyrille, Tanguy, Darshan, Julian, Richard, Jim, Rajnish, Rodrigo, Mimi, Jane, Ayah. All of you have made my PhD journey far more enjoyable. I thank you for all the love, fun, laughter and intelligent discussions we've had other lunch, pirate and conference trips, and countless beers. To all of my friends back in Italy, or here in CH: Sara, RobiBacchia, Giulia e Nico, Olga, Cate, Martuccia, Anna, Benni, Amir, Luca, Giada, AleBacchio, Rasha, Cami, Amal, Jenny, Ewa, Mari, Silvia, Isa, Till, Marissa, Michela, Alice, Marta and all the uni friends, and many others (such as friends who taught me the importance of the .eps format): thank you for your presence and your support, I love you all so much.

To my family: my parents to whom this thesis is dedicated and (all) my siblings. I love you. To Andrea, especially: you are the best brother that anybody could hope for. Thank you for being there for me, always.

To the epic neuromodulation team at BBP: Armando Romani and Alberto Antonietti. You guys deserve a whole section for yourselves. I cannot thank you enough for the support; truly this thesis could not exist without your precious help. You are amazing people and I am proud and honored to work with you. Alberto, thanks for everything: your eagle eye, for verifying my code, finding (so many) bugs and fixing them. You are a truly complete scientist, and I have learned much from you.

Special thanks go to Cyrille Favreau and Elvis Boci for the incredibly efficient support with visualizations and figures: you guys rock!

To Michael Reimann, Max Nolte and Giuseppe (Captain) Chindemi: the old guard. Thank you for all the fun times and great hikes and trips and lunches and discussions. You guys have taught me a lot, and sometimes challenged my zen: you have been really great team mates, and even better friends. I miss the old times together.

Vishal Sood, thank you for your incredible patience and for teaching me how to debug code. Without you, I would still be debugging BluePyEfe. Of course, thanks for all the lovely discussions as well, related to science, biryani, and mangoes.

Natali Barros-Zulaica, my sweet friend. I cannot even begin to cover what you have meant for me in this journey. You have been my true and loyal friend throughout this whole process, and your post-doc finger has changed the course of my PhD multiple times. The countless adventures and hard

times that we have been through together ... I am truly thankful to you, from the bottom of my heart.

Taylor H. Newton: if it weren't for you, I would still be reading programming books. You have been fundamental in anything that has happened to me in the last five years. Thank you is not enough. I love you with all my heart, you are the best confidant, deskmate, roommate, birthday twin and sparring partner that I could ever have dreamed of.

Wesam Baud: one of the most incredible people I have ever met. Your white magic has guided me throughout these years like nothing before. I consider you my mentor and true friend. Without you, and your teachings I could never have maintained (or generated) the mental health necessary to complete a PhD journey. You changed me in ways that I couldn't even conceive before, and for that I am truly grateful.

ومن اعماق قلبي احب ان اوجه كل الشكر الي صديقتي وسام والتي اعتبرها من
اروع الاشخاص اللي قابلتهم في حياتي. سحرك يا وسام كان داعم ليا جدا خلال السنين
اللي فاتت وكان مهم في حياتي انا حقيقي باعتبرك صديقه مخلصه ومعلمه فاضله.
تعليمك ليا الفتره اللي فاتت كان مهم ليا ومن غيرك انا مكنتش متخيله ازاي اقدر
احافظ علي سلامتي النفسيه في وقت صعب جدا خلال رحله الدكتوراه بتاعتي. انتي
غيرتيني للافضل بشكل انا متخيلتهوش قبل كده وعلشان كده انا باشكرك جدا.
انا بحبك يا حبيبتي. شكرا!

Abstract

Neuromodulation of neocortical microcircuits is one of the most fascinating and mysterious aspects of brain physiology. Despite over a century of research, the neuroscientific community has yet to uncover the fundamental biological organizing principles underlying neuromodulatory release. Phylogenetically, Acetylcholine (ACh) is perhaps the oldest neuromodulator, and one of the most well-studied. ACh regulates the physiology of neurons and synapses, and modulates neural microcircuits to bring about a reconfiguration of global network states. ACh is known to support cognitive processes such as learning and memory, and is involved in the regulation of arousal, attention and sensory processing. While the effects of ACh in the neocortex have been characterized extensively, integrated knowledge of its mechanisms of action is lacking. Furthermore, the ways in which ACh is released from *en-passant* axons originating in subcortical nuclei are still debatable. Simulation-based paradigms play an important role in testing scientific hypotheses, and provide a useful framework to integrate what is already known and systematically explore previously uncharted territory. Importantly, data-driven computational approaches highlight gaps in current knowledge and guide experimental research. To this end, I developed a multi-scale model of cholinergic innervation of rodent somatosensory cortex comprising two distinct sets of ascending projections implementing either synaptic (ST) or volumetric transmission (VT). The model enables the projection types to be combined in arbitrary proportions, thus permitting investigations of the relative contributions of these two transmission modalities. Using our ACh model, we find that the two modes of cholinergic release act in concert and have powerful desynchronizing effects on microcircuit activity. Furthermore we show that this modeling framework can be extended to other neuromodulators, such as dopamine and serotonin, with minimal constraining data. In summary, our results suggest a more nuanced view of neuromodulation in which multiple modes of transmitter release - ST vs VT - are required to produce synergistic functional effects.

Keywords: Acetylcholine, Neuromodulators, Neocortex, Models, Simulation, Projections, Synaptic Transmission, Volumetric transmission

Abstract

La neuromodulazione dei microcircuiti corticali è uno degli aspetti più affascinanti e misteriosi della fisiologia cerebrale. Nonostante più di un secolo di ricerche, la comunità neuroscientifica deve ancora svelare i fondamentali principi biologici che sottendono al rilascio neuromodulatorio. Filogeneticamente, l'acetilcolina (ACh) è forse uno dei neuromodulatori più antichi, e uno dei più studiati. ACh regola la fisiologia di neuroni e sinapsi e modula i microcircuiti neurali per realizzare una riconfigurazione globale delle reti neurali. ACh è nota per la modulazione che apporta a processi cognitivi come l'apprendimento e la memoria, ed è coinvolta nella regolazione dell'attenzione, degli stati di allerta e nell'elaborazione degli stimoli sensoriali. Nonostante gli effetti di ACh in neocorteccia siano stati ampiamente caratterizzati, manca tuttora una conoscenza integrale dei suoi meccanismi d'azione. Inoltre, le modalità attraverso le quali ACh è rilasciata da assoni *en-passant* provenienti da nuclei sotto-corticali sono ancora oggetto di dibattito. Modelli computazionali e simulazioni giocano un ruolo importante nel testare ipotesi scientifiche e offrono la possibilità di integrare nozioni preesistenti per poter esplorare sistematicamente territori precedentemente sconosciuti. Gli approcci computazionali basati su dati biologici evidenziano le lacune nella letteratura e aiutano a guidare la ricerca sperimentale. A tal fine, ho sviluppato un modello dell'innervazione colinergica della corteccia somatosensoriale del ratto, costituito da due tipi di proiezioni distinte, implementando la trasmissione sinaptica e quella volumetrica. Il modello permette di combinare i due tipi di proiezioni nelle proporzioni desiderate, consentendo quindi di indagare i relativi ruoli delle due modalità di trasmissione. Utilizzando il nostro modello del rilascio di ACh, abbiamo scoperto che le due modalità di trasmissione del segnale colinergico agiscono in sinergia e hanno potenti effetti di desincronizzazione sull'attività del microcircuito. Inoltre, mostriamo che il modello può essere aumentato per includere altri neuromodulatori, come la serotonina e la dopamina, purché siano disponibili i dati biologici di partenza. In sintesi, i nostri risultati suggeriscono che sia ora di introdurre una visione della neuromodulazione più sfumata, nella quale molteplici modalità di rilascio sono necessarie per produrre effetti funzionali sinergici.

Keywords: Acetilcolina, Neuromodulatori, Neocorteccia, Modelli, Simulazioni, Proiezioni, Trasmissione sinaptica, Trasmissione volumetrica

Table of contents

List of Figures	3
List of Tables	3
1 Introduction	7
1.1 Motivation	7
1.1.1 Neuromodulation of the neocortex	7
1.1.2 Acetylcholine as a use-case	9
1.1.3 Reconstructing and simulating neuromodulation . . .	11
1.2 Thesis outline	11
2 Cellular, synaptic and network effects of ACh in the neo-cortex	14
2.1 Abstract	14
2.2 Introduction	15
2.3 Volume vs synaptic transmission	17
2.4 Cholinergic receptors	20
2.4.1 Muscarinic receptors	20
2.4.2 Nicotinic receptors	28
2.5 Nicotinic and muscarinic kinetics	39
2.6 Subcellular nicotinic and muscarinic pathways	42
2.7 Transcriptome cell-specific predictions of cholinergic receptors	45
2.8 Global network effects and modulation of brain states	47
2.8.1 Basal forebrain modulation of brain states	47
2.8.2 ACh and GABA co-transmission	48
2.8.3 ACh involvement in neuroplasticity	49
2.8.4 ACh enhancement of sensory processing	51
2.8.5 ACh modulation of thalamo-cortical transmission . . .	52
2.8.6 Sensory-modality specific information processing and ACh	54
2.9 Summary and outlook	55
3 Modelling the neuromodulation of neural microcircuits: a first-draft data-driven framework	57
3.1 Introduction	57

3.2	Data-driven modelling of cholinergic modulation of neural microcircuits: bridging neurons, synapses and network activity .	60
3.2.1	Abstract	60
3.2.2	Introduction	61
3.2.3	Methods	63
3.2.4	Results	67
3.2.5	Discussion	77
3.3	Extending the framework to other neuromodulators	79
3.3.1	Dopamine	79
3.3.2	Serotonin	80
4	Modelling the neuromodulation of neural microcircuits: a multi-scale framework to investigate the effects of cholinergic release	83
4.1	Influence of neuromodulatory systems in the hindlimb representation in the developing somatosensory cortex of the rat	84
4.1.1	Abstract	84
4.1.2	Introduction	85
4.1.3	Materials and methods	87
4.1.4	Results	98
4.1.5	Discussion	109
4.1.6	Conclusions and future directions	115
5	Discussion and concluding remarks	117
	References	123
	Curriculum Vitae	153

List of Figures

1.1	Cholinergic transmission	8
1.2	The big five	9
1.3	Behavioral correlates of ACh	10
1.4	The Neural Microcircuit model	12
2.1	Summary of mAChRs effects on cells	22
2.2	Summary of nAChRs effects on cells	31
2.3	Cholinergic mediated modulation of neocortical synaptic dynamics	33
2.4	Differential expression of cholinergic receptors in various neuronal compartments across cell-types.	34
2.5	Effect of nAChRs and mAChRs activation on the membrane potential of various neocortical cell types.	40
2.6	Effect of nAChRs and mAChRs activation on neocortical synaptic dynamics.	41
2.7	Nicotinic receptor kinetics	42
2.8	Subcellular nicotinic and muscarinic signaling processes at the glutamatergic synapse being modulated by ACh.	44
2.9	Differential expression of cholinergic receptors in transcriptome-derived cell types.	46
3.1	Summary of the biologically detailed tissue model of neocortical microcircuitry.	61
3.2	Validation of anatomical and physiological properties in the tissue model of neocortical microcircuitry.	62
3.3	Integrated summary of the cellular, synaptic and microcircuit effects of acetylcholine (ACh) in the tissue model of neocortical microcircuitry.	64
3.4	ACh effects on cells	67
3.5	ACh effects on synapses	68
3.6	ACh modulates synaptic transmission failures and reorganizes network connectivity.	69
3.7	Predicting only the pre- and postsynaptic effects of ACh on network activity.	73

3.8	ACh shapes spike-spike cross-correlations.	76
4.1	Visualization of neuromodulatory release in the neocortex . .	83
4.2	Modelling workflow	86
4.3	Implementation of volumetric vs synaptic release	97
4.4	ChAT, TH and 5-HT immunoreactivity	99
4.5	In silico predictions of neuromodulatory innervation	102
4.6	ACh network effects	104
4.7	DA network effects	108
4.8	5-HT network effects	110

List of Tables

4.1	ACh literature-reported effects	91
4.2	DA literature-reported effects	92
4.3	5-HT literature-reported effects	93
4.4	ACh parameters	94
4.5	DA parameters	94
4.6	5-HT parameters	95
4.7	Fiber length and densities of the three projection systems . .	98

Chapter 1

Introduction

1.1 Motivation

1.1.1 Neuromodulation of the neocortex

The vertebrate brain is an incredibly complex structure that exists for the purpose of coordinating all the other organs in the body, creating the sense that the animal is a coherent unit, capable of navigating the external world and maximize their chances of survival and the generation of fertile offspring. In order to do that, evolution set up a centralized information-processing machine that resides in the cephalic region of vertebrates and is responsible for the coordination of sensori-motor loops (whether visceral or somatic) which ultimately encapsulate behavior. The mammalian brain, in particular, was subject to evolutionary pressures that endorsed an extensive and unprecedented development of telencephalic cortical regions that we now label as neocortex, a term that highlights the novelty of this structure. A key feature of the neocortex is that it is organized in six layers and that it sits on top of all other brain structures, hiding them from view. Moreover, the neocortex can be subdivided in multiple areas that seem to be involved in specific forms of cognitive processing (sensory processing, decision-making, associative memory etc.) and importantly, motor planning. All of these operations are orchestrated by ensembles of neuronal (and glial) cells that are connected to each other.

The process by which cells organized in a network communicate is defined as neurotransmission. There exist two main forms of neurotransmission in the central nervous system (CNS) which are supported by specific signaling molecules secreted by neurons: glutamate (GLUT) and gamma amino-butyric acid (GABA). While GLUT is prevalently an excitatory neurotransmitter (NT), GABA plays an inhibitory role in the adult neocortex. Although the proportion of excitatory neurons is much larger, inhibitory neurons take part in the regulation of their excitatory counterpart and show

considerable diversity [Markram et al., 2004]. Excitatory and inhibitory neurons are arranged in neural circuits that support a vast assortment of cognitive and motor operations, ultimately sustaining behavior.

In an ever-changing environment, there emerges a need for animals to constantly switch between behavioral states [Lee and Dan, 2012], which are in turn associated with wide-spread changes in global neural activity. The high-dimensional coordinate system that characterizes the activity of a brain at a given moment in time can be defined as brain state [Kringelbach and Deco, 2020]. Brain states in a broad sense can be referred to for instance, as states of sleep, wakefulness, alertness etc. and they are dynamical by nature. One proposed mechanism that supports transitions between brain states is a physiological process known as neuromodulation. Neuromodulation is a form of neurotransmission in that it involves the secretion of a signaling molecule that is released by one neuron and that binds and reacts with receptors present on the surface of other neurons, thus regulating their activity.

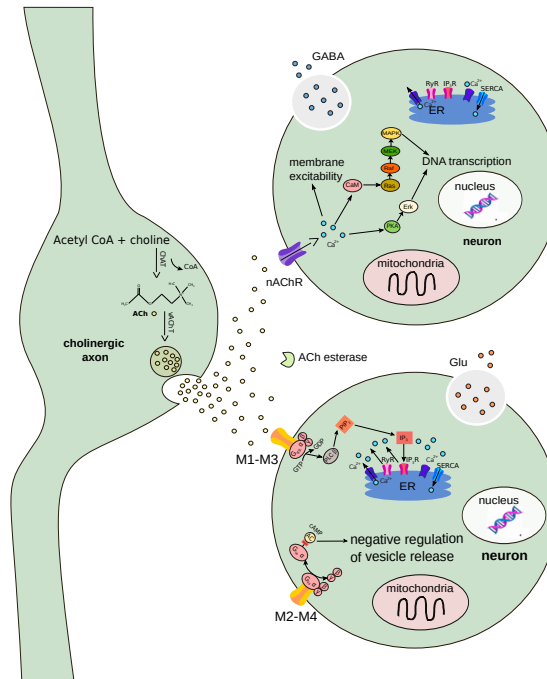


Figure 1.1: An example of neuromodulatory transmission: cholinergic transmission

However, it differs from classic neurotransmission because it acts via a wide variety of receptors, whose activation can lead to diverse effects in different contexts. Thus, it's not possible to predict the ultimate effect of the release of a neuromodulator on a cell, without knowing the target cell-type,

the receptor types involved and even the current state of the network. Given their broad-ranging actions, neuromodulators (NMs) are ideal candidates to support the reconfiguration of neural networks and to govern transitions between brain states. NMs are also involved in regulating the activity of glial cells, and can be released through the blood stream [Marder, 2012], thus influencing the activity of multiple organs in the body. In the brain, NMs reconfigure neural circuits and tremendously alter their output. More in general, they add astonishing richness to the dynamics of neural circuits and are involved in the fine-tuning of network activity. Neuromodulation extraordinarily complexifies our understanding of brain circuits and astounds our wish for linear and straightforward answers to how the brain works. Given the high complexity of neuromodulatory systems, the effort to disentangle the effects of neuromodulation in the neocortex has posed a great challenge for the neuroscientific community, so much that wide gaps are still present in the literature.

1.1.2 Acetylcholine as a use-case

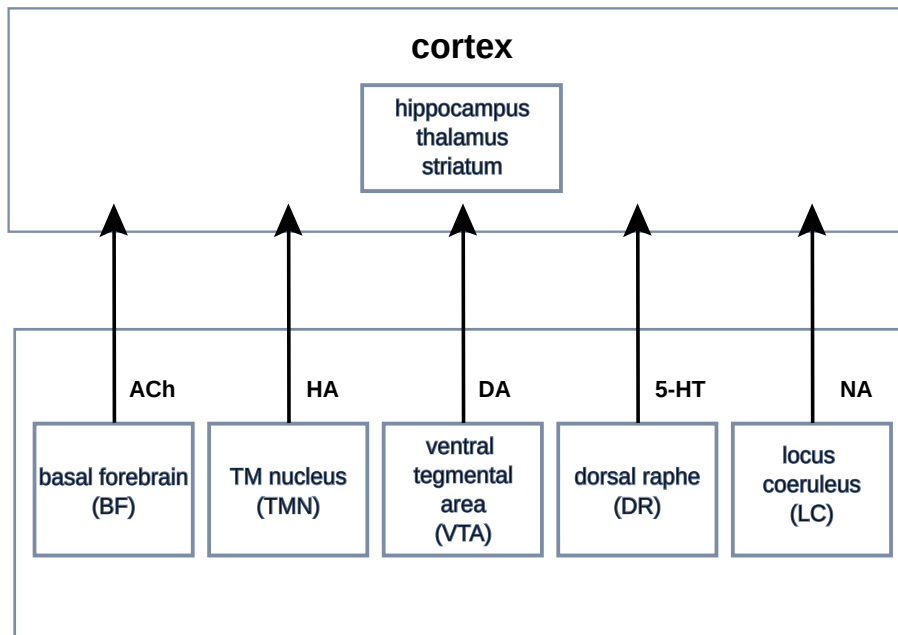


Figure 1.2: Five major neuromodulators in the CNS

There exist five major neuromodulators in the CNS: acetylcholine (ACh), dopamine (DA), serotonin (5-HT), noradrenaline (NA) and histamine (HIS). A key feature of neuromodulatory systems is that they mainly originate from subcortical structures or neuromodulatory regions: the basal forebrain

complex (BF) secreting ACh, the substantia nigra and the ventral tegmental area (SN and VTA) releasing DA, the dorsal raphe nucleus (DR) in the case of 5-HT, the locus coeruleus (LC) where NA is synthesized and the tuberomammillary nucleus (TMN), regulating the production of histamine.

Acetylcholine is the most well-studied neuromodulator, and its effects on neocortical cells and synapses have been extensively researched [Muñoz and Rudy, 2014]. The cholinergic system comprises projections to the cortex originating mainly in the nucleus basalis of Meynert (NBM) of the BF complex and cortical choline acetyl-transferase (ChAT) positive cells. The NBM in turn receives cholinergic projections from the laterodorsal tegmentum (LTD) and the pedunculo-pontine tegmentum (PPT) in the brain stem. The role played by ACh in network states transitions has been characterized to a large extent: ACh has a desynchronizing effect on neural microcircuits that supports specific cognitive functions such as attention and memory. More in general, ACh levels in the cortex correlate with enhanced alertness and arousal, and heightened sensory processing [Anacleto et al., 2015]. Thus, while it is clear that ACh modulates cortical states, we are still lacking

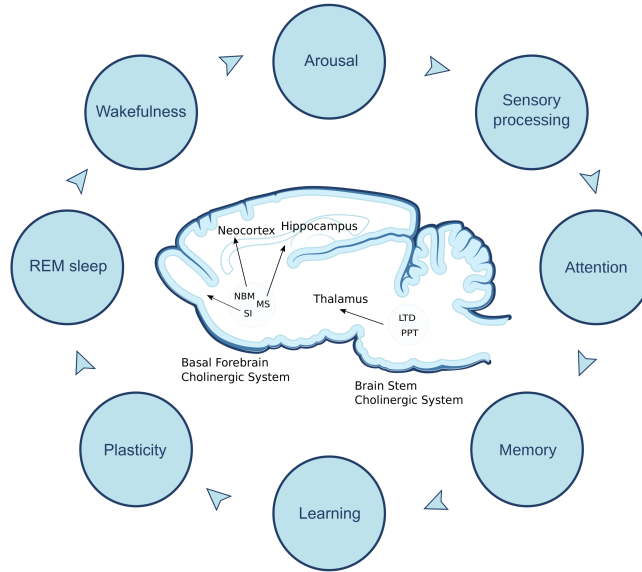


Figure 1.3: Behavioral correlates of ACh

an understanding of how its local effects on cell types and synapses bring about the documented network desynchronization. Furthermore, there is no factual agreement in the neuromodulation community on what even are the effects of ACh on cell-types, perhaps also because classification of cell-

types in the brain is still a matter of debate. Another important aspect of cholinergic modulation is its transmission mode, which remains controversial [Picciotto et al., 2012]. In this case, the discussion is focused on whether ACh signaling occurs via wired (synaptic) or diffuse (volumetric) transmission: cholinergic synapses are difficult to find in the neocortex, but evidence of fast cholinergic signaling contradicts these observations. Additionally, a reliable quantification of extracellular levels of ACh is still lacking [Coppola et al., 2016], although some research groups have estimated that it might lie between the (high) nanomolar to (low) micromolar range. Therefore, we still do not know how ACh impacts cell types, how and how much of it is released in the neocortex, and how this whole process can lead to network desynchronization.

1.1.3 Reconstructing and simulating neuromodulation

Therefore, it is crucial to fill in the knowledge gaps about cholinergic modulation with state-of-the-art tools. Computational models play an increasingly important role in testing scientific hypotheses. A recent data-driven digital model of the microcircuitry of juvenile rat somatosensory cortex [Markram et al., 2015] uses anatomical and physiological rules derived from sparse experimental data to algorithmically reconstruct neocortical tissue. Identifying rules and principles of organization provide constraints to build models of ion channels, single cells, synaptic dynamics and microcircuits at different levels of granularity. The ‘building blocks’ models can then be integrated to create a multi-scale digital replica of an ensemble of cortical columns, that is, a virtual brain slice. This unifying framework enables a systematic exploration of how ACh is released in the neocortex, regulates the physiology of local neurons and synapses and how these changes shape the emergence of global network states. To record electrical or synaptic activity from a great number of neurons at the same time is still quite a challenging task, and even if it were possible to study the effect of cholinergic modulation on every cell-type, the occurrence of volume transmission would not be considered in the picture, given that it is very hard to detect the levels of physiological extracellular ACh concentrations and therefore, virtually impossible to accurately replicate the phenomenon in vitro. Supercomputer-based simulations therefore turn the understanding of the brain into a more tractable problem, providing a new tool to study the complex interactions within different levels of brain organization.

1.2 Thesis outline

This thesis is structured as several chapters:

- **Chapter 1 - Introduction:** an overview of the high-level motiva-

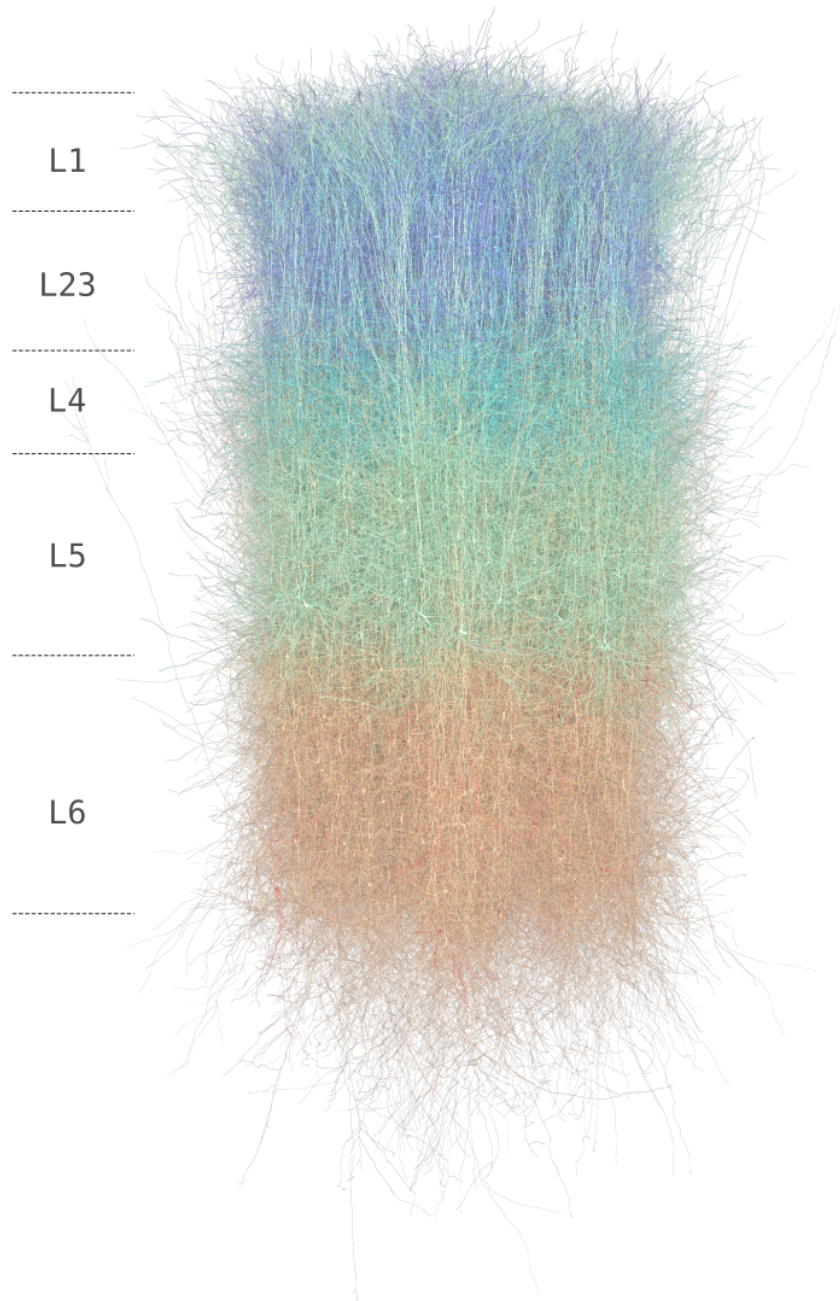


Figure 1.4: The neural microcircuit model: a biologically detailed model of the neocortical microcircuit

tions for this thesis, that is, the problem of bridging the gap between sparse datasets and the necessity to integrate all that is known in a comprehensive framework, with particular attention to the fact that this approach is remarkably well suited to address the problem of understanding neuromodulation in the cortex.

- **Chapter 2- Literature review:** in this chapter, I review and summarize extensively the state-of-the-art literature on cholinergic modulation of the neocortex and identify gaps in the current knowledge with the aim of developing a comprehensive map of the effects of ACh to guide experimental and theoretical research. This review was published in *Frontiers in neural circuits* [Colangelo et al., 2019].
- **Chapter 3- Modelling neuromodulation: a first-draft data-driven digital model:** In this chapter, after a brief overview where I re-frame the research question highlighted in the Introduction chapter in the light of the recent advances in modelling and simulation-based paradigms, I present a first-draft data-driven model of cholinergic neuromodulation. This published study [Ramaswamy et al., 2018] was conducted in the early stages of this project, and serves as a proof of concept that it is possible to build multi-level models of neuromodulation and integrate them in a coherent framework to have a chance to study otherwise technically challenging aspects of the problem.
- **Chapter 4 – Modelling neuromodulation: a multi-scale framework to model cholinergic release** The assumptions on which a model rests can be re-visited as long as they are supported by experimental data, so this chapter presents a study that builds on the data-driven framework described in Chapter 3 by refining it with additional data and further assumptions. In addition, we predict the relative functional contributions of two release modalities - synaptic vs volumetric - on cortical computation.
- **Chapter 5 – Discussion and concluding remarks** An extended commentary on the results discussed in the preceding chapter with a discussion on the limitations of our modelling approach and future directions of this research.

Chapter 2

Cellular, synaptic and network effects of ACh in the neocortex

Cristina Colangelo, Polina Shichkova, Daniel Keller, Henry Markram and Srikanth Ramaswamy

Front. Neural Circuits, 12 April 2019
<https://doi.org/10.3389/fncir.2019.00024>

2.1 Abstract

The neocortex is densely innervated by basal forebrain (BF) cholinergic neurons. Long-range axons of cholinergic neurons regulate higher-order cognitive function and dysfunction in the neocortex by releasing acetylcholine (ACh). ACh release dynamically reconfigures neocortical microcircuitry through differential spatiotemporal actions on cell-types and their synaptic connections. At the cellular level, ACh release controls neuronal excitability and firing rate, by hyperpolarizing or depolarizing target neurons. At the synaptic level, ACh impacts transmission dynamics not only by altering the presynaptic probability of release, but also the magnitude of the postsynaptic response. Despite the crucial role of ACh release in physiology and pathophysiology, a comprehensive understanding of the way it regulates the activity of diverse neocortical cell-types and synaptic connections has remained elusive. This review aims to summarize the state-of-the-art anatomical and physiological data to develop a functional map of the cellular, synaptic and microcircuit effects of ACh in the neocortex of rodents and non-human primates, and to serve as a quantitative reference for those intending to build data-driven computational models on the role of ACh in governing brain states.

2.2 Introduction

The cholinergic system is one of the most well-studied neuromodulatory systems, and perhaps phylogenetically the oldest. Acetylcholine (ACh) is found in both vertebrates and invertebrates and together with adrenaline and noradrenaline (NA), it acts as one of the main effectors of the autonomic nervous system. In the central nervous system (CNS), ACh impacts cellular and synaptic physiology and may switch network dynamics resulting in behavioral transitions such as from sleep to wakefulness, distraction to attention, and learning and recall [Hasselmo and Sarter, 2011, Lee and Dan, 2012]. Cholinergic effects have been studied for more than a century. In 1869, Schmiedeberg and Koppe [Schmiedeberg and Koppe, 1869] demonstrated how extracts of a common mushroom, *Amanita muscaria*, could slow, and at a higher concentration arrest the beat of the frog heart. They purified the extract and named it muscarine. This substance, when applied to the brain and spinal cord was able to produce flaccidity and weaken the peripheral reflexes. However, the pharmacology of the nitrite ester of choline was different in that it had considerable nicotinic activity (nicotine is the major alkaloid of tobacco, first isolated by Posselt and Reiman from *Nicotiana tabacum* leaves in 1828; [Koukouli et al., 2017]). In 1921 experimental proof was obtained for ACh’s role as a chemical transmitter at the cardiac vagal endings. The active substance was initially named “vagusstoff” by Otto Loewi in 1921 [Loewi, 1924]. Sir Henry Dale further described that muscarinic responses were antagonized by atropine, whereas the nicotine actions were antagonized by curare [Dale, 1914]. It has long been known that ACh is also present at the level of the CNS, however, it was not until 1953 that evidence of the release of ACh in the brain was provided [Eccles et al., 1953]. Prior to this discovery, it was known that anti-cholinergic drugs could influence learning and memory—pharmacological activation of muscarinic ACh receptors (mAChRs) was known to produce delirium symptoms, while receptor blockade generates severe anterograde amnesia. Moreover, the dementia of Alzheimer’s and Parkinson’s diseases has been associated with the loss of cortical cholinergic innervation [Little, 1998, Giacobini, 2003, Sabri et al., 2008, Hasselmo and Sarter, 2011], and chronic administration of nicotine reverses hypofrontality in animal models of addiction and schizophrenia [Koukouli et al., 2017].

Classical notions sustain the view that the central cholinergic system works by a diffuse release of ACh across the cortex, activating its receptors globally and producing slow responses. While this view might be applicable to long-lasting behavioral phenomena, such as cortical arousal, it does not explain the modulation of processes that happen on a much faster scale, such as sensory gating, or plasticity [Muñoz and Rudy, 2014]. ACh release in the neocortex originates from neurons distributed within the basal forebrain

(BF) nuclei, including the medial septum, the vertical and horizontal diagonal band of Broca, the substantia innominata, and the nucleus basalis of Meynert (NBM). Release occurs through topographical projections, and all the projections arise from six groups of choline acetyl-transferase (ChAT)-positive neurons in the BF (Ch1–Ch4) and brainstem (Ch5–Ch6) [Wevers, 2011]. The innervation sparsely reaches all cortical layers, but layer 5 is more heavily innervated, particularly in the motor and sensory areas; cholinergic pathways often provide en passant innervation [Dani and Bertrand, 2007] to the neocortex. Additionally, ACh-releasing cells are found in cortical layer 2/3. These cells exhibit a bipolar morphology, stain positive for calretinin (CR) and vasoactive intestinal peptide (VIP), and are GABAergic [Engelhardt et al., 2007, Granger et al., 2018]. The function of a neuromodulatory system is largely defined by the anatomy of its projections. Projections from the BF selectively control cortical activity and target neocortical regions more specifically than previously assumed [Hasselmo and Sarter, 2011, Muñoz and Rudy, 2014, Obermayer et al., 2017]. Recent evidence suggests that a roughly topographical organizational scheme exists in the rostro-caudal sequence of neurons of the BF [Zaborszky et al., 2015a] and that specific BF nuclei innervate specific cortical areas, as opposed to what happens with noradrenergic fibers originating from the locus coeruleus [Chaves-Coira et al., 2016, Kim et al., 2016]. Cholinergic fibers can take one of four different routes to cortical structures: the septal pathway (which projects mainly to the hippocampal cortex) the medial pathway, the lateral pathway, or the internal capsule projection (which preferentially project to the neocortex; [Poorthuis et al., 2014]). Cholinergic terminals that reach the neocortex, mainly via layer 1 or layer 6 [Obermayer et al., 2017], can either exert a spread out control of cortical activity and regulate processes such as the transition from sleep to wakefulness and arousal, or contact a restricted number of cortical elements and have cell-type specific effects; here contextual cholinergic signals act in concert with local processing of sensory inputs in order to guide behavior. The aim of this review is to bring together current knowledge of cholinergic modulation in the neocortex and to identify the gaps to propose future directions to advance the field of neuromodulation. Here, we summarize existing literature on ACh release in the neocortex of rodents and non-human primates, specifically focusing on how ACh-induced effects on the diversity of cell-types and synapses shape the emergence of network states and review theories that bridge the modulation of local circuit properties and the consequent reconfiguration of cortical states. Data-driven computational models allow predictions on the potential role of ACh in reconfiguring neocortical states [Ramaswamy et al., 2018]. Therefore, this review reconciles the minimal, although sparse, datasets required to build a multi-scale computational model of the neocortical cholinergic system.

2.3 Volume vs synaptic transmission

A major factor that determines the spatiotemporal precision of ACh action is the transmission mode at cholinergic terminals. Cholinergic cortical signaling has historically been considered a slow and diffuse process, which was established upon examination of the functional organization of cholinergic projections and was mainly based on reports indicating a nearly complete absence of classical synapses at the level of cholinergic terminals [Muñoz and Rudy, 2014]. Before optogenetic techniques were available, cholinergic pathways could not be activated in a selective manner, and thus evidence of the existence of fast cholinergic synaptic transmission was lacking, although some proof of fast nicotinic responses was already available from hippocampal recordings [Kalmbach et al., 2012, Obermayer et al., 2017]. In the cerebral cortex, cholinergic fibers are distributed in an intricate network with a characteristic laminar pattern. They have a higher density in the deeper layers. Cholinergic innervation reflects the classic organizational scheme of information processing systems [Kennedy and Bullier, 1985], with a higher number of projections being present in higher-order areas. Presumed cholinergic release sites have been ultra-structurally inspected and the subtle presence of synapse-like contacts has indeed been revealed; however, a relatively large number of these small varicosities, which are often associated with accumulated synaptic vesicles, do not seem to effectively establish synaptic contact with neighboring neurons, or exhibit only a few morphologically identifiable synapses. Furthermore, the scarceness of astrocytic processes in the immediate vicinity of ChAT-immuno-reactive axons (when compared to glutamatergic terminals) may also allow greater diffusion of ACh within the extracellular space [Aoki and Kabak, 1992]. Thus, relatively low concentrations of ACh will reach locations that are distant from the release site. This produces volume transmission or bulk release: neuro-modulators slowly diffuse in a wide cortical area and bind to a large pool of extra-synaptic receptors [Dani and Bertrand, 2007]. Many studies [Umbriaco et al., 1994, Descarries and Mechawar, 2000, Sarter et al., 2009, Yamasaki et al., 2010] conducted in the neocortex have suggested that ACh acts preferentially non-synaptically; however, central cholinergic synapses had already been observed in the early '90s. Actual synapses were found on cholinergic varicosities in the cingulate cortex of the rat [Umbriaco et al., 1994], and in macaque more than 40 percent of cholinergic varicosities contained synaptic specializations [Mrzijek et al., 1995]. Later, [Turrini et al., 2001] provide definitive evidence that suggests that synaptic mechanisms of cholinergic transmission not only exist but prevail in the rat neocortex. Ultrastructural observations that most (66 %) cholinergic boutons—as revealed by IR assays for the specific cholinergic marker, vesicular ACh transporter (vAChT)—establish classical synapses in layer 5 of the rat parietal cortex. By applying an improved fixation protocol and by using an anti-

body for vAChT, Turrini and others demonstrated that cholinergic boutons predominantly established symmetric synapses on layer 5 dendritic shafts. The authors also found that immuno-stained varicosities occasionally established asymmetric contacts, but always on dendritic spines. Another study probed the molecular-anatomical relationship between detectable cholinergic varicosities and the most abundant receptor subtype in the cortex—the muscarinic receptor subtype M1 [Yamamoto et al., 2010]. This study established that in the mouse neocortex M1 can be found almost exclusively on the extra-synaptic membrane of pyramidal cells (PCs). Here, they observed that M1 distribution is far denser than the putative cholinergic release sites and that it does not show any apposition pattern to the varicosities, nor to the cytomatrix active zone proteins that are normally found at glutamatergic terminals. Hence, M1’s function in cortical PCs may be to sense ambient ACh released from cholinergic terminals at variable distances, and the main modality through which it is recruited is likely to be volume transmission. These approaches not only contribute to building a more refined knowledge of the subcellular localization of receptor subtypes but also provide a method to qualitatively discriminate between two major modes of transmission. Because of a substantial difference in the distribution pattern of cholinergic receptors across species, it is very likely that experiments performed in different species will yield conflicting results. For instance, even though a low incidence of classical synapses was reported for the rodent brain, a much higher proportion of cholinergic synapses was found in primates [Smiley et al., 1997]. In the human cerebral cortex, the same authors found that up to 67 % of all cholinergic varicosities established synaptic contacts, suggesting that ACh signaling in humans is mostly mediated by point-to-point synaptic transmission; this mechanism appears to prevail in the primate brain, but whether the same can be said for rodents is still a matter of open debate.

Cholinergic innervation from the BF is more specific than previously considered; ACh can control cortical activity on a fine spatial scale as well. Indeed, these findings agree with the evidence of ACh signaling occurring through direct fast point-to-point synaptic transmission brought about by the application of optogenetic tools [Kalmbach et al., 2012]. Overall, it is not completely clear yet whether one mode of cholinergic transmission prevails over the other. Instead, a growing body of evidence suggests that volume and synaptic transmission may be complementary mechanisms by which ACh modulates cortical function [Sarter et al., 2009]. While bulk release is thought to cause a more tonic change in extracellular ACh concentration, in the scale of seconds and minutes, and is mainly mediated by activation of extra-synaptic receptors, ACh release occurring at junctional sites would have a more circumscribed influence, with the modulation of

circuit activity being restricted to the contacted cortical elements and to a much more delimited spatiotemporal scale [Muñoz and Rudy, 2014]. Taken together, evidence shows that ACh modulates microcircuit activity with different modalities, ranging from synaptic release to volume transmission, and exerts its effects by modifying membrane excitability or synaptic activity. Instead of trying to proclaim one modality over the other, future research should address the issue of whether they can occur simultaneously and have a differential impact on the temporal aspects of the response.

Traditional bath application of agonists results in broad spatial and temporal activation that might not reflect the accuracy of endogenous ACh release [Urban-Ciecko et al., 2018]. It is thus of crucial importance to determine whether the different ways in which cholinergic agonists are experimentally applied reflect different transmission modalities, and how faithfully stimulation protocols replicate physiological conditions. In the future, ACh application should be standardized according to precisely obtained dose-response and sensitization kinetics curves, and ascending concentrations should be used in order to detect eventual dose-dependent responses. Furthermore, it would be of outstanding interest to better understand how ACh release obtained by optogenetic stimulation of cholinergic afferents compares against bath application of cholinergic agonists. In a recent study, optogenetic recruitment of cholinergic fibers was performed in parallel with 1 mM ACh bath-application to detect changes in Martinotti cells (MCs) activity: the two techniques yielded very similar results [Obermayer et al., 2018]. Perhaps the high concentration of ACh used in this case is comparable with a more physiological activation of the cholinergic system. Further clarification is required on the matter, and future studies should, therefore, consider this issue and design their experiments accordingly. Cholinergic projections are likely to be arranged according to a modular pattern, with isolated bands of neighboring ChAT⁺ cells in the BF having defined cortical targets that are, in turn, functionally associated. When retrograde dyes are injected in distant cortical areas, labeled regions of cholinergic cells in the BF still largely overlap, even though the innervated cortical space is quite restricted [Muñoz and Rudy, 2014]. Furthermore, [Zaborszky et al., 2015b] assert that the degree of overlap of labeled neuronal locations within the BF is positively correlated to the connection strength between the different injected cortical regions. Such an organization could induce widespread modulation even when the system is only focally activated [Muñoz and Rudy, 2014]. Nevertheless, the response to neuromodulatory inputs is determined by the interplay of multiple factors, such as post-synaptic target, receptor type and subunit composition, subcellular localization of the receptors and their sensitivity. This way, a diffusely-organized projection system can fine-tune microcircuit activity. The cholinergic projection system should be viewed

as a highly dynamic structure, able to propagate inputs either selectively or diffusely, switching from one modality to another, depending on the needs. The next section aims to unravel the contribution of each subtype of cholinergic receptor to microcircuit modulation and attempts to determine the physiological relevance of their compartmentalized distribution and differential activation.

2.4 Cholinergic receptors

Even though the differential pharmacological effects had already been characterized, it was not until the early 1950s that the idea of “receptors” as the binding site for ACh was firmly established by [Eccles et al., 1953]. Cholinergic receptors are composed of two classes of transmembrane macromolecular complexes, the muscarinic and the nicotinic receptor families, each of which is further divided into subclasses. The occurrence of many ACh receptor subtypes and their differential dendritic, somatic, axonal, and synaptic localization contribute to the varied roles that these receptors play in the CNS. Cholinergic receptors have been found on axons originating from thalamic, cortical or basalo-cortical fibers as well as on cortical pyramidal excitatory neurons and inhibitory GABAergic interneurons [Groleau et al., 2015]. The precise layer-wise distribution of cholinergic terminals, the identification of cell-types that actually express cholinergic receptors, and the subcellular localization of these receptors are described in the following sections.

2.4.1 Muscarinic receptors

Cholinergic synapses throughout the CNS are composed of muscarinic receptors (mAChRs), which can be further differentiated into subtypes that are encoded by a single gene [Venter et al., 1988, Van der Zee and Luiten, 1999]. Five genetically defined and pharmacologically characterized (M1 to M5) mAChR subtypes have been identified in the CNS with high levels of expression in subcortical structures and the cerebral cortex [Wevers, 2011]. Immunocytochemical approaches have identified different levels of expression of mAChRs throughout the cerebral cortex. These studies have detected moderate levels of mAChRs in the frontal cortex, parietal cortex, temporal cortex, entorhinal cortex, occipital cortex, insular and cingulate cortex, with the highest values for the temporal and occipital cortex. M1 receptors are the most abundantly expressed among all subtypes of mAChRs [Wevers, 2011]. The density of cholinergic terminals in the rat neocortex differs between the six layers and depends on the cortical region studied [Eckenstein et al., 1988, Lysakowski et al., 1989]. The pattern of cellular staining for mAChRs in the neocortex is characterized by a clear laminar distribution: in most of the cortical mantle, especially in neocortical areas, predominantly layer 5 PCs (L5PCs) show strong immunoreactivity

across mammals such as the mouse, golden hamster, rat, cat, and human [Van der Zee and Luiten, 1999]. The density of each mAChR subtype differs throughout the brain with M1 being the most abundantly expressed and M5 the least [Alger et al., 2014]. In the hippocampus and neocortex, M1 is present at high levels, M3 is moderately represented (though generally low elsewhere) and M4 is present in high density, as almost anywhere else in the brain, even though its concentration is considerably lower than M1. M2 instead, is found at very low densities, and this class of receptors seems to be distributed according to a precise pattern. M2 receptors frequently reside on presynaptic axonal terminals, whereas M1 receptors are often located on somato-dendritic regions of neurons. The M5 subtype is believed to play an important role in cortical perfusion, and it is mainly expressed on endothelial cells of the cerebral vascular system [Elhusseiny and Hamel, 2000, Gericke et al., 2011] even though recent evidence suggests that the M3 subtype is also involved in this kind of process [Zuccolo et al., 2017]. In the rodent visual cortex, the subtypes M1 and M2 predominate, while in primates the subtypes M1, M2 and M4 prevail. Besides a few regional variations, highest labeling densities have been observed in the superficial layers of most cortical areas for both M1 and M2 [Wevers, 2011].

Most cholinergic receptors are metabotropic and mediate slow responses, which are typically associated with volume transmission. In the neonatal and adult cortices of rodents and primates, M1–M5 subtypes of mAChRs occur in both pre-synaptic and post-synaptic positions [Mrzljak et al., 1993, Groleau et al., 2015]. All mAChRs are transmembrane macromolecular complexes that are coupled to membrane-embedded G-proteins of different kinds; g-proteins act as intracellular effectors and initiate signaling cascades that ultimately have an effect on intracellular processes, leading to the opening or closing of some ion channel, or to the production of long-term modifications of genetic activity and protein expression. Different mAChRs are coupled to specific G-proteins. The pre-synaptic mAChRs M2 and M4 preferentially couple to G_i and G_o proteins that generally have inhibitory effects on voltage-activated calcium channels or extend the opening of potassium channels. The resulting decrease in c-AMP signaling suppresses neurotransmitter release [Groleau et al., 2015]. M1, M3 and M5 subtypes are preferentially coupled to G_q and G_{11} proteins and are mainly located post-synaptically. Their activation seems to trigger membrane depolarization and increases the input-resistance of the cell membrane. M1-like (M1-M3-M5) receptors are known to potentiate NMDA currents and also influence and modulate voltage-dependent calcium currents, mostly by upregulating phospholipase C (PLC) signaling and inositol triphosphate (IP_3) turnover. One major effect that can be attributed to M1-type receptors is the inhibition of potassium currents, including the I_m and the I_{AHP} (both medium and slow

rate). However, M1-type receptors can also potentiate cationic currents like the I_h and the TRP currents, and the I_{cat} (Teles-Grilo Ruivo and Mellor, 2013). For a more detailed description of the effects of ACh on various currents and their associated intracellular signaling pathways, we direct the reader to the section “Subcellular Nicotinic and Muscarinic Pathways” of this review.

Cell type	Receptor	Effect	Area	Technique—Reference
L5 PC	M1 (soma)	Transient hyperpolarization	Rat PMC/V1/PFC	Optogenetics (Hedrick and Waters, 2015)
	M1 (soma)	Slow depolarization	Rat PMC/V1/PFC	1. Optogenetics (Hedrick and Waters, 2015)
				2. Somatic puff 100 μ M ACh/CCh (Gulledge and Stuart, 2005)
				3. 100 μ M ACh focally applied (Gulledge et al., 2007)
	M1 (soma)	Hyperpolarization	Rat SSC	100 μ M ACh focally applied (Gulledge et al., 2007)
	M1 (soma)	Depolarization	Rat mPFC	30 μ M muscarine or oxotremorine bath application (Haj-Dahmane and Andrade, 1996)
L2/3 PC	Muscarinic	Depolarization	Mouse V1	<i>In vivo</i> 2-photon imaging (Alitto and Dan, 2013)
	Muscarinic	Prolonged depolarization	Rat EC layer II	100 mM CCh bath application (Shalinsky et al., 2002)
	M2–M4	Hyperpolarization	Mouse SSC (p12–p16)	Optogenetics (Dasgupta et al., 2018)
L4 PC	M2–M4	Persistent hyperpolarization	Rat SSC	100 μ M ACh, puff (Eggermann and Feldmeyer, 2009)
L4 SS	M4 (soma)	Persistent hyperpolarization	Rat SSC	100 μ M ACh, puff (Eggermann and Feldmeyer, 2009)
L1 BC	Muscarinic	Depolarization	Mouse V1	<i>In vivo</i> 2-photon imaging (Alitto and Dan, 2013)
L1 DBC	Muscarinic	Depolarization	1. Mouse V1	1. <i>In vivo</i> 2-photon imaging (Alitto and Dan, 2013)
			2. Rat PFC	2. 10 μ M CCh or 3 μ M muscarine bath application (Kawaguchi, 1997)
L2/3 DBC	M2	1. Hyperpolarization	1. Rat SSC	1. 100 μ M ACh focally applied (Gulledge et al., 2007)
		2. Hyperpolarization + slow depolarization	2. Rat PFC	2. 10 μ M CCh or 3 μ M muscarine bath application (Kawaguchi, 1997)
L2/3 MC	M1–M3	Depolarization	Mouse SSC	1. Muñoz et al. (2017; M1–M3 KO lines)
				2. Optogenetics (Dasgupta et al., 2018)
L2/3 BC	Muscarinic	Depolarization	Mouse V1	1 μ M/10 mM ACh application (Chen et al., 2015)
		Not responsive (NR)	1. Rat SSC	1. 100 μ M ACh focally applied (Gulledge et al., 2007)
			2. Rat PFC	2. 10 μ M CCh or 3 μ M muscarine bath application (Kawaguchi, 1997)
L5 BC		NR	Rat SSC	100 μ M ACh focally applied (Gulledge et al., 2007)
L5 MC	Muscarinic	NR/slight depolarization	Rat SSC	100 μ M ACh focally applied (Gulledge et al., 2007)

The table links the distribution and localization (when known, in brackets) of muscarinic receptors across neocortical cell types, with respect to cortical layers, with the effect of their activation. The effect of receptor activation is represented in terms of variation of membrane potential. Age of the specimen is given in brackets, when known. When biphasic effects occur, they are listed as multiple effects. Inclusion criteria for the listed studies comprise: (1) recordings performed in the rodent neocortex; (2) knowledge of the morphological type involved; and (3) knowledge of the receptor subtype involved in the response. Abbreviations: PC, pyramidal cell; SS, spiny stellate cell; IN, interneuron; MC, Martinotti cell; BC, basket cell; DBC, double-bouquet cell; NGFC, neurogliaform cell; BPC, bipolar cell; NBC, nest basket cell; RS, regular spiking. PMC, primary motor cortex; V1, primary visual area; PFC, prefrontal cortex; mPFC, medial prefrontal cortex; EC, entorhinal cortex; SSC, somatosensory cortex; ACh, acetylcholine; CCh, carbachol.

Figure 2.1: Table 1 links the distribution and localization (when known, in brackets) of muscarinic receptors across neocortical cell types, with respect to cortical layers, with the effect of their activation. The effect of receptor activation is represented in terms of variation of membrane potential. Age of the specimen is given in brackets, when known. When biphasic effects occur, they are listed as multiple effects. Inclusion criteria for the listed studies comprise: 1) recordings performed in the rodent neocortex, 2) knowledge of the morphological type involved and 3) knowledge of the receptor subtype involved in the response. Abbreviations: PC, pyramidal cell; SS, spiny stellate cell; IN, interneuron; MC, Martinotti cell; BC, basket cell; DBC, double bouquet cell; NGFC, neurogliaform cell; BPC, bipolar cell, NBC, nest basket cell; RS, regular spiking. PMC, primary motor cortex; V1, primary visual area; PFC, prefrontal cortex; mPFC, medial prefrontal cortex; EC, entorhinal cortex; SSC, somatosensory cortex, ACh, acetylcholine; CCh, carbachol

Presynaptic localization

What anatomical and functional evidence exists on the distribution of mAChRs in the neocortex? Muscarinic cholinergic activity influences sensory processing by facilitating or depressing neuronal responses to specific stimuli, and by modulating connections strength and neural synchronization: this results in the fine-tuning of cellular and network properties during developmental processes, the execution of attention tasks and perceptual learning [Groleau

et al., 2015]. These effects can largely be attributed to M1 and M2 subtypes, which appear to be highly prevalent in the neocortex. The presence of M1 and M2 mAChRs on PC somata and apical dendrites in non-human primates is well established, but M2 receptors are also found on excitatory and inhibitory axons in the primate neocortex [Mrzljak et al., 1993]. Disney et al. [Disney et al., 2006] report that M1 and M2 receptor labeling can be observed, but is quite weak in axons and terminals in the macaque visual cortex, whereas mAChRs are mostly expressed at the level of the soma of GABAergic neurons and in the dendritic compartments of glutamatergic cells. Among the presynaptic receptors in the rodent and human visual cortex, M2 is very abundant while M4 is less prevalent [Groleau et al., 2015]. M2 and M4 are mostly found at the presynaptic terminals; activation of these receptor subtypes causes membrane hyperpolarization and conveys a self-inhibitory signal. Thus, extracellular levels of ACh are regulated by means of negative feedback. In the rat’s primary visual cortex (V1) M2 is mainly found at the level of cholinergic terminals in layer 4 and layer 5. Being the main inhibitory auto-receptor, it contributes to the suppression of presynaptic ACh release [Mrzljak et al., 1993]. It is not yet clear whether the presence of M2-like subtypes at the level of the presynaptic terminal is a distinctive feature of cholinergic axons innervating the neocortex. Conflicting results emerge when looking at rodent studies, while experiments done on non-human primates and cats corroborate M2 receptors as the main auto-receptors localized on BF cholinergic axons. Subsequent research should, therefore, address this issue and determine the extent to which presynaptic M2-like receptors account for negative feedback via auto-inhibition, since this type of self-regulatory process is crucial for the fine-tuning of the response. Moreover, given that BF fibers originating from distinct neuron clusters differentially innervate separate cortical areas [Zaborszky et al., 2015a, Chaves-Coira et al., 2016, Kim et al., 2016], discrepancies should be expected when assessing receptor subtype distributions across neocortical regions. Estimation of the physiological presynaptic distribution profile of inhibitory auto-receptors in the rodent sensory cortex is of key importance to understanding the system’s self-calibrating features. A systematic anatomical profiling of receptor expression should be performed in the rodent models, and quantitative comparisons should be made across sensory areas.

Postsynaptic localization

Neocortical PCs and inhibitory interneurons are strongly innervated by cholinergic axons, with L5PCs being the most densely innervated cells; however, numerous immuno-reactive interneurons can be found in all layers, but most frequently in layer 2/3 and layer 5. Here, the mAChR positive interneurons are intermingled with labeled PCs, but in general, the immunostaining

of interneurons is less dense than that of the PCs [Van der Zee and Luiten, 1999]. While mAChRs are more easily found in the dendritic compartments of PCs, their expression profile throughout the diversity of inhibitory interneurons is quite homogeneous, as these receptors are detected in proximity of the somatic compartment [Disney et al., 2006]. mAChRs are expressed by different types of interneurons. In macaque, M2 receptors are found in 31 % of PV neurons, 23 % of CB neurons, and 25 % of CR neurons. 87 % of PV⁺ neurons, 60 % of CB⁺ neurons and 40 % of CR⁺ neurons however, express M1-type mAChRs. The M1 subtype is found across the cortical mantle on the cell bodies and dendrites of post-synaptic PCs, and it appears to be present mainly in layers 2/3 and 6, but it can be found across all cortical layers. In macaque V1, M1 is mostly expressed on GABAergic interneurons, but it is also found on cortico-cortical fibers [Mrzljak et al., 1993, Groleau et al., 2015]. M1 immuno-reactivity is also observable in interneurons of the rat neocortex [Levey et al., 1991], although other studies have pointed to a low expression of M1 in primary sensory cortices of rats, such as S1 and V1. Some found M1 expression on PV⁺ neurons to be low or even undetectable in mice neocortex [Yamasaki et al., 2010]. The significant difference in expression between rodents and primates could be explained by the fact that M1 receptors are much more associated to the extra-synaptic membrane compartments and are usually activated by volume transmission. Given that the BF cholinergic projection system is scaled-up in primates relative to rodents, there could be a more widespread distribution of M1 receptors throughout cortical interneurons. M1 immuno-reactivity is also detected at the synaptic level, in both inhibitory and excitatory synapses across cortical layers, but more frequently on asymmetric synapses, and here, preferentially on dendritic spines, as opposed to symmetric synapses where M1 is found mostly on dendritic shafts [Mrzljak et al., 1993]. This preferential distribution perspective is challenged though, by experimental evidence that cholinergic boutons form synapses mainly with dendritic shafts, much fewer with dendritic spines and only occasionally on neuronal somata [Beaulieu and Somogyi, 1991, Mrzljak et al., 1993, Umbriaco et al., 1994]. However, in mice, the highest density of M1 immuno-particles is observed in small-caliber oblique dendrites (smaller than 0.66 μm in diameter) of PCs [Yamamoto et al., 2010]. In L5PCs, M2 mAChRs are mainly localized postsynaptically, where they bring about a decrease in excitatory conductances, but M2 and M4 receptors are also present on the cell bodies of GABAergic interneurons in layers 2/3 and 4; here, M2 activation inhibits GABA release. The M3 subtype is localized postsynaptically in rodent inhibitory neurons and dendrites, where it enhances inhibitory transmission [Mrzljak et al., 1993, Groleau et al., 2015]. Finally, M4 mAChRs are expressed in cortical excitatory neurons, in particular, in layer 4 spiny stellate neurons (L4SS) across different neocortical regions—S1, V1, and prefrontal cortex (PFC)—where they generate a persistent hyperpolarizing response

[Radnikow and Feldmeyer, 2018]. Perhaps the presence of M4 mAChRs is a marker to tell apart layer 4 from other layers. Cholinergic inputs to the cortex generate different responses depending on which receptor is recruited: while M1-like (M1-M3-M5) receptors activation generally leads to an increase in postsynaptic conductance, M2-like receptors (M2-M4) have the opposite tendency to decrease synaptic transmission, by regulating presynaptic ACh release or by directly hyperpolarizing the post-synaptic membrane.

mAChRs thus seem to be distributed both at the presynaptic and the postsynaptic level, and the resulting effect depends mostly on which subtype is activated. A detailed understanding of the cellular localization of each receptor subtype for every cell-type is still lacking; some generalizations can be made (as can be seen in Figure 3), but in order to precisely understand how neuromodulatory signals affect neural computation, a detailed knowledge of the amount and distribution of receptor subtypes at the level of each compartment is essential. Furthermore, it is of vital importance to gather this information for each neocortical cell-type. Neuromodulatory inputs very likely affect each cell-type differently, unlocking the possibility of fine-tuning the response and allowing delicate recalibration based on contextual information processing. This is most likely achieved by differentially distributing receptors along cellular compartments, thus creating modulatory micro-domains.

Regulation of neuronal and synaptic physiology

ACh can either increase or decrease neurotransmitter release probability, consistent with its role as a neuromodulator rather than a transmitter, and the effect on synaptic release probability depends on the identity of the pre and postsynaptic partners. Cell-types in the neocortex are differentially regulated by ACh, and the effects of cholinergic release include modulation of membrane properties (Figure 1) and synaptic dynamics (Figure 2). The effects of ACh on neocortical PCs have been thoroughly investigated, and many studies [Gil et al., 1997, Disney et al., 2007] have come to the conclusion that besides generating direct PC depolarization, cholinergic modulation has an overall effect of increasing the signal to noise ratio (SNR) of incoming thalamic inputs. ACh seems to play a role in enhancing circuit responses to relevant stimuli, providing a mechanism to regulate sensory processing during learning and attention.

The involvement of mAChRs in the depolarizing response of PCs to BF cholinergic inputs has been established by numerous studies [McCormick and Prince, 1985, Delmas and Brown, 2005, Gullledge and Stuart, 2005, Carr and

Surmeier, 2007, Zhang and Séguéla, 2010], which report that muscarinic activation in PCs leads to an initial SK-mediated hyperpolarization, followed by a more sustained and slow depolarization (Table 1, Figure 1). Interestingly, the same biphasic response can be induced by bath perfusion of muscarinic agonists in hippocampal interneurons [Heys et al., 2012, Heys and Hasselmo, 2012]. The mechanism by which this depolarization emerges has not been fully clarified yet, but some authors suggest the suppression of muscarinic-sensitive and voltage-dependent K^+ conductance termed the M current (I_m) or the activation of a non-specific cationic current both support the observed depolarization [McCormick and Prince, 1986, Krnjević, 2004]. In L5PCs, transient activation of M1-type mAChRs induces calcium release from IP_3 -sensitive intracellular calcium stores and subsequent activation of an apamin-sensitive, SK-type calcium-activated potassium conductance (Gulledge et al., 2007). Conversely, M4-mediated activation of a potassium conductance (Kir_3) in L4SS generates a persistent membrane hyperpolarization and induces suppression of neurotransmitter release (Table 1, Figure 1). The observed hyperpolarizing response is supported by a decrease in presynaptic calcium conductance, at synapses between L4PCs and also at synapses between L4PCs and L23PCs (see Table 3, Figure 2; [Eggermann and Feldmeyer, 2009]). Focal application of ACh onto the soma of L5PCs evokes a biphasic response in which a transient membrane hyperpolarization precedes a slower and longer-lasting depolarization. Pharmacological evidence suggests that this effect is mediated by M1 receptors. Compared with the pressure application of ACh, activation of cholinergic synapses with brief bursts provides relatively weak activation of mAChRs that often fails to affect the somatic membrane potential at rest (Hedrick and Waters, 2015). One possible interpretation of these results might be that synaptically released ACh activates first nAChRs and usually fails to activate mAChRs, whereas pressure ejection onto the soma recruits primarily mAChRs. Muscarinic activation modulates K^+ conductances [McCormick, 1992], but the reversal potential for K^+ is approximately -90 mV: mAChR activation, therefore, exerts a little effect at resting membrane potential. However, when a neuron is depolarized, the observable mAChR-mediated hyperpolarization and subsequent depolarization are larger. The reported biphasic effect affects both cortico-pontine (CPn) and commissural (COM) pyramidal neurons; however, COM neurons show a more pronounced inhibitory phase, while CPn neurons have a larger and longer-lasting depolarizing phase (Baker et al., 2018). While these effects have been characterized thoroughly in [Baker et al., 2018] deep-layers PCs, others report that ACh has limited ability to inhibit superficial PCs via changes in membrane potential [Gulledge et al., 2007].

Cortical inhibitory interneurons are, as well as PCs, a prominent target of cholinergic neuromodulation. The ways in which ACh modulates the dynamics of local interneurons have not been completely clarified yet, because the effects of BF cholinergic stimulation and bath application of cholinergic agonists (Table 1) strongly depend on the inhibitory cell-type. Exogenous application is unlikely to mimic accurately the spatiotemporal profile of ACh release from cholinergic axons, and furthermore, there seems to be no agreement within the neuroscientific community on which concentration of cholinergic agonists should be used to promote activation of the cholinergic receptors. The applied dose ranges from 10 to 100 micromolar across different experimental groups, and in other cases, it even spans the millimolar range. These discrepancies arise from the fact that to measure the physiological extracellular concentration of ACh is experimentally challenging, because of the prompt intervention of hydrolases in the synaptic cleft. Application of acetylcholinesterase inhibitors cannot be avoided, making it extremely difficult to detect physiological levels of ACh in the extracellular space. Moreover, while mAChR agonists have been extensively used and are known to generate a multitude of responses in cortical neurons, much fewer studies [Hedrick and Waters, 2015, Dasgupta et al., 2018] have discerned muscarinic responses evoked by endogenous ACh release (see Figures 1, 2). Cholecystokinin-immunoreactive (CCK^+) cells are affected heterogeneously by cholinergic agonists depending on their sizes. For example, small CCK^+ cells are promptly depolarized by cholinergic inputs, while bigger CCK^+ cells show a biphasic response comprising an initial hyperpolarization and a subsequent depolarization similarly to PCs (Kawaguchi, 1997). There is a general consensus [Gulledge et al., 2007, Kruglikov and Rudy, 2008, Poorthuis et al., 2014] that cholinergic modulation of fast-spiking PV positive (PV^+) interneurons does not produce any effect on membrane excitability (Table 1). However, evidence also shows the opposite. For example, [Alitto and Dan, 2013] report in their review that PV^+ interneurons are depolarized via muscarinic activation, but when mAChRs are blocked by antagonist application, the excitation is converted to inhibition; in turn inhibition of PV^+ cells is converted to excitation when nAChRs are blocked, suggesting that excitation and inhibition compete in the same population of PV^+ interneurons through the activity of the different receptors. The subpopulation of dendrite-targeting interneurons, that is identified as somatostatin (SST) expressing (SST^+) interneurons (MCs), can be depolarized by activation of mAChRs [Fanselow et al., 2008]. However, some studies report that only very few SST^+ interneurons display excitation or inhibition in response to BF stimulation and that the inhibitory cells displaying the strongest excitation by ACh are L1 and VIP^+ interneurons). Recent findings outlined by [Muñoz and Rudy, 2014] challenge these results. In their study, they claim that cholinergic modulation of SST^+ interneurons via M1 and/or M3 mAChRs provides a major excitatory drive to these cells dur-

ing whisking activity. VIP expressing interneurons are highly responsive to cholinergic inputs and show a mixed activation profile that is partially blocked by both nicotinic and muscarinic receptor antagonists [Kawaguchi and Kubota, 1997].

In summary, muscarinic activation has differential effects on membrane potential, based on which subtypes are expressed in a specific cell-type and in cellular compartments. These heterogeneous responses might play different roles in neocortical information processing: the initial hyperpolarizing phase observed in PCs and some CCK⁺ cells could be used to push the cell away from threshold, while the subsequent depolarization selectively augments inputs that are strong enough to reach threshold, therefore increasing the SNR, and at the same time promoting synchronization of neural activity. At the same time, the presynaptic inhibition of excitatory feedback could serve as a mechanism to prevent interference during the encoding of new stimuli and reduce top-down influences on perceptive processes. In addition, muscarinic receptors contribute to the generation of the gamma rhythm by inducing synchronized oscillations in both excitatory and inhibitory neurons [Heys et al., 2012]. Another class of receptors contributes to cholinergic signaling in the neocortex. Nicotinic receptors exert fast cortical actions, playing a key role in many cognitive processes [Dani and Bertrand, 2007], as described in the following section.

2.4.2 Nicotinic receptors

ACh is primarily regarded as a neuromodulator rather than a neurotransmitter in the CNS because its physiological effects have a latency of onset of tens of milliseconds to minutes [Van der Zee and Luiten, 1999]. This great variability in the response of cortical neurons to ACh stimulation originates from the fact that there are two main types of ACh receptor proteins. Neuronal nicotinic receptors (nAChRs) are ionotropic receptors which are composed of combinations of twelve different nAChR subunits: $\alpha 2$ to $\alpha 10$ and $\beta 2$, $\beta 3$, $\beta 4$. Each receptor is made of five subunits. It is generally assumed that nicotinic actions are fast and precise; however, the depolarization rate produced by the opening of the nicotinic channel can vary depending on the specific subunit composition. Because mAChR signaling acts through G-proteins, mAChR signaling might be expected to be slower than ionic nAChR signaling. However, homomeric ($\alpha 7$) nAChRs can also mediate slow responses, and the time course of muscarinic action may also vary widely, depending on the signal pathways involved [Muñoz and Rudy, 2014]. The nicotinic branch of the AChR family can be further divided into at least two classes, based on the affinity that their binding sites have for nicotine itself or the snake toxin α -bungarotoxin. At their simplest neuronal nAChRs are homomeric (constituted from five identical subunits) while the more complex forms are

heteromeric, composed of at least one α and one β subtype.

Binding studies using [3H]-nicotine have shown that high-affinity nAChR binding sites are very common for the human cerebral cortex, while autoradiographic labeling of nAChRs shows an inhomogeneous distribution over architectonically identified cortical areas of the rat brain, with highest concentrations in the medial PFC (mPFC) and generally frontal areas. As for mAChRs, the expression of different subunit combinations varies across layers and across cortical areas. Given the involvement of the cholinergic system in the treatment of tobacco addiction, many studies have been performed in the human brain. Most data on the distribution of nAChRs has been obtained from human autopsy tissue homogenates using techniques such as ligand binding, RT-PCR, immunoprecipitation, and Western blot. Currently-available nAChR agonists and antagonists used for receptor autoradiography are not subtype specific, although they act on nAChR subtypes with a distinct profile: labeling experiments carried out with different probes revealed that nAChRs are widely expressed in the cortex, both at the level of gray and white matter; many fibers show immunoreactivity at the neuropil level [Schröder, 1992]. Five α subunits (3–7) and three β subunits (2–4) are expressed in the human brain. The expression of $\alpha 4$ and $\beta 2$ subunits in the frontal cortex, parietal cortex, and temporal cortex shows a characteristic laminar distribution. Higher receptor binding is observed in layers 1, 3 and 5. These results are in agreement with the observed distribution of $\alpha 3$ and $\alpha 4$ mRNAs that are mostly found in PCs of layer 2/3 and layer 5 of the frontal cortex (Wevers, 2011). However, other studies report that the $\alpha 3$ mRNA is exclusively expressed in layer 4, while $\alpha 4$ subunit is moderately expressed in all layers (Radnikow and Feldmeyer, 2018). The $\alpha 7$ subunit is found mostly in layer 1–3 and 5 and is virtually absent in layer 4, while $\alpha 4$ and $\beta 2$ immunoreactive fibers were observed in layer 4 of the PFC [Sparks et al., 1998]. The $\alpha 2$ subunit is a characteristic feature of L5MCs that project to layer 1 and specifically target L5TTPCs [Hilscher et al., 2017]. The detection of nicotinic subunits is possible because of the existence of specific antisubunit-antibodies and the introduction of nAChR subunit-Cre mouse lines. Nevertheless, nicotinic receptors are made up of multiple subunits and are either homomeric or heteromeric. The most abundant receptor subtypes in the neocortex are the homomeric receptor $\alpha 7$ and the heteromeric $\alpha 4\beta 2$ channel (which is often associated with the regulatory subunit $\alpha 5$; [Radnikow and Feldmeyer, 2018]). Nicotinic receptors can be activated both via volume transmission and fast synaptic activity [Dani and Bertrand, 2007, Hedrick and Waters, 2015, Hay et al., 2016].

Presynaptic localization

None of the studies mentioned above investigates the precise cellular localization of cholinergic receptors, which is crucial in determining the outcome of the response. This is especially true for nAChRs, because their activation directly leads to a cation influx into the cell, and immediately results in a voltage change in the underlying compartment. nAChRs are expressed on glutamatergic inputs to layer 5, mostly contacting layer 5 interneurons and L5/L6 PCs. L5PCs and L6PCs are modulated by $\alpha 7$ and $\beta 2$ nAChRs, respectively, while L23PCs and glutamatergic inputs to these cells do not contain nAChRs. Interneurons across layers contain mixed combinations of nAChRs [Poorthuis et al., 2014]. Some subtypes, such as $\alpha 7$ homomeric receptors, are preponderantly expressed in presynaptic areas, whereas heteromeric receptors are more expressed on cell bodies and main dendrites [Bertrand, 2010]. Cholinergic axons that diffusely innervate the cortex are thought to make *en passant* connections in the area of the main dendrite of the PCs from layer 5 and 6, therefore causing a volume release of ACh. Pre-synaptically, nAChRs generally increase the release of GABA and glutamate [Dani and Bertrand, 2007]. However, both nAChR and mAChRs can reduce EPSPs by acting pre-synaptically [Levy et al., 2008].

Postsynaptic localization

The distribution of nAChRs at the light and electron microscopic level was studied in the human cerebral cortex using anti-nAChR monoclonal antibody (mAb) WF-6, which is not subunit selective (Schröder et al., 1990): nAChR immunoreactivity revealed a pattern for the frontal and temporal cortex that was very similar to that obtained with the auto-radiography. In the frontal cortex, in situ hybridization techniques display numerous labeled neurons, mostly PCs bearing the $\alpha 7$ mRNA in the cell body and in the apical dendrite. In the motor cortex, many PCs showed signals in the proximal part of their apical dendrite. As reported by [Schröder et al., 1989] and [Schröder, 1992] nAChR localization is predominant in L23 and L5 PCs; a few nAChR-expressing fusiform cells can be detected in layer 4 and 6. Many PCs show nAChRs on basal dendrites that originate in layer 5, cross the superficial layers of the cortex perpendicular to the pial surface, and branch between layers 1 and 2. Immuno-precipitate is detectable both in cell bodies and in their apical dendrites, in branches of various diameters, and in the PSD of synaptic junctions. In a double-labeling approach conducted in the temporal cortex, it was further demonstrated that PV⁺ interneurons express $\alpha 4$ and $\alpha 7$ subunit protein (Wevers, 2011). Double-labeling studies have shown that at least 30% of cortical neurons contain both nAChR and mAChR proteins, the majority of these being PCs. In the human cortex, nicotinic immuno-staining in individual neurons appears generally compara-

Cell type	Receptor	Effect	Area	Technique—Reference
L5 PC	$\alpha_4\beta_2$ (soma and main dendrite)	Medium depolarization	Mouse PMC/V1/PFC	Optogenetics (Hedrick and Waters, 2015)
	$\alpha_4\alpha_5$	Depolarization Persistent spiking (starting from subthreshold)	Mouse PMC/V1/PFC	Optogenetics (Hedrick and Waters, 2015)
L6 PC	$\alpha_4\alpha_5$ (soma and main dendrite)	Depolarization	Mouse PMC/V1/PFC	Optogenetics (Hedrick and Waters, 2015)
	$\alpha_4\beta_2$	Depolarization	Rat PFC (p7–p27)	Kassam et al. (2008; bath application of 10 μ M ACh to 1 mM)
L1 NGFC	Nicotinic (non- α_7)	Depolarization (from RP) Suppression of activity (from subthreshold)	Rat SSC	Iontophoretic application or bath application of 100 μ M ACh (Brombas et al., 2014)
L1 BC	Nicotinic	Suppression of activity (at low levels of cortical desynchronization)	Mouse V1	<i>In vivo</i> 2-photon imaging (Alitto and Dan, 2013)
L1 INs	Nicotinic	Fast depolarization (from RP)	Rat SSC	100 μ M ACh focally applied (Christophe et al., 2002) and (Gulledge et al., 2007)
NBC	Nicotinic	Depolarization	Rat SSC	100 μ M ACh focally applied (Gulledge et al., 2007)
BPC	Nicotinic	Depolarization	Rat SSC	100 μ M ACh focally applied (Gulledge et al., 2007)
DBC	Nicotinic	Depolarization	Rat PFC	10 μ M CCh or 3 μ M muscarine bath application (Kawaguchi, 1997)
L23 MC	Nicotinic	Depolarization	Mouse V1	1 μ M/10 mM ACh application (Chen et al., 2015)
	Nicotinic	Depolarization	Rat SSC	Optogenetics (Dasgupta et al., 2018)
	$\alpha_4\beta_2$	Depolarization	Mouse S1 and mPFC	Optogenetics or 1 mM ACh bath-application (Obermayer et al., 2018)
L23 BC	Nicotinic	Some are depolarized Some are hyperpolarized	Mouse V1	<i>In vivo</i> 2-photon imaging (Alitto and Dan, 2013)
L23 CHAT+ BPC	$\alpha_4\beta_2$	Depolarization	Mouse SSC (P20–P40)	Optogenetics (Arroyo et al., 2012)
L23 BPC	$\alpha_4\beta_2$ and α_7	Depolarization	Mouse and rat SSC	Optogenetics (Arroyo et al., 2012) and (Dasgupta et al., 2018); 100 μ M ACh focally applied (Gulledge et al., 2007)
L5 MC	$\alpha_4\beta_2$	Depolarization	Mouse S1 and mPFC	Optogenetics or 1 mM ACh bath-application (Obermayer et al., 2018)

The table links the distribution and localization (when known, in brackets) of nicotinic receptors across neocortical cell types, with respect to cortical layers, with the effect of their activation. The effect of receptor activation is represented in terms of variation of membrane potential. Age of the specimen is given in brackets, when known. When biphasic effects occur, they are listed as multiple effects. Inclusion criteria for the listed studies comprise: (1) recordings performed in the rodent neocortex, (2) knowledge of the morphological type involved and (3) knowledge of the receptor subtype involved in the response. Abbreviations: PC, pyramidal cell; SS, spiny-stellate cell; IN, interneuron; MC, Martinotti cell; BC, basket cell; DBC, double-bouquet cell; NGFC, neurogliaform cell; BPC, bipolar cell; NBC, nest basket cell; RS, regular spiking. PMC, primary motor cortex; V1, primary visual area; PFC, prefrontal cortex; SSC, somatosensory cortex; ACh, acetylcholine; CCh, carbachol; RP, resting potential; NR, not responsive.

Figure 2.2: Table 2 links the distribution and localization (when known, in brackets) of muscarinic receptors across neocortical cell types, with respect to cortical layers, with the effect of their activation. The effect of receptor activation is represented in terms of variation of membrane potential. Age of the specimen is given in brackets, when known. When biphasic effects occur, they are listed as multiple effects. Inclusion criteria for the listed studies comprise: 1) recordings performed in the rodent neocortex, 2) knowledge of the morphological type involved and 3) knowledge of the receptor subtype involved in the response. Abbreviations: PC, pyramidal cell; SS, spiny stellate cell; IN, interneuron; MC, Martinotti cell; BC, basket cell; DBC, double bouquet cell; NGFC, neurogliaform cell; BPC, bipolar cell; NBC, nest basket cell; RS, regular spiking. PMC, primary motor cortex; V1, primary visual area; PFC, prefrontal cortex; mPFC, medial prefrontal cortex; EC, entorhinal cortex; SSC, somatosensory cortex; ACh, acetylcholine; CCh, carbachol; RP, resting potential; NR, not responsive

ble to that seen in the rodent model [Schröder et al., 1989, Schröder, 1992]: as in the rat occipital cortex, nAChRs can be detected on the cell bodies and dendrites of L2/3 and L5 PCs. Most studies agree that nAChRs are preferentially found in infragranular layers, mostly at the level of L5 and L6 PCs, but also at the level of inhibitory interneurons; CB-immunoreactive neurons, as well as PV⁺ neurons all express nAChRs, while that is not true for CR-immunoreactive neurons [Coppola and Disney, 2018]; furthermore, nAChRs are expressed at the level of layer 2/3 as well, both in PC bodies and in the apical dendrites of deeper-layer placed cells. However, only a small subset of layer 2/3 excitatory neurons and no layer 4 neurons express nAChRs; layer 6 expression profile can be set apart from the rest, given that these neurons predominantly express the slowly desensitizing heteromeric $\alpha 4\beta 2$ channel [Radnikow and Feldmeyer, 2018].

The distribution of nAChRs and the subunits combination, therefore, depends on cell-types, laminar position and on the cortical area studied, similarly to mAChRs; nowadays the possibility of systematically studying the distribution profile of cholinergic receptors has greatly increased, due to the advancement in the production of anti-subunit-specific antisera and to the development of better immunoprecipitation and ligand binding techniques. Such studies exist and are quite informative as regards, for instance, the striatum [Zoli et al., 2002], but a comprehensive and detailed investigation of the expression of subunits in the neocortex is still lacking. Nicotinic activation prevalently modulates the excitability of deep cortical layers: in the next section, we move on and explore the contribution of nicotinic stimulation to local circuit properties and examine studies that investigated the involvement of the nicotineric system in the modulation of neocortical activity.

Regulation of neuronal and synaptic physiology

Even though nAChRs are predominantly expressed pre-synaptically, where their activation modulates neurotransmitter release through calcium influx or terminal depolarization [Nashmi and Lester, 2006], there is evidence that nAChRs may also influence post-synaptic signaling and that these effects vary based on the subcellular localization of the receptor (Tables 2, 3). nAChRs expressed on distal dendrites are thought to cause the generation of fast excitatory post-synaptic potentials since activation of nAChRs on distal apical dendrites promotes PC depolarization and leads to an increase in action potential firing. On the contrary, activation of nAChRs on the proximal apical dendrites (closer to the cell body) reduces membrane impedance and shunts signal incoming from the apical tuft: when the nAChRs opens, the membrane resistance of the PC decreases and signals incoming from the apical dendrites get attenuated [Dani and Bertrand, 2007].

Connection type	Receptor	Effect	Area	Technique—Reference
L5 PC-L5 PC	Muscarinic	Reduction in depression rate of consecutive EPSPs	Rat SSC	Bath application of 50 μ M ACh (Tsodyks and Markram, 1997)
	M1 (perisomatic)	Enhancement of EPSCs	Rat SSC (p14–p16)	1–10 μ M ACh local puff (Núñez et al., 2012)
	M2 (basal dendrites)	Reduction of IPSCs	Rat SSC (p14–p16)	50–100 μ M ACh local puff (Núñez et al., 2012)
	Nicotinic	Increase in EPSPs	Rat SSC (p14–p16)	1–10 μ M ACh local puff (Núñez et al., 2012)
L5 PC-L5 MC	Nicotinic heteromeric	Decrease in onset delay, increase in time course; no change in EPSP size	Mouse S1 and mPFC	Optogenetics or 1 mM ACh bath-application (Obemayer et al., 2018)
L4 PC-L4 PC	M4	Reduction in first EPSP amplitude	Rat SSC	Bath application of 100 μ M ACh (Eggermann and Feldmeyer, 2009)
L4 SS-L4 SS				
L4 PC-L23 PC	M4	Reduction in first EPSP amplitude	Rat SSC	Bath application of 100 μ M ACh (Eggermann and Feldmeyer, 2009)
L23 PC-L23 PC	M1/M3	Reduction in EPSC amplitude	Rat A1 (p21–p28)	Bath application of 10 μ M oxotremorine or muscarine (Alzori et al., 2009)
	Muscarinic (apical dendrite)	Reduction in EPSP amplitude	Rat PFC	Iontophoretic application of 0.05 M muscarine (Vidal and Changeux, 1993)
	Nicotinic (apical dendrite)	Increase in EPSPs	Rat PFC	Iontophoretic application of 0.05 M muscarine (Vidal and Changeux, 1993)
TC fibers-L4 PC	Muscarinic	Increase in EPSP depression rate	Rats and mice TC slice (p21–p28)	Bath application of 5–10 μ M muscarine (Sli et al., 1997)
CHAT+ fibers—L4 PC	Muscarinic	IPSC	Mouse TC slice (p12–p16)	Optogenetic activation (Dasgupta et al., 2018)
L23 PC-L23 MC	Nicotinic	Increase in EPSPs	Mouse SSC	Bath application of 20 μ M CCh (Urban-Ciecko et al., 2018) and optogenetics
	Nicotinic heteromeric	No change in EPSP size	Mouse S1 and mPFC	Optogenetics or 1 mM ACh bath-application (Obemayer et al., 2018)
L1 NGF-L23 PC	M1 (perisomatic)	Connection is silenced (L23 PC is disinhibited)	Rat SSC (p24–p31)	Iontophoretic application or bath application of 100 μ M ACh (Brombas et al., 2014)
	Nicotinic (non $\alpha 7$)	Connection is silenced	Rat SSC (p24–p31)	Iontophoretic application or bath application of 100 μ M ACh (Brombas et al., 2014)
L23 BC-L5 PC	Muscarinic	Reduction in IPSPs amplitudes (connection is silenced)	Mouse SSC	Bath application of 10 μ M muscarine (Kruglikov and Rudy, 2008)
L5 BC-L5 PC	M2/M4	Reduction in u-IPSC amplitude	Mouse SSC	Bath application of 10 μ M muscarine (Kruglikov and Rudy, 2008)
	Muscarinic	Reduction in u-IPSC amplitude	Rat insular cortex	Bath application of 10 μ M CCh (Yamamoto et al., 2010)
L5 MC-L5 PC	Nicotinic heteromeric	Decrease in onset delay, no change in IPSP size	Mouse S1 and mPFC	Optogenetics or 1 mM ACh bath-application (Obemayer et al., 2018)
	Nicotinic	Increase in IPSP size	Mouse A1	Bath application of 10 μ M CCh (Hiltscher et al., 2017)
L5 BC-L5 BC	Muscarinic	Decrease in IPSCs amplitudes	Rat insular cortex	Bath application of 10 μ M CCh (Yamamoto et al., 2010)
L5 RS IN-L5 PC	Muscarinic	Decrease in IPSCs amplitudes	Rat insular cortex	Bath application of 10 μ M CCh (Yamamoto et al., 2010)
L5 BC-L5 RS IN	Muscarinic	Increase in first IPSCs amplitudes	Rat insular cortex	Bath application of 10 μ M CCh (Yamamoto et al., 2010)
L5 RS IN-L5 RS IN	Muscarinic	Increase in first IPSCs amplitudes	Rat insular cortex	Bath application of 10 μ M CCh (Yamamoto et al., 2010)

The table links the distribution and localization (when known, in brackets) of nicotinic and muscarinic receptors across neocortical cell types, with respect to cortical layers, with the effect of their activation on synaptic dynamics. Effect is represented in terms of increase or decrease in PSP/EPSC size. Age of the specimen is given in brackets, when known. Inclusion criteria for the listed studies comprise: (1) recordings performed in the rodent neocortex; (2) knowledge of the pre and post synaptic morphological types involved; and (3) knowledge of the receptor subtype involved. Abbreviations: PC, pyramidal cell; SS, spiny stellate cell; IN, interneuron; MC, Martinotti cell; BC, basket cell; DBC, double bouquet cell; NGFC, neurogliaform cell; BPC, bipolar cell; NBC, nest basket cell; RS, regular spiking; A1, primary auditory area; PFC, prefrontal cortex; SSC, somatosensory cortex; TC thalamo-cortical; ACh, acetylcholine; CCh, carbachol; EPSP, excitatory post-synaptic potential; IPSP, inhibitory post-synaptic potential; EPSC, excitatory post-synaptic current; IPSC, inhibitory post-synaptic current.

Figure 2.3: Table 3 links the distribution and localization (when known, in brackets) of nicotinic and muscarinic receptors across neocortical cell types, with respect to cortical layers, with the effect of their activation on synaptic dynamics. Effect is represented in terms of increase or decrease in PSP/PSC size. Age of the specimen is given in brackets, when known. Inclusion criteria for the listed studies comprise: 1) recordings performed in the rodent neocortex, 2) knowledge of the pre and post synaptic morphological types involved and 3) knowledge of the receptor subtype involved. Abbreviations: PC, pyramidal cell; SS, spiny stellate cell; IN, interneuron; MC, Martinotti cell; BC, basket cell; DBC, double bouquet cell; NGFC, neurogliaform cell; BPC, bipolar cell; NBC, nest basket cell; RS, regular spiking; A1, primary auditory area; PFC, prefrontal cortex; SSC, somatosensory cortex; TC thalamo cortical; ACh, acetylcholine; CCh, carbachol; EPSP, excitatory post synaptic potential; IPSP, inhibitory post synaptic potential; EPSC, excitatory post-synaptic current; IPSC, inhibitory post synaptic current

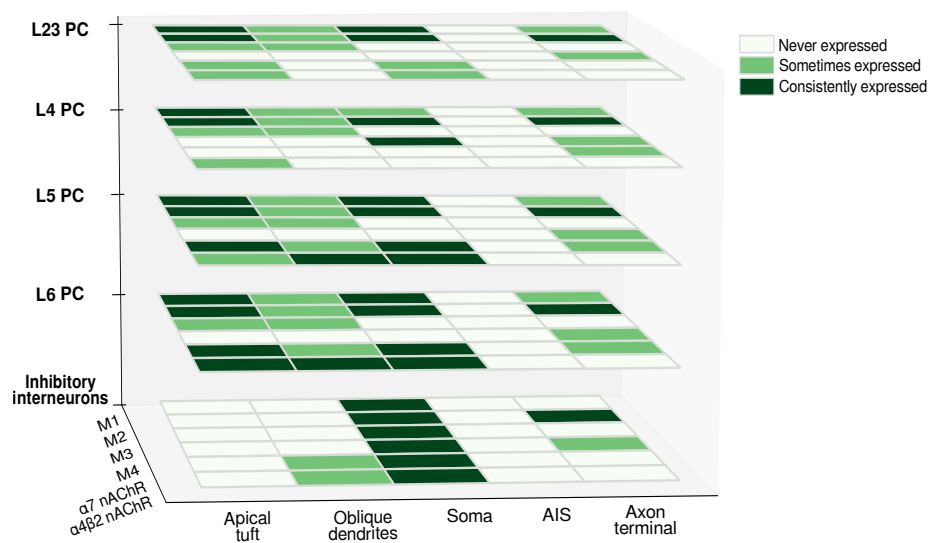


Figure 3

Figure 2.4: Differential expression of cholinergic receptors in various neuronal compartments across cell-types. Heatmap matrices show the occurrence of cholinergic receptor subtypes at the level of different cell-types. The presence of a given subtype in a cellular compartment is classified as consistently expressed (consistent findings across experimental studies), sometimes expressed (evidence of its presence is only partial) and never expressed (presence of a given subtype is undetectable). Abbreviations: PC, pyramidal cell; M1, M2, M3, M4, muscarinic cholinergic receptors 1–4; nAChR, nicotinic acetylcholine (ACh) receptor.

Optogenetic activation of cortical cholinergic input generates an increase in membrane excitability (Table 2) mediated by nAChRs and promotes spiking in L5PCs [Hedrick and Waters, 2015]. When the stimulation is paired with additional depolarization, spiking activity becomes persistent and can be blocked by BAPTA application, suggesting that the observed depolarization is mediated by intracellular Ca^{++} transients. As suggested by kinetic analysis it is likely that non- $\alpha 7$ nAChRs determine this response. The depolarizing response spans all layers, but occurs with laminar and regional differences; additionally, the effect of the depolarization can be moderate and transitory or pronounced and persistent depending on the cell membrane potential. Although the modulatory effect was found to be stronger in deeper layers, the authors report that it was similar in M1, V1 and prefrontal (PF) cortices. The preferential modulation of deep neocortical layers is likely to influence the flow of excitation occurring throughout the neocortex that originates in layer 4 and then propagates to the superficial layers, whose role is to modify the output of layer 5. Altogether this study showed that nAChR activation increases the excitability of neocortical PCs; in the light of previous evidence that $\alpha 4$ and $\alpha 5$ subunits are highly expressed in layer 6 [Tribollet et al., 2004], and nAChR-mediated responses in layer 6 of the PFC have already been reported by many studies [Kassam et al., 2008, Bailey et al., 2010, Poorthuis et al., 2014], the authors suggest that the presence of $\alpha 4$ and $\alpha 5$ -mediated PSPs could be a characteristic feature of L6PCs across neocortical regions (see Table 2, Figure 1). Pyramidal-to-PCs connections in layer 5 can be potentiated by using a spike-timing-dependent-plasticity (STDP) protocol. Bath-application of $10\text{ }\mu\text{M}$ (or 300 nM) nicotine impairs L5PC to L5PC potentiation and favors the induction of LTD. When monitoring spontaneous synaptic events, application of nicotine increases the frequency and amplitude of sEPSCs. Evoked excitatory post-synaptic currents (EPSCs) behave differently and are reduced in amplitude by nicotine. However, puffing nicotine directly on PCs fails to elicit an inward current, and application of gabazine prevents the de-potentiation. Therefore, the effects of nicotine on L5PC to L5PC synapses should be attributed to an enhancement of GABAergic transmission, rather than the direct activation of a PCs [Couey et al., 2007]. nAChRs are known to be distributed throughout the dendritic trees of cortical PCs [van der Zee et al., 1992], but a comprehensive mapping of cholinergic synapses apposition remains elusive. To provide concomitant information on receptor localization while recording electrical responses more researchers should apply the strategy used by [Hedrick and Waters, 2015], who measured nicotinic PSPs during restricted illumination of the slice: illumination of the tuft dendrites failed to evoke a nicotinic PSP at the soma and therefore the authors concluded that nAChRs that contribute to the somatic depolarization are likely to be within $300\text{ }\mu\text{m}$ of the soma and many are probably located in the proximal $50\text{ }\mu\text{m}$ of the apical and basal arbor. This technique sheds light on the

compartmental origin of the observed response and it is immensely useful to causally link the distribution of cholinergic receptors and their physiological role. A subsequent investigation should combine this strategy with pharmacological inactivation of specific receptor subunits and provide further proof that PCs responses to cholinergic inputs in different layers are mediated by specific receptor subunits and that their distribution profile is greatly involved in determining the outcome of neural computations.

Although nAChRs are mainly found on PCs, there is extensive evidence that nAChRs are expressed on the membrane of cortical interneurons (Table 2), such as MC, chandelier cells (ChCs) and basket cells (BCs), where they contribute to the modulation of GABAergic signaling [Couey et al., 2007, Wevers, 2011]. The subpopulation of serotonin receptor 5-HT_{3a}R expressing GABAergic interneurons is depolarized by ACh via nAChRs [Gulledge et al., 2007, Poorthuis et al., 2013]; this embryologically distinguished subpopulation, that accounts for about 30% of the total number of cortical inhibitory interneurons, is heterogeneous and includes all the VIP⁺ interneurons, as well as the VIP⁻ neurogliaform cells (NGCs; [Rudy et al., 2011]). VIP⁺ interneurons show a mixed activation profile in which both nicotinic and muscarinic receptors are involved (Figure 1; [Kawaguchi and Kubota, 1997]). Prominent nAChRs expression is a hallmark of layer 1 inhibitory interneurons both in rodents and humans [Letzkus et al., 2011, Alitto and Dan, 2013] and endogenous cholinergic release is known to rapidly recruit this receptor subpopulation during locomotion and attentive processes. These fast, nicotinic responses are mediated by $\alpha 7$ and $\beta 2$ containing receptors [Poorthuis et al., 2018]. When at rest, all layer 1 interneurons are depolarized via nicotinic activation (Figure 1, Table 2); however, when these interneurons are engaged in repetitive firing, ACh inhibits the activity of L1 NGCs [Brombas et al., 2014]. Conversely, single bouquet cells (SBCs) are activated by ACh in the regime of repetitive firing [Jiang et al., 2013]. Layer 1 interneurons responses are abolished by application of nAChR antagonists (Figure 1; [Christophe et al., 2002]). ACh enhances the activation of neocortical deep-layers PCs by ascending thalamic inputs via mAChR-mediated depolarization and subsequent enhanced glutamate release from thalamocortical terminals in layer 4 [Gil et al., 1997, Metherate, 2004, Disney et al., 2007], but it also releases inhibition on superficial layers PCs. There is extensive evidence that ACh mediates activation of layer 1 and layer 2/3 non-fast spiking PV⁻ cortical interneurons via non- $\alpha 7$ nAChRs. These interneurons, in turn, inhibit MCs and BCs that directly target PCs: nAChR-mediated inhibition of superficial interneurons reduces inhibition of superficial PCs [Gulledge et al., 2007, Arroyo et al., 2012, Brombas et al., 2014]. Photostimulation of ChAT⁺ neurons in the BF evokes a prolonged disynaptic inhibition in PCs; pharmacological manipulation of the response suggests

that it is supported by non- $\alpha 7$ mediated excitation of specific interneurons subtypes. This finding indicates that nicotinic cholinergic input originating from BF fibers is also comprised of a slow component. The observed delayed barrage of inhibitory post-synaptic current (IPSC) in L23PCs exhibits a long latency (of about 26 ms) characteristic of dysynaptic inhibition. Layer 1 and layer 2/3 inhibitory interneurons, and in particular in late-spiking cells and L23 ChAT⁺ bipolar cells are responsible for this phenomenon [Arroyo et al., 2012]. In agreement with previous reports [Poorthuis et al., 2014] fast-spiking cells such as BCs and ChCs do not exhibit EPSPs in response to optogenetic stimulation of ChAT⁺ BF neurons, but rather respond similarly to PCs and are swamped by an IPSC barrage as well. While layer 1 and layer 2/3 late spiking cells (LS) exhibit both a fast and a slow response, L23 ChAT bipolar cells display only a slow response. This study demonstrates that the fast and slow components are mediated by $\alpha 7$ receptors and non- $\alpha 7$ receptors, respectively, and that non- $\alpha 7$ receptor-mediated excitation elicits action potentials in cortical interneurons that in turn produce a delayed and prolonged wave of inhibition in L23PCs and FS cells. One proposed explanation for the slow response is that it may arise from a cholinergic bulk transmission and that it may sustain the high metabolic demand of processes such as attention and memory [Cauli et al., 2004].

Cortical ChAT⁺/VIP⁺ interneurons have been shown to dilate local microvasculature to increase blood supply during periods of elevated neuronal activity [Kocharyan et al., 2008] during the execution of memory and attention tasks, following electrical BF stimulation. The fast component of the cholinergic response may also be implicated in the emergence of a broader phenomenon like synchronized neuronal activity; it has been shown that LS cells are connected via gap junctions, and this fast response may thus play a fundamental role in the emergence of network oscillations that sustain plasticity and attention mechanisms. [Couey et al., 2007] realized that the effect of nicotine on L5PC to L5PC connections is mostly due to an enhancement of GABAergic transmission, and they decided to dissect the effects of nicotine on three different interneurons types. First, they looked at the activity of FS cells in layer 5, and observed no effect when adding nicotine to the bath; later they stained the cells for certain neuropeptides and several nAChR subunits and found an extremely low amount of mRNA coding for nicotinic subunits in FS cells, which might explain their unresponsiveness. Once again, another piece of evidence emerges confirming that (putative) BCs have a tendency not to respond to the application of cholinergic agonists. The authors identified another type of interneuron as a regular-spiking-non-PC (RSNPC), and observed a fast inward current after application of nicotine. LTS cells (putative MC) showed an even bigger inward current response; in both cell-types the most abundantly stained

nicotinic subunit was $\alpha 4$, but $\beta 2$ and $\alpha 7$ were also present. In this study, nicotine application increases the frequency and amplitude of spontaneous EPSCs in putative BCs and MCs; as for putative ChC (RSNP) a decrease in the frequency, but not the amplitude of sEPSCs can be observed [Couey et al., 2007]. Pyramidal to SST⁺ interneurons neocortical connections are relatively weak, but local excitatory input to SST neurons is selectively enhanced during cholinergic modulation of network activity. In a recent 2018 study, it was shown that endogenous ACh release activates presynaptic nAChRs and boosts glutamatergic input in a target-cell specific manner [Urban-Ciecko et al., 2018]. Thus, there is evidence that local excitatory input to SST neurons is selectively enhanced during nicotinic modulation of network activity (Table 2, Figure 2).

In a recent study by [Obermayer et al., 2018] examined PC-MC-PC disynaptic connections in both layer 2/3 and layer 5 and found that the typical delayed disynaptic inhibitory response in the post-synaptic PC is faster and stronger when cholinergic inputs are activated optogenetically, or by means of 1 mM ACh bath application. When looking at the activity of a single MC, they observed that ACh inputs lead to a significant decrease of the onset delay of AP firing and increases the number of APs fired in MCs, which can account for the earlier onset and prolonged duration of disynaptic inhibition. This effect was abolished by application of 10 μM DH β E demonstrating that it is mediated by heteromeric nicotinic receptors (Table 2, Figure 2). However, when they recorded from synaptically connected PC-MC pairs during concurrent activation of cholinergic fibers, they could only observe an increase in the membrane depolarization level, but not in EPSP sizes. The same effect was found in MC-PC connections, and this as well was confirmed to be nicotinic in nature, contradicting the result obtained by Urban-Ciecko and others and others. The setups of the two experiments are comparable: both studies were performed in the adult mouse somatosensory cortex. However, the first remarkable difference lies in the nature of the cholinergic input used in the two experiments: while [Obermayer et al., 2018] used bath-application of 1 mM ACh and optogenetic activation, [Urban-Ciecko et al., 2018] decided to record activity in the presence of 20 μM CCh, a non-hydrolyzable analogue of ACh. Not only the two concentrations differ by two orders of magnitude, but the two cholinergic agonists work in fundamentally different ways. While ACh is almost immediately hydrolyzed by the cholinesterase in the synaptic cleft (within a few milliseconds), carbachol has a much more prolonged effect [Katz and Miledi, 1973]. Nevertheless, the results obtained by bath-application of ACh are in agreement with the results achieved by optogenetic activation of the cholinergic system, which is supposed to be a more physiological way of stimulating cholinergic release [Obermayer et al., 2018]. Interestingly, optogenetic acti-

variation of cholinergic inputs did not affect the typical fast disynaptic post-PC response mediated by BCs, which provides yet another example of how BCs tend to be unresponsive to cholinergic release in both layer 2/3 and layer 5, or more generally show a more heterogeneous response profile to ACh inputs [Obermayer et al., 2018]. This could be explained by the lack of a precise morphological identification of various subtypes of BCs, which could express cholinergic receptors in different subcellular locations or in a different amount, and therefore show differential responses to ACh inputs. These findings indicate that subcortical neuromodulatory projections recruit nicotinic receptors to alter network function through increased inhibition and provide a potential mechanism by which attention controls the gain of local circuits.

2.5 Nicotinic and muscarinic kinetics

What are the receptor affinities to various agonists and can this be related to the actual amount of nicotinic modulation? The relative activation of receptors vs. the concentration of agonist has been measured (Table 4). Muscarine reversibly reduces Ca^{2+} currents in a dose-dependent manner. The modulation is rapid, with an onset time constant of 1.2 s. A slowly developing component of the modulation also is observed, with a time constant of 17 s. Under elevated Ca^{2+} conditions, the fast component is due to a reduction in both N- and P-type calcium currents, whereas the slow component involves L-type current [Stewart et al., 1999]. Receptor properties such as conductance, open time, and sensitivity to ACh depend on the nicotinic subunit composition (Table 4). $(\alpha 4)_2(\beta 2)_3$ nAChRs are sensitive to micromolar scale changes, while $(\alpha 7)_5$ receptors have a half-maximal sensitivity of more than a hundred micromolar. Extracellular choline is normally 3–5 μM but can attain 20 μM in some pathological cases. However, ACh reaches the millimolar range at the site of release [Alkondon and Albuquerque, 2004]. Responses mediated by $\alpha 7$ nAChRs are short-lasting, whereas those mediated by $\alpha 4\beta 2$ nAChRs are long-lasting. This is because the mean open time of $\alpha 7$ nAChRs is shorter than that of $\alpha 4\beta 2$ nAChRs. Also, $\alpha 7$ nAChRs desensitize much faster than $\alpha 4\beta 2$ nAChRs [Alkondon et al., 1999]. An interesting hypothesis was put forward by [Albuquerque et al., 2000]. $\alpha 7$ but not $\alpha 4\beta 2$ nAChRs can be fully activated by choline [Nguyen et al., 1995, Alkondon et al., 1999]. Choline and acetate are the products of hydrolyzation of synaptically released ACh by ACh-esterase in the synaptic cleft. This process occurs quickly, but reuptake of choline into presynaptic terminals is slow. Therefore, the ACh concentration in the synaptic cleft should decay rapidly, with only low levels of diffusing ACh reaching peri-synaptic sites. But choline levels should rapidly rise in the synaptic cleft with high levels of diffusing choline reaching peri-synaptic

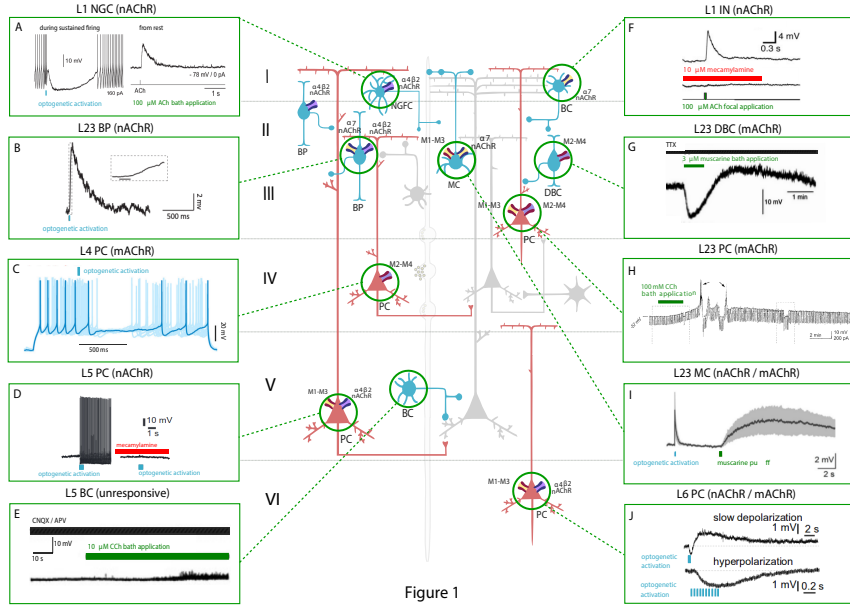


Figure 1

Figure 2.5: Effect of nicotinic acetylcholine receptors (nAChRs) and muscarinic ACh receptors (mAChRs) activation on the membrane potential of various neocortical cell types. The central schema represents the main cell types in the neocortex. Excitatory neurons are shown in red and inhibitory GABAergic neurons are shown in blue. The electrophysiological responses to the optogenetic activation of cholinergic fibers (in light blue) or the application of a cholinergic agonist (shown in green) or antagonist (shown in red) of each cell type are depicted in the inserts. Timing of cholinergic manipulation is shown as a vertical or horizontal bar. Muscarinic and nicotinic cholinergic receptors associated with the observed response, when known, are shown as four main subtypes: M1-M3-M5 like receptors (yellow and red), M2-M4 like receptors (violet and red), $\alpha 4\beta 2$ heteromeric nAChRs (violet and blue) and $\alpha 7$ homomeric nAChRs (yellow and blue). All shown experimental traces reflect studies listed in Tables 1, 2. Selected traces were recorded in sensory areas of the rodent neocortex. Inclusion criteria for the experimental traces comprise knowledge of the cell-types and the receptor subtype (nicotinic or muscarinic) involved in the electrophysiological response. Abbreviations: PC, pyramidal cell; SS, spiny-stellate cell; IN, interneuron; MC, Martinotti cell; BC, basket cell; DBC, double-bouquet cell; NGFC, neurogliaform cell; BPC, bipolar cell. Reproduced and adapted from: (left, top to bottom): (A). [Brombas et al., 2014]; (B) [Arroyo et al., 2012]; (C) [Dasgupta et al., 2018]; (D) [Hedrick and Waters, 2015]; (E) [Kawaguchi and Kubota, 1997] (Right, top to bottom): (F) [Gulledge et al., 2007]; (G) [Kawaguchi, 1997]; (H) [Shalinsky et al., 2002]; (I) [Dasgupta et al., 2018]; (J) [Hedrick and Waters, 2015]. For more exhaustive information on agonist concentration, species and cortical area examined, see Tables 1, 2.

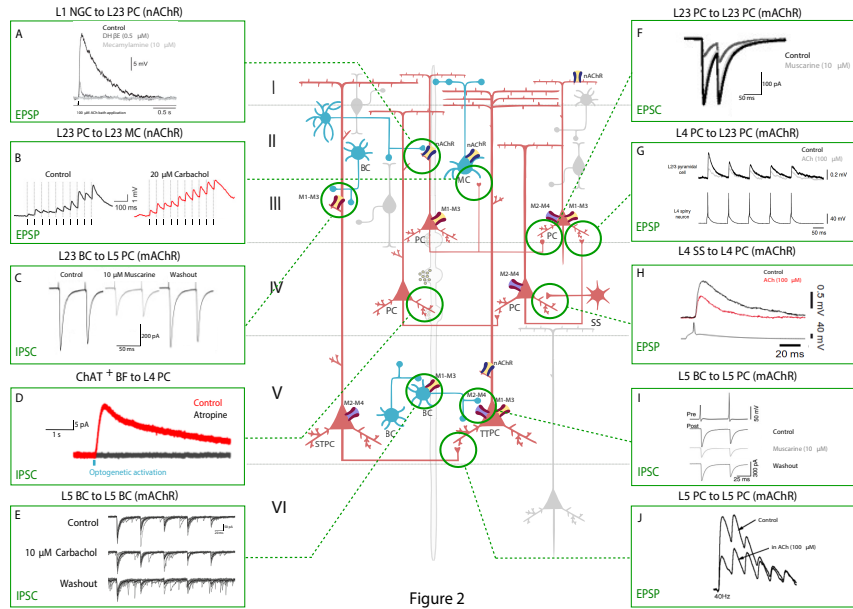


Figure 2

Figure 2.6: Effect of nAChRs and mAChRs activation on neocortical synaptic dynamics. The central schema represents the main neocortical cell types and their synaptic connections. A fiber of subcortical provenance associated with cholinergic boutons is also shown. Excitatory neurons are shown in red and inhibitory GABAergic neurons are shown in blue. The electrophysiological responses to the application of a cholinergic agonist or antagonist or to basal forebrain (BF) optical stimulation are depicted in the inserts. Panels show the modulation of synaptic dynamics in terms of increase or decrease in PSP/PSC size. Muscarinic and nicotinic cholinergic receptors associated with the observed response, when known, are shown as four main subtypes: M1-M3-M5 like receptors (yellow and red), M2-M4 like receptors (violet and red), $\alpha 4 \beta 2$ heteromeric nAChRs (violet and blue) and $\alpha 7$ homomeric nAChRs (yellow and blue). All shown experimental traces reflect studies listed in Table 3. Selected traces were recorded in sensory areas of the rodent neocortex. Inclusion criteria for the experimental traces comprise knowledge of the pre and postsynaptic cell-types and the receptor subtype (nicotinic or muscarinic) involved in the response. Abbreviations: PC, pyramidal cell; TTPC, thick tufted pyramidal cell; STPC, slender tufted pyramidal cell; SS, spiny-stellate cell; MC, Martinotti cell; BC, basket cell; NGFC, neurogliaform cell; BPC, bipolar pyramidal cell; IPC, inverted pyramidal cell. Reproduced and adapted from: (left, top to bottom): (A) [Brombas et al., 2014]; (B) [Urban-Ciecko et al., 2018]; (C) [Kruglikov and Rudy, 2008]; (D) [Dasgupta et al., 2018]; (E) [Yamamoto et al., 2010]; (F) [Salgado et al., 2007]; (G,H) [Eggermann and Feldmeyer, 2009]; (I) [Kruglikov and Rudy, 2008]; (J) [Markram et al., 1997]. For more exhaustive information on technique, species and cortical area examined, see Table 3.

Receptor type	Single channel conductance	Open time	PO_{max}	EC50 for ACh or nicotine	Kinetics
Nicotinic heteromeric ($\alpha 3\beta 4$)	29 pS	0.71 \pm 0.14 and 3.5 \pm 0.4 ms			
Nicotinic heteromeric ($\alpha 3\beta 2\delta 4$)	29 pS (Stetzer et al., 1999), 18.2 \pm 0.46 (Rovira et al., 1999)	147 ms (Stetzer et al., 1999)			
($\alpha 3\beta 2$) $\alpha 5$				EC50 ACh 1.70–1.83 μ M for ACh EC50 Nicotine 2.91 μ M IC50 Nicotine 2.92 μ M (Kuryatov et al., 2011) EC50 ACh 115–122 μ M EC50 Nicotine 4.64 IC50 Nicotine 16.7 μ M (Kuryatov et al., 2011) High affinity is 1.6 μ M, low affinity is 62 μ M (Buisson and Bertrand, 2001) EC50 for ACh in activating $\alpha 7$ is 3 μ M (Albuquerque et al., 2000) EC50 ACh 1.44–1.64 μ M for variants tested EC50 Nicotine 0.62 μ M IC50 Nicotine 0.0872 μ M (Kuryatov et al., 2011) Choline: EC50 1.6 mM; IC50 37 μ M (Abbondon and Albuquerque, 2004). 200 μ M ACh (Buisson and Bertrand, 2001). EC50 for ACh in activating $\alpha 7$ 130 μ M (Albuquerque et al., 2000)	Fast: 40–121 ms; slow: 274–1039 ms (Figl and Cohen, 2000)
Nicotinic heteromeric ($\alpha 4\beta 2$)	31.3 pS, 40.5 pS (high state) and 21.9 pS (low; Halls et al., 2009)	207 \pm 38 ms (Hsiao et al., 2008)	0.8 (Li and Steinbach, 2010)		Fast 4–6 ms; slow 30–53 ms (Figl and Cohen, 2000)
Nicotinic heteromeric ($\alpha 4\beta 2$) $\alpha 5$					
Nicotinic homomeric ($\alpha 7$)	82.9 pS (Albuquerque et al., 2000)	108 μ s and 92.7 μ s for channels activated by 11 and 10 mM ACh, respectively (Albuquerque et al., 2000)			

The table lists properties of nicotinic homomeric and heteromeric receptors (single-channel conductance, open time and open probability and EC50 and kinetics).

Figure 2.7: Table 4 lists properties of nicotinic homomeric and heteromeric receptors (single channel conductance, open time and open probability and EC50 and kinetics).

sites. This implies that extrasynaptically located $\alpha 4\beta 2$ nAChRs (i.e., the high affinity nAChRs) could be activated by diffusing, low levels of ACh, extrasynaptically located while low-affinity $\alpha 7$ nAChRs may be activated by diffusing choline. Thus, $\alpha 7$ and $\alpha 4\beta 2$ nAChRs might exhibit differential control [Albuquerque et al., 2000].

2.6 Subcellular nicotinic and muscarinic pathways

ACh affects membrane conductance through several subcellular pathways, as illustrated in Figure 4, leading to both hyperpolarizing and depolarizing effects (Tables 1, 2). ACh can act on both pre and post-synaptic membranes, binding to muscarinic and nicotinic receptors. The interplay among intracellular pathways leads to a dynamically changing outcome, such as the transient hyperpolarization and following long-term depolarization resulting from the binding of ACh to M1 mAChR [Dasari et al., 2017]. When ACh interacts with M1, the exchange of coupled GDP for GTP produces the dissociation of the G-protein complex from the receptor. The released α subunit of the G_q protein then activates the enzyme phospholipase C (PLC β) which hydrolyzes phosphatidyl-inositol 4,5 bisphosphate (PIP₂), leading to its dissociation from the membrane and the subsequent formation of diacylglycerol (DAG) and IP₃. IP₃ initiates calcium ions release from the endoplasmic reticulum (ER), serving as a trigger for this process. Refilling of the ER with Ca²⁺ ions is then obtained by the activity of the sarco-ER Ca²⁺-ATPase (SERCA). Extracellular calcium ions are therefore crucial for the maintenance of calcium cycling. M1 activation facilitates voltage-dependent refilling of calcium stores by promoting excitation. Thus, fine-tuned calcium dynamics govern complex reciprocal relations among many different proteins contributing to changes in membrane potential. Ultimately, changes in K⁺, Ca²⁺-activated K⁺-currents and non-specific cationic currents support a shift from transient hyperpolarization

to a sustained excitation. Meanwhile, DAG together with Ca^{2+} ions activate kinases such as protein kinase C (PKC), causing multiple downstream effects. PKC controls the function of many proteins including members of both pre and post-synaptic membranes. PKC is also involved in synaptic plasticity regulation and causes the internalization of AMPARs and NMDARs, leading to LTD phenomena [Callender and Newton, 2017]. PKC can also phosphorylate metabotropic glutamate receptor 5 (mGluR₅; [Hwang et al., 2005] Hwang et al., 2005) as well as many other proteins. Moreover, PKC activates heme-oxygenase 2 (HO-2; [Artinian et al., 2001]) and inhibits NO-synthase (NOS), interfering with the calcium/calmodulin activation of NOS enzyme [Borda et al., 1998]. These effects contribute to the downstream processes involving carbon monoxide (CO) and nitric oxide (NO) as interacting messengers [Mathes and Thompson, 1996, Artinian et al., 2001]. Long-term effects of PKC activation include changes in DNA transcription that are mediated by MAPK/Erk signaling. Furthermore, there is recent evidence for the direct interaction of M3 mAChR with PLC β , which increases signaling efficiency [Kan et al., 2014].

The downstream signaling pathways of M3 and M5 receptors overlap with that of M1, and therefore they are grouped as M1-like receptors; similarly, M2-type mAChRs comprise both M2 and M4 receptors. Binding of ACh to M2-type mAChRs results in the inhibition of adenylyl cyclase (AC) by the α subunit of G_i or G_O protein and in the subsequent reduction of cAMP levels [Muñoz and Rudy, 2014]. However, there are some differences between the G_i and G_O mechanisms of AC regulation [Jiang and Bajpayee, 2009]. The $\beta \gamma$ -complex of the dissociated G-protein can activate the G-protein activated inward rectifier K^+ channels (GIRK) and inhibit voltage-gated calcium channels (VGCCs). Moreover, G_O proteins can also regulate Na^+ channels [Jiang and Bajpayee, 2009]. Particular effects of M1 and M2 receptors on different ion channels have been already summarized by [Thiele et al., 2012]. A significant increase in intracellular calcium concentration comes from the direct flow of ions due to the permeability of nAChRs to Ca^{2+} . However, nAChR activation also leads to the activation of VGCC and subsequent Ca^{2+} influx. [Dajas-Bailador and Wonnacott, 2004, Shen and Yakel, 2009]. Moreover, functional cross-talk among presynaptic nAChRs has been shown to affect signal transduction [Marchi and Grilli, 2010]. Therefore, the action of one receptor might depend on the function of co-existing receptor subtypes in the same cell. The interaction between presynaptic nicotinic receptors with other ionotropic or metabotropic receptors serves the purpose of producing an integrated response.

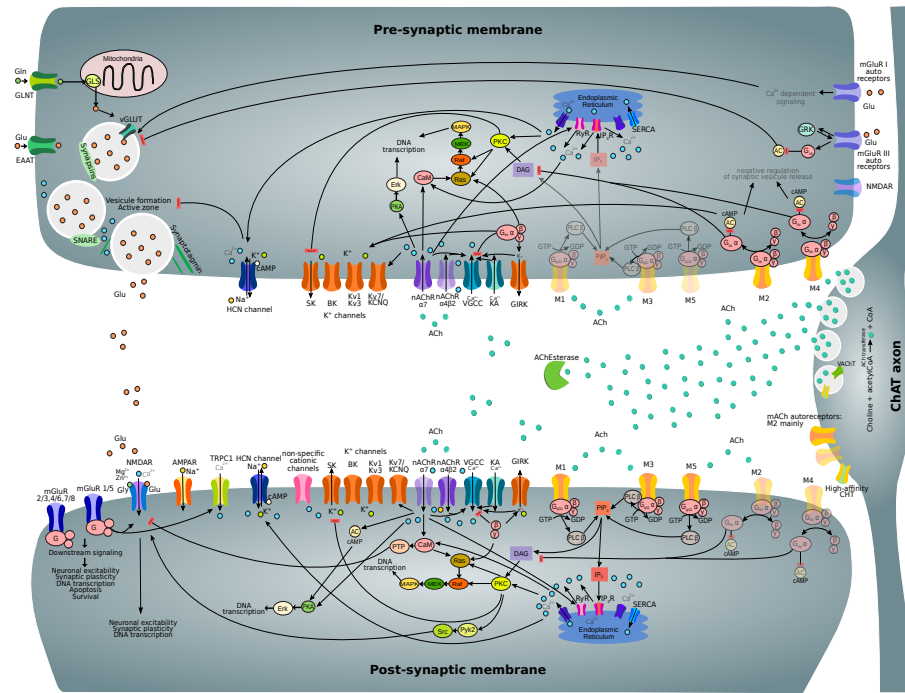


Figure 4

Figure 2.8: Subcellular nicotinic and muscarinic signaling processes at the glutamatergic synapse being modulated by ACh. Only the main relevant pathways and components are shown. Receptor subtypes which are less expressed on pre and post-synaptic membranes and related downstream processes are shown in semi-transparent colors. Abbreviations: ACh, acetylcholine; ACh Esterase, acetylcholinesterase; M1-M5, muscarinic acetylcholine receptor types 1–5; nAChR ($\alpha 7$, $\alpha 4\beta 2$), nicotinic acetylcholine receptor; VGCC, voltage-gated calcium channel; KA, kainate receptor; GIRK, G-protein activated inward rectifier K⁺ channel; PKA, protein kinase A; CaM, calmodulin; AC, adenylyl cyclase; DAG, diacylglycerol; PKC, protein kinase C; NOS, NO-synthase; HO-2, heme oxygenase 2; sGC, soluble guanylyl cyclase; PKG, cGMP-dependent protein kinase; HCN, hyperpolarization-activated cyclic nucleotide-gated channel; TRPC1, transient receptor potential cation channel 1; mGluR, metabotropic glutamate receptor; Pyk2, protein-tyrosine kinase 2; PiP₂, phosphoinositol-1,4,5-bisphosphate; PLC β , phospholipase C β ; IP₃, inositol triphosphate; IP₃R, IP₃ receptor; RyR, ryanodine receptor; SERCA, sarco-endoplasmic reticulum Ca²⁺ ATP-ase.

2.7 Transcriptome cell-specific predictions of cholinergic receptors

In recent years, a wealth of transcriptomic data from the mouse brain has become available [Saunders et al., 2015, Zeisel et al., 2018]. Many different cell types may exist; one study found 565 different cell groups, for example [Saunders et al., 2018]. Since a standard classification of cortical cell types is still emerging, most articles employ different approaches to arrive at cell type specific transcriptomes. We examined a representative data set from the somatosensory cortex in order to interpret possible cell-specific differences in cholinergic receptor expression (Figure 5). We chose this data set since excitatory cell types are mapped to layer-specific types, allowing the easiest comparison with the types referenced in this review. In this dataset, normalized expression of M1 receptors is highest in L4 PCs. There is a strong expression of M2 in deep layer neurons, particularly in layer 5a. M3 is highly expressed in layer 2/3 and layer 5a, while M4 is highest in layer 4. $\alpha 3$ nAChR subunits are highest in layer 4, but also in the deep layers. β subunit expression is highest in layer 6 and layer 6a neurons. Inhibitory interneuron expression of cholinergic receptors is definitely cell-type specific, though heterogeneous. PV cells express more nAChR $\alpha 3$ than do somatostatin-expressing interneurons (Figure 5B). Somatostatin expression is best correlated with M2 expression and nicotinic β subunit expression and negatively correlated with M1 expression (Figure 5C). VIP and Htr3a expression is correlated with nAChR $\alpha 3$, nAChR $\alpha 4$, and nAChR $\alpha 5$. Furthermore, ChAT expression is correlated with M1 expression. In layer 5a, the effects of the predominantly-expressed nAChR and mAChRs seemed to be synergistic. We also examined an additional dataset for frontal cortex (Figure 5E; [Saunders et al., 2018]). M5 is expressed in a subset of interneurons, including some cholinergic and MCs. The nicotinic receptor ChRNA5 is expressed in a subset of deep PCs. ChRNA6 is most expressed in a particular type of layer 5 PC. This dataset illustrates that the degree of sub-classification of PCs is likely to be important. For example, there are many subtypes of L5PCs, which have different cholinergic receptor expression. Both datasets showed consistency in M3 expression in L2/3 and L5a PCs but not L4 and L5 PCs. In addition to cell-type specific correlation, nAChR genes that encode heteromeric α/β subunits are well correlated among themselves [Zoli et al., 2015, Saunders et al., 2018]. The genes encoding the α subunits correlate well with the corresponding β subunit. Cholinergic neurons can be identified by cluster analysis [Zeisel et al., 2018]. In particular, separate types have been identified in the red nucleus and habenular nucleus of the thalamus (ibid). ACh often is released in neurons releasing other neurotransmitters. In the habenular nucleus, the glutamate transporter Slc17a6, in cholinergic cells, suggesting co-release of glutamate and ACh [Mancarci et al., 2017]. In the

ventral midbrain, a neuron type that was both dopaminergic and cholinergic was identified [Zeisel et al., 2018]. Many forebrain cholinergic neurons also are GABAergic [Mancarci et al., 2017] (Mancarci et al., 2017), consistent with the co-release of these two substances [Saunders et al., 2015].

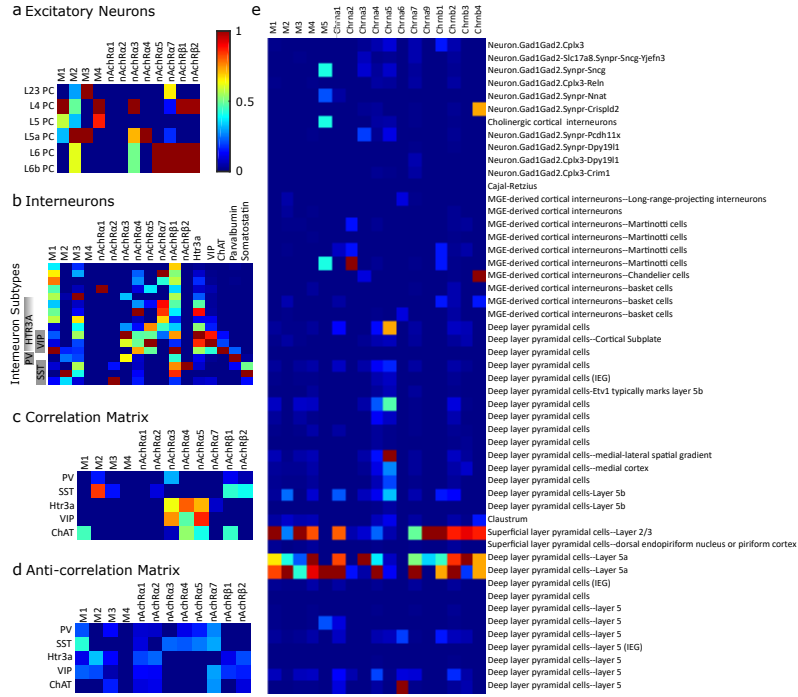


Figure 2.9: Figure 5 - Differential expression of cholinergic receptors in transcriptome-derived cell types. (A) Excitatory cell types. (B) Interneurons in somatosensory cortex. Gene expression is normalized to a maximum of 1 on a gene-by-gene basis. (C) Correlation matrix (positive values of correlation matrix Pearson correlation coefficient matrix). (D) Anti-correlation matrix (negative values of correlation matrix). The data is from Zeisel et al. (2018) and was collected with high-throughput single-cell RNA sequencing, a method which counts individual RNA molecules. Abbreviations: PV, parvalbumin; SST, somatostatin; VIP, vasointestinal peptide; ChAT, choline acetyltransferase. (E) Expression of ACh receptor genes across the Frontal cortex cell-clusters identified in Saunders et al. (2018). The data was collected using Drop-seq (a method which allows the use of older animals and elimination of certain technical artifacts) to profile the RNA expression of individual cells. Semi-supervised independent component analysis was used to group cells into the sub-clusters using network-based clustering (ibid). Expression levels were normalized to the highest expression across all the selected genes. In this data set, receptor expression was particularly high in L23 and L5a PCs.

2.8 Global network effects and modulation of brain states

The transition between different brain states that occurs whenever an organism switches from one behavioral state to another is associated with changes in the overall pattern of neural activity, which can be captured with EEG or LFP recordings. The pattern of EEG activity can change dramatically with the behavioral state of the animal [Lee and Dan, 2012], as can be seen in the transition from slow-wave sleep to wakefulness (or from deep sleep to REM sleep), when the EEG pattern shifts from large and synchronous waves of neural activity to a more desynchronized and short-amplitude wave pattern [Berger, 1929]. Ensemble neuronal activity undergoes impressive changes during behavioral state transitions, and different brain states have been associated with different brain functions; definitive evidence for these functions although, is still lacking, and the mechanism by which these transitions are achieved in the cortical network is not yet understood. Many authors have proposed that the switch between cortical states may be driven by the action of neuromodulators like ACh [Lee and Dan, 2012]. However, precisely how these neuromodulators influence global cortical processing by locally targeting specific cells is largely an unsolved mystery.

2.8.1 Basal forebrain modulation of brain states

A large body of evidence suggests that the BF, a complex and heterogeneous structure classically defined by the presence of clusters of cholinergic neurons, is crucial for the maintenance of the sleep/wake cycle and for processes that underlie arousal and attentional modulation, but it is unclear which BF neurons promote each brain state and how they interact with each other to regulate transitions between states [Anaclet et al., 2015]. Already since 1930, it was known that BF lesions could cause severe insomnia [Saper et al., 2001]; however, this evidence has been an object of constant challenge over the years, and the attempts to replicate this experiment would yield different results. Finally, [Szymusiak and McGinty, 1986] observed that sleep-active cells were confined to the ventral BF in the cat (the horizontal limb of the diagonal bands of Broca, substantia innominata, entopeduncular nucleus and ventral globus pallidus) and that these areas partially overlap with those where chemical and electrical stimulations evoke sleep, and where lesions suppress sleep. The sleep-active cells were thus considered optimal candidates for mediating some of the sleep-promoting functions attributed to the BF [Szymusiak and McGinty, 1986]. Many BF neurons are active during wake and during REM sleep [Lee and Dan, 2012], and specific lesions reduce wakefulness, in agreement with the finding that BF lesions cause significant increases in delta waves occurrence during wakefulness, and that BF stimulation induces cortical desynchronization of EEG or LFP signals,

accompanied by a decrease in correlated spiking. Furthermore, the BF receives inputs from the LDT and PPT pontine nuclei; cholinergic neurons that can be found at the level of the LDT nucleus exhibit an increase in firing rate during cortical activation, just before the transition from slow-wave sleep frequencies to faster frequencies [Saper et al., 2010].

Therefore, it seems reasonable to hypothesize the existence of functionally diverse neurons in the BF: according to [Duque et al., 2000], BF cells that exhibit different wake/sleep activity pattern, also express different molecular markers [Zaborszky and Duque, 2000]. There are three major neuronal types in the BF: cholinergic, glutamatergic and GABAergic cells [Anacleto et al., 2015, Xu et al., 2015]. There might be extensive local synaptic interactions among BF neurons mediating local reciprocal inhibition between GABAergic neurons and sleep-active and wake-active cholinergic neurons. The well-known flip-flop circuit for sleep/wake cycle control [Saper et al., 2010] could, therefore, comprise multiple loops and switches. However, some findings suggest that BF GABAergic neurons provide major contributions to wakefulness, while cholinergic and glutamatergic neurons appear to play a lesser role; chemogenetic activation of GABAergic neurons promotes wake and high-frequency EEG activity, whereas cholinergic or glutamatergic activation have a destabilizing effect on slow-wave-sleep (SWS), but has no effect on total wake [Anacleto et al., 2015]. Cholinergic neurons residing in the BF can be divided into two subpopulations, that might be involved in different functions: an early-spiking population may reflect phasic changes in cortical ACh release associated with attention, while the late-spiking group could be more suited for the maintenance of the cholinergic tone during general cortical arousal [Unal et al., 2012].

2.8.2 ACh and GABA co-transmission

Nevertheless, functional co-transmission of ACh and GABA seems to be a common feature of nearly all forebrain ACh-producing neurons [Henny and Jones, 2008, Granger et al., 2016]. BF inputs to the neocortex are therefore not only constituted of different fibers, but also use a mixture of functionally diverse neurotransmitters [Kalmbach et al., 2012]. This opens the question of whether there is a substantial difference between the cholinergic modulation and the BF modulation of neocortical activity. The contribution of GABA needs to be considered when studying the functional impact of ACh-producing neurons: electrical stimulation of BF fibers might evoke markedly different responses than optogenetically-evoked selective cholinergic release. Does the co-release happen in a target-specific modality, at different terminals branching from the same axon, or is the release site the same for both transmitters? And if so, how does GABA affect the ongoing cholinergic modulation? Release of an excitatory (ACh) and inhibitory

(GABA) neurotransmitter by the same axons seems to be functionally antagonistic. However, both transmitters could act in parallel, depending on the mode of co-transmission [Granger et al., 2016]. If both ACh and GABA are released simultaneously onto the same post-synaptic cells, then GABA may act to shunt the (supposed) excitation generated by ACh. Otherwise, they could target different postsynaptic cells, such that GABA inhibits one cell population while ACh excites another. Given previous experimental results showing that GABA release from VIP interneurons shunts activity of SST⁺ interneurons, but not other VIP interneurons, it is thought that VIP/ChAT cortical interneurons may release ACh and GABA onto different post-synaptic targets, perhaps from separate synaptic vesicle populations [Granger et al., 2016]. Indeed, a recent analysis of the molecular composition of the pre-synaptic terminals of cortical VIP/ChAT interneurons revealed that ACh and GABA vesicles are confined to separate boutons. At the post-synaptic level, the subset of GABAergic boutons seems to contact prevalently other inhibitory interneurons, while ACh boutons target mostly L1 interneurons and other VIP/ChAT cortical interneurons. Here, ACh evokes EPSCs that are mediated by nicotinic receptors [Granger et al., 2018]. Another recent study conducted in the mPFC confirms that only 10%–20% of post-synaptic targets of VIP/ChAT cortical interneurons are contacted by both cholinergic and GABAergic inputs [Obermayer et al., 2018]; here they report that VIP/ChAT neurons directly excite interneurons in layers 1–3 as well as PCs in L2/3 and L6 by fast nicotinic transmission. Immunolabeling studies [Beaulieu and Somogyi, 1991] have shown substantial co-labeling of presynaptic cholinergic terminals for both GABA and ChAT in the neo-cortex, but more studies should address the functional consequences of the synaptic co-release of these neurotransmitters and try to dissect the differential impact of each transmitter on postsynaptic cells excitability. Analysing the co-localization of post-synaptic receptors or scaffolding proteins could also allow the identification of individual synapses that are sensitive to both ACh and GABA. These possibilities should be addressed systematically in order to precisely understand the contribution of each neurotransmitter to cortical processing.

2.8.3 ACh involvement in neuroplasticity

Apart from the fine-tuning of sleep/wake transitions, cholinergic neuromodulation is tightly implicated in regulating selective attention to a given sensory stimulus by altering the activity of the sensory cortex that perceives that modality [Kim et al., 2016]. ACh is known to be especially involved in cortical arousal [Saper et al., 2010] and in the state-dependent modulation of cortical activity; cholinergic neurons are active during locomotion [Buzsaki et al., 1988] and during transition to the attentive state [Kim et al., 2016]. Studies have shown that the occurrence of relevant sensory events evokes

a transient increase in ACh concentration in the rat PFC [Hasselmo and Sarter, 2011]. Conversely, activating cholinergic transmission in the PFC determines an improvement in subject’s performance during sustained attention tasks [Saper et al., 2010]. It is, therefore, reasonable to hypothesize that ACh can induce long-lasting changes in neuronal excitability, and indeed this was demonstrated. Pioneering experiments showing that ablation of noradrenergic and cholinergic innervation in the striate cortex substantially impairs ocular dominance plasticity in kittens [Bear and Singer, 1986] opened the way for subsequent studies on the involvement of ACh in cortical plasticity. Some showed that when a tone is paired with NBM stimulation or ACh application, auditory cortex receptive fields change and prolonged enhanced responses to the paired frequency can be observed [Metherate and Weinberger, 1990, Rasmusson, 2000]. Others discovered that co-application of muscarinic agonists with glutamate induces a prolonged increase in response to glutamate in somatosensory cortical neurons [Sugihara et al., 2016], and that these effects concern as well the somatosensory cortex and the primary visual area V1. According to Metherate and Weinberger (1990), the potentiation can be blocked by cortical application of atropine, but others [Sugihara et al., 2016] report that cholinergic antagonists cannot reverse the prolonged changes, thereby confirming that ACh is necessary for the induction, but not the maintenance of these modifications. ACh seems to act more as an instructive, rather than a permissive signal [Lin et al., 2015].

ACh is as well involved in the generation of LTD at synapses between cortical pyramidal neurons and striatal medium spiny neurons through disinhibition of Ca_v channels. Here, the activation of D2 receptors reduces basal ACh release from cholinergic striatal interneurons and lowers M1 receptor tone in medium spiny neurons, which leads to enhanced opening of intraspine $\text{Ca}_v1.3 \text{ Ca}^{2+}$ channels in response to synaptic depolarization. The calcium transient results in enhanced production of endocannabinoids (ECs) such as 2-arachidonoylglycerol, and activation of presynaptic CB1 receptors that reduce glutamate release [Wang et al., 2006]. Furthermore, the role of several neuromodulatory systems in STDP induction [Pawlak, 2010] has been studied across multiple brain areas. While dopamine (DA) and NA modulation of STDP has been mostly investigated in subcortical areas, ACh’s role in STDP induction has been extensively researched in neocortical sensory areas and in the PFC. In mouse mPFC, nicotine application increases the threshold for STDP in L5PCs by reducing their dendritic calcium signals. This effect, however, is due to an enhancement in GABAergic transmission in various types of interneurons in the PFC network, that express multiple types of nAChRs [Couey et al., 2007], and not to a direct nicotinic action on PCs. Taken together, evidence suggests that cholinergic inputs to the cortex incoming from the BF should be viewed more as teaching, rather

than motivational signals. Overall, activation of the cholinergic system controls the shift from a correlated or synchronized state, to a decorrelated or desynchronized state and results in an enhancement of cortical information processing [Lee and Dan, 2012]. However, exactly how the detection of relevant stimuli is enhanced and which are the mechanisms at the basis of this ACh-induced desynchronization are still a matter of open debate.

2.8.4 ACh enhancement of sensory processing

NBM stimulation has a differential effect on spontaneous and sensory-evoked activity. In a recent study, [Meir et al., 2018] showed that NBM stimulation desynchronizes cortical LFP and increases the SNR of sensory-evoked responses while suppressing ongoing spontaneous synaptic activity. The authors recorded spontaneous PSPs occurring in L4 and showed that following NBM stimulation the frequency and amplitude of sPSPs were decreased. Moreover, the mean membrane voltage of the response became more hyperpolarized, and trial-to-trial variability was decreased, both during spontaneous and evoked activity. However, sensory stimulation did not change the amplitude of the response, whereas it caused a prominent reduction in the noise amplitude, therefore changing the SNR of the sensory response. By analyzing the coupling of V_m and LFP signals, they also showed that cholinergic activation largely reduced fluctuations in the membrane potential and caused a decorrelation in network activity. [Chen et al., 2015] were able to identify a defined microcircuit in the superficial layers of mouse V1 that supports ACh driven desynchronization. The authors measured the activity of different inhibitory interneurons while optogenetically stimulating superficial cholinergic axons, and found that cholinergic inputs facilitate SST⁺ interneurons, which in turn inhibit PV⁺ interneurons and PCs. Optogenetic inhibition of SST⁺ neurons blocks desynchronization, whereas direct activation of SST⁺ neurons is sufficient to induce desynchronization [Chen et al., 2015]. The observed desynchronization in cortical activity may explain the role of ACh in mediating transitions between phases of the sleep-wake cycle, but it fails to explain how ACh enhances sensory processing. A large body of evidence suggests that ACh enhances sensory inputs while simultaneously suppressing intrinsic cortical activation [Kimura et al., 1999, Disney et al., 2007, Newman et al., 2012], but a detailed understanding of this process is currently lacking. ACh’s role may substantially differ across sensory areas and affect different tuning properties.

Nucleus basalis activation affects sensory responses to natural stimuli of a population of cortical neurons. Before BF stimulation, multi-unit activity (MUA) in the rat’s V1 is highly correlated but poorly time-locked to the stimulus; after BF stimulation it becomes less correlated but more time-locked to the sensory event. NBM stimulation also decreases single-unit

activity (SU) correlation (between cells correlation) and increases response reliability (between trials correlation coefficient) but does not induce any significant change in receptive field size, orientation tuning nor direction selectivity. Atropine application decreases NBM induced decorrelation, indicating that mAChRs support this effect (Goard and Dan, 2009). After NBM stimulation a shift in the firing modality of the LGN resembling that found at the level of the thalamus can be observed, namely a transition from burst to tonic mode [Bazhenov et al., 2002, Castro-Alamancos and Gulati, 2014]. A similar study [Thiele et al., 2012] was conducted in the extrastriate cortex of the macaque and yielded opposing results: at the level of the middle temporal (MT) area it revealed how other tuning properties, like orientation and direction discriminability, are also affected by cholinergic modulation; in this case, ACh had little effect on response reliability, though it is still not clear whether these differences are attributable to differences existing between rodents and primates or to functional differences between sensory areas. In an effort to clarify the precise role of neocortical cholinergic modulation, [Disney et al., 2007] concentrated on the role of nAChRs in a well-studied cortical model system, the V1 of the macaque monkey. Here they showed in vivo that nicotine reliably enhances the gain of responses to visual stimuli in layer 4c, but not in other layers. Having found $\beta 2$ -nAChR in a pre-synaptic position at the level of thalamo-cortical synapses on PV⁺ interneurons, they prove that nicotine enhances detection of visual stimuli through enhanced TC transmission. These findings confirm that cholinergic activation causes an increase in cortical sensory responses through enhancement of thalamic synaptic transmission and suppression of intracortical inputs. A systematic effort to extend these results to other sensory areas is therefore needed in order to decipher whether the mechanism supporting cholinergic modulation is common throughout all cortical areas or if different tuning properties are affected each time.

2.8.5 ACh modulation of thalamo-cortical transmission

Castro-Alamancos and Gulati recorded, multi-electrode activity (MUA) and field potential from adult rat barrel cortex following multi-whisker stimulation at 0.2 Hz, while increasing concentrations of carbachol or other drugs were applied by means of micro-dialysis. The authors found that the application of 50 μM carbachol, but not norepinephrine, can stop the emergence of the 10–15 Hz oscillations that are observed during baseline recordings and that in the presence of atropine these oscillations are even enhanced [Castro-Alamancos and Gulati, 2014]. The effect of carbachol on barrel cortex LFP is thus congruent with the traditionally termed desynchronization for doses higher than 50 μM [Moruzzi and Magoun, 1949, Steriade et al., 1993]. A low tone of cholinergic activation (0.5–1 μM) however, reinforces the deactivated cortical state by enhancing synchronous slow oscillations. A very high tone

of cholinergic activation (250–2,500 μM) leads to a significant increase in tonic firing, without altering the overall firing rate. An interesting follow-up to this experiment would be to check whether the same effect can be observed in the whole somatosensory region, and across other sensory cortices. The group then tried to decipher whether cholinergic activation would also modulate thalamocortical activity: by recording from the VPM, they found that cholinergic cortical activation suppresses burst-firing in the thalamus and changes neuronal firing to a tonic mode. This result is fairly consistent with the outcome predicted by the model of thalamo-cortical slow-wave sleep oscillations and transition to activated states generated by [Bazhenov et al., 2002]. Here, the increase in ACh activity was modeled by the reduction of a K^+ leak current in pyramidal and thalamo-cortical cells and resulted in the abolishment of the hyperpolarizing phase of network activity and a consequent increase in the input/resistance relationship, accompanied by a switch to the tonic firing (15–20 Hz) modality. The transition from bursting to tonic firing thus seems to be a characteristic feature of relay diencephalic structures like the thalamus and the meta-thalamus. Enhanced thalamo-cortical transmission seems to be a constant finding across a vast number of articles and reviews [Bazhenov et al., 2002, Disney et al., 2007, Hasselmo and Sarter, 2011] with the aim of revealing the mechanisms by which cholinergic neuromodulation operates. Next studies in this field should, therefore, consider the possibility that cholinergic inputs reach the cortex not only through direct BF projections but also exploiting the thalamo-cortical loop. Voltage-sensitive dye imaging revealed that ACh application to the neocortex, upon stimulation of layer 2/3, suppresses the spread of excitation to nearby areas. Thus, ACh seems to play an important role in coding sensory stimuli by enhancing thalamocortical inputs, but at the same time, by suppressing intracortical interactions [Kimura et al., 1999]. One of the proposed models for the cholinergic mediated shift from default mode to detection mode suggests that ACh acts to enhance the glutamatergic representation of thalamic input through stimulation of nAChRs, while suppressing the cortical spread of associational input through activation of mAChRs (Hasselmo and Sarter, 2011). [Minces et al., 2017] recently evaluated the effect of increases in cortical ACh following optogenetic BF stimulation on the correlation structure of the visual network and found that transient cholinergic release in the cortex decreases the slope between signal and noise correlations. The authors propose that this mechanism acts to increase the encoding capacity of the network. Another article evaluated the impact of ACh on local circuit activation and found that cholinergic inputs exclude unreliable neurons from contributing to circuit activity while conserving neurons that were active in response to thalamic activity and showed strong correlations. Moreover, weak functional connections were pruned, thus yielding a more modular and hierarchical circuit structure. Once again, these results highlight how ACh is able to reorganize the circuit function in a way that promotes the discrim-

inability of thalamic inputs at the expense of weak pairwise relationships [Runfeldt et al., 2014].

2.8.6 Sensory-modality specific information processing and ACh

Many studies [Disney et al., 2007, Minces et al., 2017] have focused on trying to understand the role played by ACh in improving stimuli detection or modifying receptor fields size in the visual cortex. While many of them have been done in primates, others have privileged the somatosensory areas and highlight the involvement of the cholinergic system in the regulation of sensory cortical processing in rodents as well, supporting the idea that cholinergic modulation of cortical microcircuits is functionally equivalent across brain areas and model organisms, even though a canonical and anatomically equivalent system is not strictly identifiable [Coppola and Disney, 2018]. The finding that distinct neuronal clusters in the BF project selectively to specific sensory areas [Kim et al., 2016] and that cholinergic inputs to sensory cortices are spatially segregated supports the idea that cholinergic release improves sensory discrimination in a modality-selective manner and with a high degree of specificity. The authors mapped BF projections to different sensory areas and found retrobead-labeled neurons from three different sensory cortices within the BF, with a clear distinction between the clusters of cells: neurons in the HDB project preferentially to V1, the posterior part of NBM projects to A1, while the aNBM preferentially projects to S1. These results were further confirmed by another experiment in which the authors optogenetically activated cholinergic neurons in the BF subnuclei and successfully induced modality-selective desynchronization in specific sensory cortices. A similar experiment was performed by [Chaves-Coira et al., 2016], who also used retrograde anatomical procedures to demonstrate the existence of specific neuronal groups in the BF implicated in the modulation of specific sensory cortices. However, here the authors found that most of the neurons located in the HDB projected to the S1 cortex, suggesting that this area is specialized in the sensory processing of tactile stimuli, and the NBM was found to have a similar number of cells projecting to S1 as to A1. Furthermore, optogenetic HDB stimulation induced a larger facilitation of tactile evoked potentials in S1 than auditory evoked potentials in A1, while optogenetic stimulation of the NBM facilitated either tactile or auditory evoked potentials equally. These results suggest that cholinergic projections to the cortex are organized into spatially segregated pools of neurons that modulate specific cortical areas; although, additional research will be needed in order to provide a clear and definitive picture of the topographical organization of the projections arising from the BF region and innervating the cortex. Despite the many attempts to clarify this issue, it remains unclear whether there exist distinct neuronal populations in the HDB, or whether

the differences observed in the outcomes of the experiments mentioned above are due to discrepancies existing in the transgenic mouse lines used or to the slightly different techniques that were employed. ACh is thus involved both in the bottom-up attentional process that leads to a general and whole-state arousal of the cortex and in the top-down modifications of circuit activity that occur during detection of behaviorally relevant sensory stimuli. Cognitive functions of cholinergic projection systems vary according to the brain area that is being modulated. Cholinergic modulation may act as a common mechanism to improve sensory encoding in several brain areas.

2.9 Summary and outlook

ACh release in the neocortex controls transitions between brain states, such as attention, memory and wakefulness, and can occur through volume or synaptic transmission. However, it is not clear yet whether one modality prevails upon the other or if they are complementary mechanisms. Further studies are needed to establish correlations between the distribution profile of the receptor subtypes, the relative proximity and density of cholinergic varicosities to assess differences between the two modalities. Moreover, as results could vastly vary across species, a systematic effort is crucial to be able to compare quantitative measurements. The expression of muscarinic and nicotinic cholinergic receptors—the two main types—varies according to the cell-type and the pattern of receptor localization varies across cortical layers. A detailed knowledge of the subcellular localization of cholinergic receptors is, however, currently lacking. The detection of cholinergic structures such as the receptor protein has become easier with the advent of polyclonal antibodies targeting different subtypes. Future investigations should, therefore, converge on systematically measuring the amount of each receptor subtype across cellular compartments. In this review, we have endeavored to determine, in a quantitative manner, the cellular and synaptic effects of ACh release in the neocortex. While the cholinergic modulation of excitatory PCs has been extensively researched, its effect on inhibitory interneurons is still largely unknown. For example, the effect of ACh on BCs (fast-spiking, PV⁺ interneurons) remains unclear. This could be due to the lack of a thorough classification of diverse morphological types of BCs where a differential distribution of cholinergic receptors could modulate divergent cellular and synaptic effects. Furthermore, it is not clear whether bath-application of cholinergic agonists is comparable to a physiological activation of the cholinergic system. Applied concentrations of cholinergic agonists vary substantially (up to three orders of magnitude) across electrophysiological studies, which seldom use more than one concentration. To obtain carefully designed dose-response curves of the effects of cholinergic agonists is paramount to dissect the consequences of physiological ACh release

in the neocortex. The advent of optogenetics holds promise in designing physiological protocols of ACh release. Future experiments should not only merely employ traditional bath-application of cholinergic agonists but also exploit optogenetics to reconcile how doses of agonists directly map to effects of endogenous, physiological release of ACh. The effects of ACh on synaptic connections can vary drastically according to the identity of the presynaptic terminal and its postsynaptic partner. Additionally, the magnitude of the postsynaptic response also depends on the receptor subtype being activated. Therefore, there is a clear requirement for systematic investigations of the effects of ACh on different synapse-types, combined with knowledge of implicated cell-types and receptor subtypes to unravel the effects of ACh release on neocortical synaptic transmission. ACh is involved in the induction of synaptic plasticity mechanisms, which could support its role in cortical learning and memory. In addition, ACh enhances sensory processing by affecting receptor fields size and tuning properties. It is not clear, however, if the effects of ACh are modality-specific or can be generalized to all sensory processing, nor exactly which tuning properties are affected. Many studies point to a role of ACh in increasing the SNR of a sensory response, and others describe how ACh suppresses cortico-cortical interactions in favor of thalamic transmission. Therefore, further clarification is required on the matter. Moreover, special attention must be paid in integrating data from primates and rodents: neuromodulatory systems are commonly the object of evolutionary modifications, even though they might maintain some functional similarity throughout species. The mechanisms of ACh-induced changes in the physiology of neocortical neurons and their synapses, and how these changes shape the emergence of global network states still remains elusive. The impact of ACh on global cortical computations sustains cognitive functions such as attention, learning and memory, which are characterized by desynchronized network activity. Cholinergic inputs mainly originate in the BF, a structure comprising distinct multi-transmitter neuronal populations. The functional relevance of neuronal subpopulations in the BF and the co-release of two potentially antagonistic transmitters to the desynchronization of cortical activity is unknown. Furthermore, recent work identifies that a sub-population of VIP^+ cortical interneurons co-release ACh and GABA with potentially differing functions across species. Future research should, therefore, focus on dissecting the impact of each transmitter on cellular excitability. In addition, analyzing the co-localization of post-synaptic receptors could also allow the identification of individual synapses that are sensitive to multiple neurotransmitters. All these possibilities should be addressed systematically in order to precisely understand the contribution of each neurotransmitter to ACh-induced effects on the emergence of cortical network states in health and disease.

Chapter 3

Modelling the neuromodulation of neural microcircuits: a first-draft data-driven framework

3.1 Introduction

As illustrated in the previous chapter, the understanding of the cholinergic modulation of the neocortex has kept neuroscientists busy for decades and despite numerous efforts to frame the problem into a wider picture, the quest for underlying principles of biological organization has remained inconclusive. The problem when looking at cholinergic neuromodulation, is that it seems to get more complex as more research is conducted. The idea that neuromodulatory principles can be understood primarily through the lenses of experimental research is growing feebler as more evidence accumulates. Let's take for instance the problem of predicting the effects of ACh on a given cell-type. Regardless of the century-old issue of objectively classifying neuronal cell-types [Kanari et al., 2019, Tasic et al., 2018], it is not possible to answer in a simplified form, for instance that 'ACh inhibits pyramidal neurons' or 'ACh excites interneurons', because ACh modulation is dynamic and context-dependent. The effects of ACh vary based on its extracellular concentration, the types and subtypes of receptors involved, the subcellular localization of those receptors, the laminar position of the cell type examined, the neocortical area involved, the age and developmental state of the animal, and they are not necessarily conserved across species. Furthermore, the basal tone of ACh depends on the contextual cocktail of other neuromodulators, and co-release of other transmitters, modulators or peptides that in turn shape cholinergic inputs. Neuromodulation is an extremely sophisticated phenomenon, and its inherent intricacy is likely to be at the heart of

its cardinal role in the regulation of neural activity. Neuromodulation is the process by which the activity of the microcircuit is fine-tuned at the level of multiple biological scales of organization in order to achieve the desired reconfiguration of network states, and organize the appropriate behavioral response to environmental stimuli. Therefore, I think it is essential, if we want to move forward in our understanding of neuromodulatory processes, and more in general of brain structure and function, to generate new approaches to study these incredibly complex phenomena. Not everything can be measured experimentally, and even if it were possible, merely gathering more data will not deepen our understanding of the problem; as shown in the previous chapter, the current approaches have led to the generation of contradictory and often incompatible observations. Thus, there emerges a need not only to fill the gaps in current knowledge, but also to integrate all the known pieces in a coherent framework that makes the problem more tractable.

Simulation neuroscience is a recent and rapidly evolving field, fueled by advances in computing, that has nowadays been accepted as a complementary approach to experimental neuroscience to tackle the understanding of the brain [Cremonesi et al., 2020]. Simulation based paradigms offer the advantages of being comparatively low cost and high-throughput methods that allow neuroscientists to conduct investigations that would be incredibly challenging or impossible to achieve in real-life setups. Bio-physical models are constrained via laboratory acquired data and, provided with state-of-the-art computational tools, offer a way to expand a neuroscientist’s toolkit to probe brain mysteries. The neocortical microcircuit model (NMC) developed by the Blue Brain Project (BBP) [Markram et al., 2015], is an example among other approaches that were developed to bridge the gap between the necessity to integrate large albeit sparse experimental datasets and the inexplicable complexity of brain structure and function [Izhikevich and Edelman, 2008]. The NMC model is a biologically plausible digital reconstruction of rat neocortical microcircuitry constrained by experimental datasets that offers a unique opportunity to perform rigorous in-silico experiments. Thus, it is an exceptionally suitable framework to explore the mysteries of neuromodulatory phenomena. Given the multifaceted aspects of cholinergic neuromodulation it is paramount to capture the essential aspects that will be the foundations of the model: in the next section I will present a proof-of-concept study based on phenomenological models of ACh effects on neocortical cells and synapses. This first-draft data-driven framework shows that simulating cholinergic release brings about shifts in network oscillatory activity, thus validating the underlying hypothesis that neuromodulators regulate transitions between global brain states by acting on local microcircuits.

In the last section of this Chapter, I will review the state-of-the-art literature about two other neuromodulators that are particularly relevant for this thesis: DA and 5-HT.

3.2 Data-driven modelling of cholinergic modulation of neural microcircuits: bridging neurons, synapses and network activity

Srikanth Ramaswamy, Cristina Colangelo and Henry Markram

Front. Neural Circuits, 09 October 2018
<https://doi.org/10.3389/fncir.2018.00077>

3.2.1 Abstract

The neocortex is densely innervated by cholinergic neurons projecting from the basal forebrain, which release acetylcholine (ACh) [Mesulam et al., 1992, Levey et al., 1987, Gielow and Zaborszky, 2017]. Diffuse release of ACh targets neurons and synapses in neocortical microcircuits, and regulates behavioral states, such as attention, wakefulness, learning and memory [Metherate et al., 1992, Hasselmo, 1995, Hasselmo, 1999, Lee and Dan, 2012]. It is thought that the actions of ACh on the physiology of neurons and synapses plays a key role in switching cortical rhythms that underlie a diversity of behavioral states [McCormick, 1992, Steriade et al., 1993, Xiang et al., 1998a, Picciotto et al., 2012, Zagha and McCormick, 2014]. Much of our knowledge on the regulation of neuronal and synaptic physiology by ACh comes from studies in cortical slices that have combined whole-cell somatic recordings and bath-application of ACh agonists, such as carbachol (CCh), to the extracellular recording medium [Wang and McCormick, 1993, Kawaguchi and Kubota, 1997], [Gulledge et al., 2007, Gulledge and Stuart, 2005, Gulledge et al., 2009, Levy et al., 2008], [Eggermann and Feldmeyer, 2009, Brombas et al., 2014, Chen et al., 2015, Poorthuis et al., 2014, Urban-Ciecko et al., 2018]. Emerging data suggest that ACh controls the excitability of neocortical neurons, enhances the signal-to-noise ratio of cortical responses, and modifies the threshold for activity-dependent synaptic modifications by activating postsynaptic muscarinic (mAChR) or nicotinic (nAChR) receptors. At the cellular level, it is understood that ACh mostly activates mAChRs to depolarize neurons and initiate action potentials (APs) [Krnjević, 2004, Kawaguchi and Kubota, 1997, Gulledge et al., 2009, Eggermann et al., 2014]. However, a handful of studies also suggest that ACh transiently activates mAChRs and strongly inhibits the initiation of APs in neocortical pyramidal neurons [Gulledge and Stuart, 2005, Gulledge et al., 2007]. At the level of synapses, it is known that ACh reduces the efficacy of excitatory connections in the neocortex. For example, in synaptic connections between thick-tufted layer 5 pyramidal cells (TTPCs), which are marked with pronounced short-term depression, bath-application of 5–10 μM of CCh during presynaptic stimulation, rapidly reduces the rate

of depression in a train of postsynaptic potentials (PSPs) without affecting the so-called stationary PSPs [Tsodyks and Markram, 1997, Levy et al., 2008]. In contrast, administering a similar amount of CCh on facilitating synaptic connections between TTPCs and Martinotti cells (MCs) increases the strength of successive PSPs [Levy et al., 2008]. Although some of the cell-type, and connection-type specific effects of ACh in the neocortex have been experimentally mapped, the vast majority remains unknown.

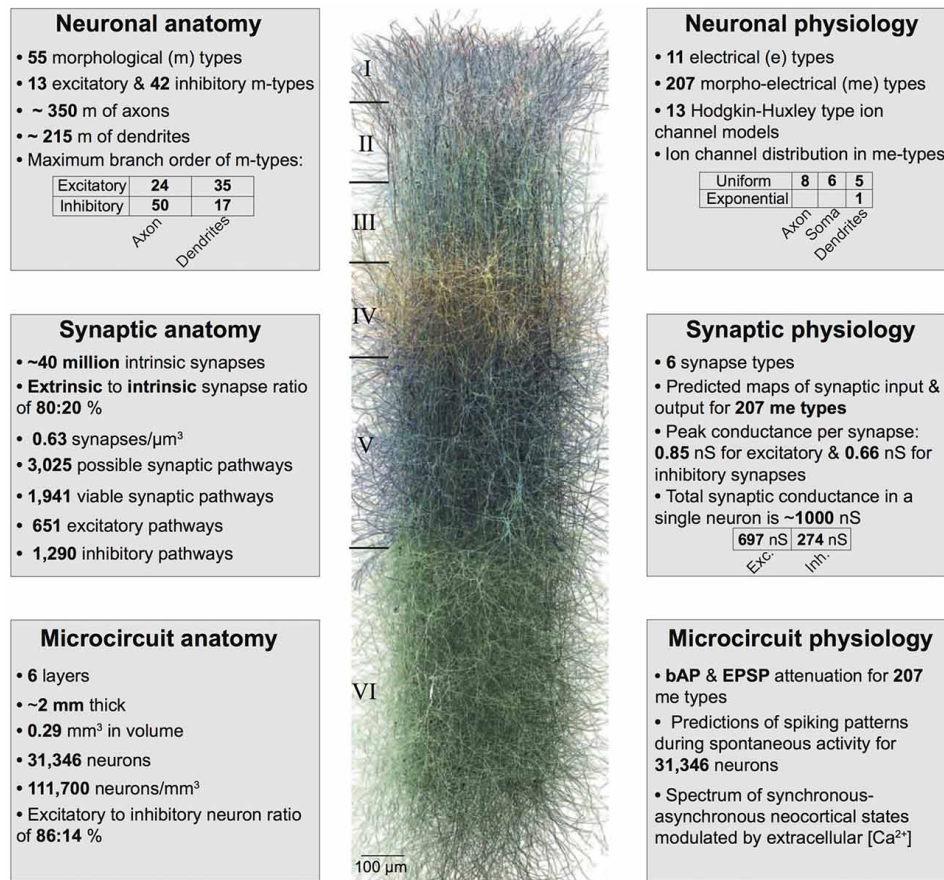


Figure 3.1: Figure 1 - Summary of the biologically detailed tissue model of neocortical microcircuitry. Top left: overview of neuronal anatomy in the reconstruction. Top right: summary of neuronal physiology. Middle left: overview of synaptic anatomy. Middle right: fact and figures on synaptic physiology. Bottom left: summary of microcircuit anatomy. Bottom right: overview of microcircuit physiology.

3.2.2 Introduction

It is thought that ACh and its interactions with other neuromodulators such as dopamine, noradrenaline and histamine is important in regulating cognitive functions including arousal and attention, sleep-wake cycles, reward,

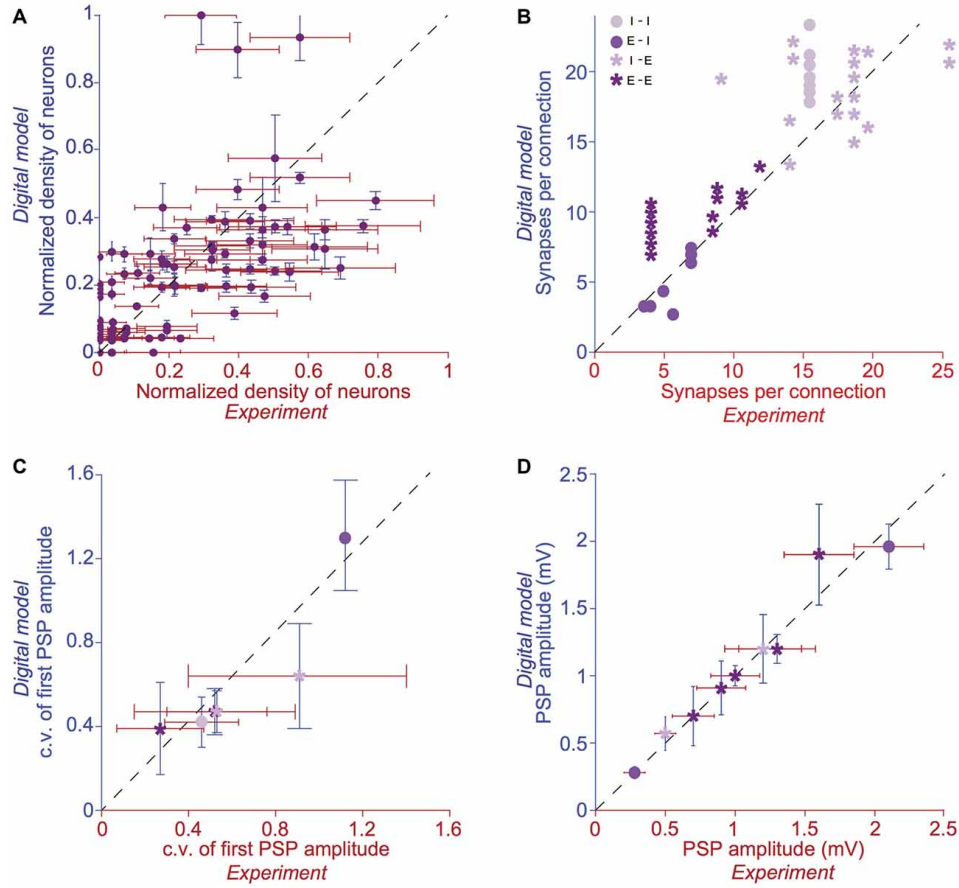


Figure 3.2: Figure 2 - Validation of anatomical and physiological properties in the tissue model of neocortical microcircuitry. (A) Normalized neuronal densities. Number of stained neurons per 100 μm bin from layers 1 to 6. Red: experiment (counts/bin), blue: digital model (counts/bin; mean \pm SD, $N = 100$ bins). Dashed line has unit slope. (B) Mean number of synapses per connection in excitatory-excitatory (E-E), excitatory-inhibitory (E-I), inhibitory-excitatory (I-E) and inhibitory-inhibitory (I-I) pathways. Red: experiment, blue: digital model. Dashed line has unit slope. (C) Mean coefficient of variation (c.v.; defined as standard deviation/mean) of the amplitude of the postsynaptic potential (PSP) for pathways some of the pathways in (B). (D) same as in C, but for the mean amplitude of the PSP for some of the pathways in (B).

learning and memory [Blandina et al., 2004, Calabresi et al., 2006, Lester et al., 2010, Constantinople and Bruno, 2011]). Yet, it has been difficult to develop a unifying view of how ACh controls neuronal and synaptic physiology and impacts neocortical network dynamics. An impediment in this direction is probably due to the fact that ACh differentially controls the activity of neocortical neurons and synapses in complex ways, making it difficult to reconcile its systemic effects [Muñoz and Rudy, 2014]. Computational models of neocortical microcircuitry at the cellular and synaptic level of biological detail not only offer an integrative platform to bring together experimental data capturing the specific effects of ACh on dendrites, neurons and synapses, but also make it possible to generate predictions on the actions of ACh at the network level. As a way forward, we developed a first-draft, data-driven framework that leverages a recent, rigorously validated digital model of the microcircuitry of juvenile rodent somatosensory cortex [Markram et al., 2015, Ramaswamy et al., 2015] (Figure 1) comprising 31000 neurons distributed across six layers, 55 layer-specific morphological (m), 11 electrical (e) and 207 morpho-electrical (me) neuron subtypes that are connected through 40 million synapses and six dynamical synapse (s) types (Figure 2). Next, we augmented the model by integrating the phenomenological cell-type specific effects of ACh neuronal and synaptic physiology from published literature [Kawaguchi and Kubota, 1997, Tsodyks and Markram, 1997, Chen et al., 2015, Gullledge and Stuart, 2005, Gullledge et al., 2007, Eggermann and Feldmeyer, 2009]. This data-driven approach enabled us to bridge how the local impact of ACh on neurons and synapses are broadcast to the global level and influence the emergence of neocortical network activity. Model parameters were not tuned to replicate any specific ACh-induced network effects. Using this framework, we derive preliminary predictions, which suggest that a dose-dependent change in ACh levels shifts neocortical network state from highly synchronous to asynchronous activity, and distinctly shapes the structure of spike-spike cross-correlations between specific neuronal populations.

3.2.3 Methods

A digital model of the microcircuitry of juvenile rodent somatosensory cortex was reconstructed as previously described [Markram et al., 2015, Ramaswamy et al., 2015, Reimann et al., 2015]. In brief, the reconstruction process comprised the following.

Microcircuit dimensions

Thicknesses of individual layers and the diameter of the microcircuit were used to construct a virtual hexagonal prism. A virtual slice was generated from a 1×7 mosaic of microcircuits as a cortical sheet with a thickness of

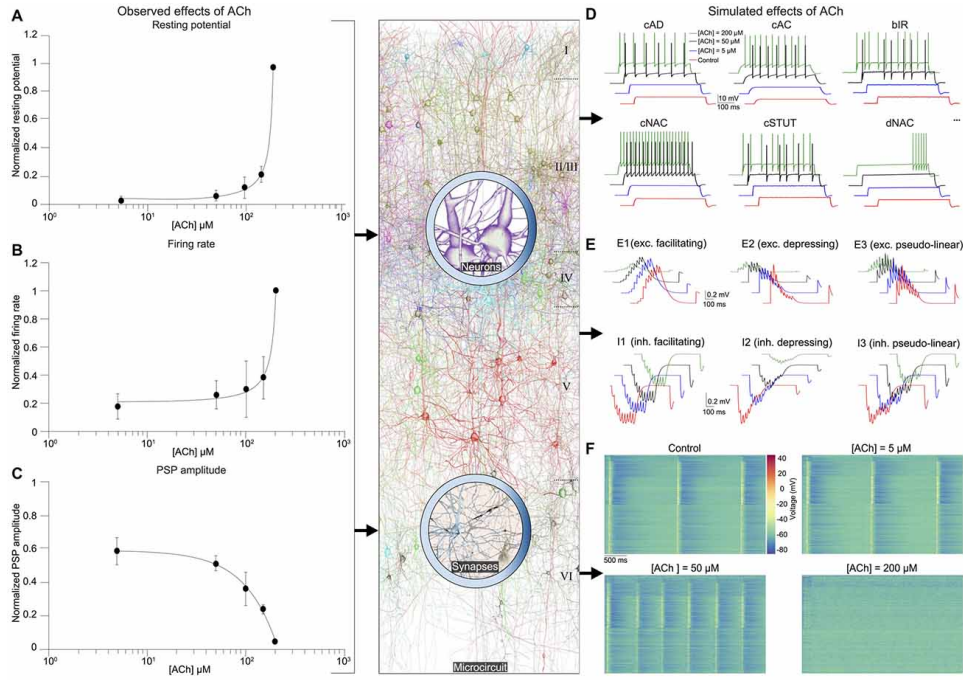


Figure 3.3: Figure 3 - Integrated summary of the cellular, synaptic and micro-circuit effects of acetylcholine (ACh) in the tissue model of neocortical micro-circuitry. (A) Integrated sparse data-sets from published literature on the dose-response effects of ACh on the normalized resting membrane potential of neocortical neurons. Error bars show SD. (B) same as in A, but for neuronal firing rate. (C) same as in A, but for the first PSP amplitude. (D) Predicted effects of different ACh levels on the resting potential and firing rate of neocortical e-types. Only six e-types are shown. cAD, continuous accommodating (all pyramidal cells); cAC, continuous accommodating (interneurons); bIR, burst irregular, cNAC, continuous non-accommodating; cSTUT, continuous stuttering; dNAC, delayed non-accommodating. (E) Predicted effects of different ACh levels on the physiology of all neocortical s-types. (F) Prediction of the effect of ACh concentration on network dynamics. Clockwise from left, voltage rasters of 1000 randomly sampled neurons across layers 1–6 at different ACh concentrations.

230.9 μm and a width of 2,800 μm .

Cellular composition

Measurements of neuronal densities across neocortical layers and fractions of m- and me-types were used to generate the position of individual neurons in the reconstructed microcircuit, constrained by layer-specific proportions of excitatory and inhibitory neurons. Each neuron was assigned the optimal morphology for its location in the microcircuit.

Digital Neuron morphologies

Neuronal morphologies were obtained from digital 3D reconstructions of biocytin-stained neurons after whole-cell patch-clamp recordings in 300 μm -thick, sagittal neocortical slices from juvenile rat hind-limb somatosensory cortex. Severed neurites of morphologies due to the slicing procedure were algorithmically regrown). Neurites were digitally unraveled to compensate for shrinkage. Neuronal morphologies were then cloned to obtain a sufficient representation of all m-types.

Electrical neuron models

Conductance based, multi-compartmental electrical models of neurons were produced using up to 13 active ion channel mechanisms and a model of intracellular Ca^{2+} dynamics. Axon initial segments (AIS), somata, basal and apical dendrites were modeled as separate, but interconnected compartments. Pyramidal neurons contained two dendritic regions, whereas interneurons contained only one dendritic region. Each region received a separate set of ion channels (see NMC portal; [Ramaswamy et al., 2015]). With respect to the axon, only the AIS was simulated due to technical limitations in simulating complete axons of all 31000 neuron models. Each AIS was represented by two fixed length sections, each with a length of 30 μm ; diameters were obtained from the reconstructed morphology used for model fitting. APs detected in the AIS were propagated to the synaptic contacts with a delay corresponding to the axonal delay required to propagate to each synapse, assuming an axonal velocity of 300 $\mu m/ms$. As previously described, electrical models were fitted using a feature-based multi-objective optimization method.

Synaptic anatomy

The number and location of synaptic contacts were derived using an algorithm, described previously [Reimann et al., 2015]. The algorithm removes axo-dendritic appositions that do not obey the multi-synapse and plasticity reserve rules and ensures compatibility with biological bouton densities.

Synaptic physiology

Excitatory synaptic transmission was modeled using both AMPA and NMDA receptor kinetics. Inhibitory synaptic transmission was modeled with a combination of GABA-A and GABA-B receptor kinetics. Stochastic synaptic transmission was implemented as a two-state Markov model of neurotransmitter release, a stochastic implementation of the Tsodyks-Markram dynamic synapse model. Biological parameter ranges for the three model parameters—neurotransmitter release probability, recovery from depression and facilitation—were obtained from experimental measurement for synaptic connections between specific m- and me-types or between larger categories of pre and postsynaptic neurons.

Microcircuit simulation

The digital model of neocortical microcircuitry was simulated using the NEURON simulation environment, augmented for execution on a supercomputer [Hines and Carnevale, 1997, Hines et al., 2008], along with custom tools to setup and configure microcircuit simulations, and read output results. We simulated spontaneous background activity by injecting tonic background depolarization to the somata of all neurons, and by modeling miniature PSCs, which were implemented using an independent Poisson process (of rate λ_{spont}) at each individual synapse to trigger low release. Spontaneous release rates for inhibitory and excitatory synapses were parameterized to match biological observations [Ling and Benardo, 1999, Simkus and Stricker, 2002]. The excitatory spontaneous rate was scaled up per layer to account for missing extrinsic excitatory synapses projecting from subcortical regions, such as the thalamus. The resulting spontaneous release rates for unitary synapses were low enough (0.01 Hz–0.6 Hz) so as not to significantly depress individual synapses.

Implementation of dose-dependent effects of ACh on cellular excitability

Dose-dependent effects of ACh on cellular excitability was achieved by depolarizing somatic step current injection, which caused an increase in the resting membrane potential and firing frequency. Step currents were expressed in terms of percentage of the minimum step current injection required for each cell to spike at least once (rheobase).

Implementation of dose-dependent effects of ACh on synaptic transmission

Dose-dependent effects of ACh on synaptic physiology was achieved by changing the utilization of synaptic efficacy parameter (U) in the stochastic

synapse model. The effect of ACh on excitatory and inhibitory synaptic response amplitudes were simulated by modifying the neurotransmitter release probability for all synaptic contacts underlying m-type specific connections according the extrapolated dose-dependence curve compiled from literature. Due to lack of data for specific synaptic connection-types, we assumed that all excitatory and inhibitory connections showed the same dose-dependent effects to ACh.

Cross-correlations

Mean spike-spike cross-correlations were computed as the average of all spike-times measured in 10000–20000 randomly sampled pairs of excitatory–excitatory (E-E), excitatory–inhibitory (E-I), inhibitory–excitatory (I-E) and inhibitory–inhibitory (I-I) neurons. Cross-correlograms were computed in Matlab (version 9.1).

3.2.4 Results

ACh modulation of neuronal physiology

Cell-type	Experimental technique	Physiological effect	References
L23 PC	Bath-application of ~5–100 μ M of CCh in Rat/Mouse cortical slices (P13–28)	Prolonged depolarization; increased firing rate	Vidal and Changeux (1993); Levy et al. (2008); Eggermann and Feldmeyer (2009); Chen et al. (2015)
L23 MC	Bath-application of ~10–100 μ M of CCh in Rat/Mouse cortical slices (P13–28)	Depolarization; increased firing rate	Chen et al. (2015)
L23 SBC/DBC/BP	Bath-application of ~10–100 μ M ACh in Rat/Mouse cortical slices (P18–28)	Depolarization; increased firing rate	Kawaguchi (1997); Chen et al. (2015)
L5 PC	Bath-application of ~100–200 μ M ACh in Rat cortical slices (P18–60)	Slow depolarization; Increased firing rate	Gulledge and Stuart (2005); Eggermann and Feldmeyer (2009); Dasari et al. (2017)

Figure 3.4: Table 1 - Summary of input data sources on ACh-induced effects on the excitability of neocortical cell-types

Next, we integrated experimental data on the impact of ACh on the resting membrane potential and cellular excitability of neocortical neurons, which enabled us to build a dose-dependent activation profile across a range of ACh concentrations obtained from published literature (Figures 3A,B; see Table 1). We have previously shown that a piece of neocortical tissue, 0.3 mm³ in volume, consists of 55 m-types and 11 e-types, resulting in 207 me-types (for a description of m-, e- and me-types see <https://bbp.epfl.ch/nmc-portal/glossary>) distributed across six layers (Figure 1). Next, we used validated digital models of 207 me-types that were optimized to reproduce diverse electrophysiological features of excitatory and inhibitory neocortical neurons such as AP amplitudes and widths, mean firing frequency and accommodation index [Ramaswamy et al., 2015, Van Geit et al., 2016]. We extended these models by identifying an appropriate level of depolarizing step current injection into the soma, which led to an increase in the resting

membrane potential and firing frequency of each me-type to mimic the dose-dependent effects of ACh on cellular excitability (Figure 3D; see “Methods,” section). The amount of injected step current used to simulate cellular excitability at different ACh levels was expressed in terms of percentage of the minimum current injection required for each me-type model to generate at least a single AP (rheobase; see “Methods,” section). In this first-draft implementation of the framework, obtained by augmenting an existing detailed model of neocortical microcircuitry, we began by assuming that all excitatory and inhibitory me-types respond similarly to ACh levels. Excitatory me-types including PCs in all layers and L4 spiny neurons were grouped together. All me-types responded with a change in intrinsic excitability that was predicted to switch from sub-threshold to supra-threshold behavior at an ACh concentration of $50 \mu M$ (Figure 3D; six randomly chosen me-types are shown). The mean AP firing frequency in all me-types increased significantly from 5 Hz to 10 Hz for a four-fold change in ACh from $50 \mu M$ to $200 \mu M$ (Figure 3D).

ACh modulation of synaptic physiology

Connection-type	Short-term dynamics	Experimental technique	Physiological effect	Reference
L23 PC \rightarrow L23 BC	E2 Excitatory, depressing	Bath-application of $\sim 5 \mu M$ of CCh in Rat S1 slices (P11–26)	Reduction of first PSP amplitude to $\sim 60\%$ of control	Levy et al. (2008)
L23 PC \rightarrow L23 PC	E2 Excitatory, depressing	Bath-application of $\sim 10 \mu M$ oxotremorine or muscarine in Rat A1 slices (P21–28)	Decreases first EPSC amplitude to $\sim 53\%$ of control	Atzori et al. (2005)
L4 excitatory \rightarrow L4 excitatory	E2 Excitatory, depressing	Bath-application of $\sim 100 \mu M$ ACh in Rat S1 slices (P18–24)	Diminishes first PSP amplitude to $\sim 40\%$ of control	Eggermann and Feldmeyer (2009)
L5 PC \rightarrow L5 PC	E2 Excitatory, depressing	Bath-application of ~ 100 – $150 \mu M$ ACh in Rat S1 slices (P13–15)	Reduction of first PSP amplitude to $\sim 25\%$ of control	Tsodyks and Markram (1997)
L5 PC \rightarrow L5 PC	E2 Excitatory, depressing	Bath-application of $\sim 200 \mu M$ ACh in Rat S1 slices (P13–15)	Decreases first PSP amplitude to $\sim 5\%$ of control	Tsodyks and Markram (1997)

Figure 3.5: Table 2 - Summary of input data sources on ACh-induced effects on the physiology of neocortical synaptic connections

As the next step, we unified relevant published data, and extrapolated a dose-dependent activation curve of the effects of varying concentrations of ACh on the response amplitude of the first PSP for all neocortical s-types (Figure 3C; see Table 2). It is known that neocortical synapses exhibit at least six distinct forms of excitatory (E) and inhibitory (I) short-term plasticity that are used to distinguish synaptic connections into facilitating (E1 and I1), depressing (E2 and I2), and pseudo-linear (E3 and I3) dynamic s-types [Reyes et al., 1998, Gupta et al., 2000, Thomson, 2007]. We have previously shown that 55 m-types establish around 1,941 morphology-specific synaptic connection types, whose dynamics are governed by one of the six s-types dictated by the pre-post combination of m-types [Markram et al., 2015, Ramaswamy et al., 2015, Reimann et al., 2015]. We augmented this model to include the effects of ACh modulation of the first PSP amplitude

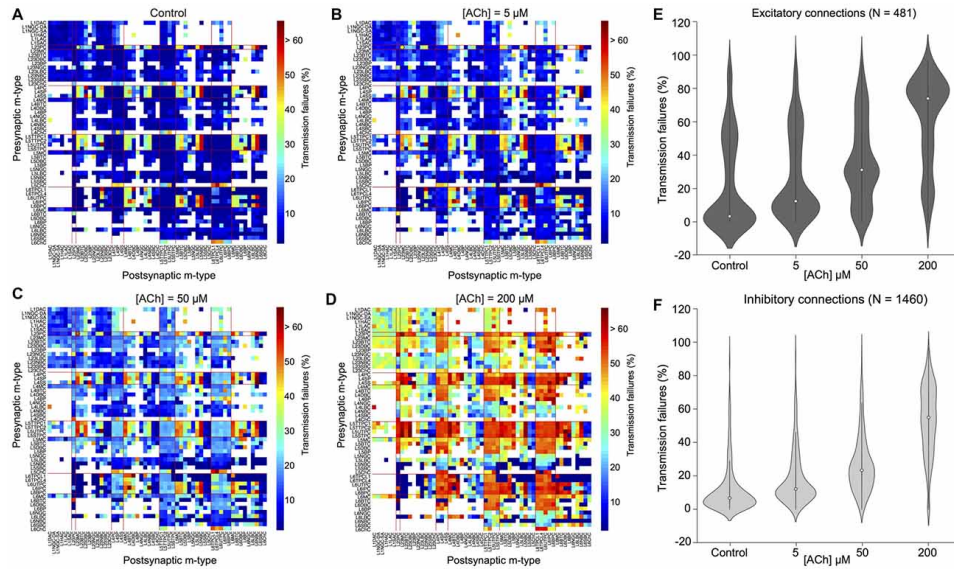


Figure 3.6: Figure 4 - ACh modulates synaptic transmission failures and reorganizes network connectivity. (A) A matrix representation of the average synaptic transmission failures for 1941 connections formed between the 55 m-types (presynaptic on x-axis; postsynaptic on y-axis) in the control condition. Red lines separate excitatory and inhibitory m-types. Black circle shows the L23PC to L23MC connection. (B) Same as in A, but for $[ACh] = 5 \mu M$. (C) Same as in A, but for $[ACh] = 50 \mu M$. (D) Same as in A, but for $[ACh] = 200 \mu M$. (E) Violin plot showing the complete probability density distribution of synaptic transmission failures for all excitatory connections ($N = 481$) in the control condition and across different ACh levels. White circle inside the violin plot shows the median of the distribution. Black line shows the interquartile range. (F) Same as in E, but for all inhibitory connections ($N = 1460$).

of s-types and derived predictions on how their short-term facilitating, depressing and pseudo-linear dynamics are controlled by ACh (Figure 3E). It is known that ACh powerfully modulates the PSP amplitude of synaptic connections between excitatory neocortical m-types, very likely by modifying the probability of glutamate release [Levy et al., 2008, Eggermann and Feldmeyer, 2009]. However, it remains unclear if ACh controls inhibitory synaptic transmission in the neocortex by modulating GABA release in similar ways to glutamate [Kruglikov and Rudy, 2008, Yamamoto et al., 2010]. Therefore, in this first-draft implementation, we assumed that ACh regulates the physiology of both excitatory and inhibitory synaptic connections in comparable ways (Figure 3C; see Table 2). In order to simulate the change in PSP amplitude as a function of ACh concentration, we modified the neurotransmitter release probability for all synaptic contacts underlying m-type specific connections according the extrapolated dose-dependence curve compiled from literature (Figure 3C).

We found that ACh exerted highly diverse effects on the PSP amplitude for the six s-types (Figure 3E). The impact of ACh concentrations (5–200 μM) on the first PSP amplitude evoked by injecting a train of nine APs at 30 Hz into the presynaptic soma was superficial compared to control for both E1 (between a L23 PC and a MC) and I1 (between a L23 small basket cell (SBC) and a PC) s-types (Figure 3E, top left; maximum responses are normalized to control). However, the very pronounced facilitation typically observed for the E1 s-type was strongly suppressed at higher (200 μM), rather than lower concentrations (5–100 μM) of ACh (Figure 3E, top left). We found that the amplitude of the first PSP and the subsequent facilitating dynamics for the I1 s-type was not substantially modulated by ACh, despite a four-fold increase in concentration (Figure 3E, bottom left; from 5 μM to 200 μM). The physiology of both E2 (between L5 two thick-tufted pyramidal cells; Figure 4E, top center) and I2 (between a L5 MC and a TTPC; Figure 3E, bottom center) s-types was crucially impacted by different ACh levels (5–200 μM). On average, the first PSP amplitude for both E2 and I2 s-types was reduced to about 75%, 50% and 10% of control at ACh concentrations of 5, 50 and 200 μM ACh, respectively (Figure 3E, top and bottom center). Amplitude of subsequent PSPs decreased to 50%–80% of control with markedly diminished rates of depression, but consistent with previous observations, did not critically impact the amplitude of stationary PSPs [Tsodyks and Markram, 1997, Levy et al., 2008, Eggermann and Feldmeyer, 2009]. Higher concentrations of ACh at 200 μM almost completely shutoff depressing synaptic transmission (Figure 3E, top and bottom center). For E3 (between two L6 PCs; Figure 4E, top right) and I3 (between a L5 Nest basket cell (NBC) and a TTPC; Figure 3E, bottom right) pseudo-linear s-types ACh concentrations between 5–100 μM did not cause an increase

in the amplitude of the first PSP in a train. At ACh concentrations of 5 and 50 μM , the mean amplitude of the first PSP for E3 and I3 s-types was approximately 70% and 85% of control, respectively (Figure 3E, top and bottom right). Whereas, the amplitude of the first PSP at 200 μM ACh was diminished to about 10% and 50% for E3 and I3 s-types, respectively (Figure 3E, top and bottom right). However, despite an exponential increase in ACh levels from 5 μM to 200 μM the modulation of pseudo-linear dynamics for E3 and I3 s-types appeared to be insensitive to ACh. We predict that an increase in ACh concentration, more than an order of magnitude, has a steep modulatory effect on the physiology of E2 and I2 s-types, but only a superficial impact on E1, I1, E3 and I3 s-types.

The diversity of the effects of ACh on the dynamics of the six s-types is somewhat surprising because we implemented homogeneous ACh-induced effects on excitatory and inhibitory synaptic connections in this first-draft framework. Although an exhaustive exploration is beyond the scope this study, it is very likely that the predicted differences in ACh-induced effects on synaptic transmission could arise due to the fact that the anatomical and physiological properties for each of the six s-types in the detailed digital model of neocortical microcircuitry, which forms the foundation for the framework presented here, are quite diverse [Markram et al., 2015]. For example, in the detailed digital microcircuit model, there is a large variability in the mean number of synapses for each of the six s-types, which ranges from 5 to 20 contacts per connection, the clear-cut innervation patterns by which synaptic contacts are distributed due to distinct axo-dendritic morphologies, and the specific parameter sets used to model synaptic transmission—peak quantal conductances, release probabilities, time constants for recovery from facilitation and depression [Markram et al., 2015, Ramaswamy et al., 2015, Reimann et al., 2015]. Given that ACh levels modulate the first PSP amplitude by modifying the probability of neurotransmitter release, it should also influence the efficacy and reliability of synaptic transmission. We, therefore, took advantage of our framework to investigate how ACh concentration impacts the reliability of transmission for all 1,941 morphology-specific synaptic connections formed by 55 m-types in neocortical microcircuitry. The average transmission failures for all synaptic connections in the control condition without any ACh was $14.3 \pm 19.1\%$ (mean \pm SD, $N = 1,941$ connections), $22.6 \pm 27.1\%$ for all excitatory connections ($N = 481$) and 11.6 ± 14.7 for all inhibitory connections ($N = 1460$). Transmission failures for all synaptic connections at simulated ACh levels of 5, 50 and 200 μM increased nearly fourfold in comparison against control to $20.5 \pm 19.3\%$, $29 \pm 19.7\%$ and $55.3 \pm 22.6\%$, respectively. Figures 4A–D shows the predicted average transmission failures for all the 1,941 synaptic connections across different simulated levels of ACh. Upon closer examination, we found

that the average transmission failures for all excitatory synaptic connections ($N = 481$) at simulated ACh concentrations of 5, 50 and 200 μM changed nearly threefold compared against control to $27.3 \pm 25.5\%$, $36.3 \pm 24.7\%$ and $61 \pm 26.7\%$, respectively (Figure 4E). Transmission failures for all inhibitory connections ($N = 1460$) at simulated ACh levels of 5, 50 and 200 μM changed nearly four fold in comparison against control to $18.3 \pm 16.2\%$, $26.6 \pm 17.5\%$ and $53.5 \pm 20.8\%$, respectively (Figure 4F).

Our preliminary predictions could provide insight on how ACh modulates local cell-type specific connectivity maps between pairs of pre-postsynaptic neurons to reorganize network architecture. In the control case, without ACh, failures between most of the 1,941 morphology-specific synaptic connections are low, which results in highly reliable transmission, and therefore, translates to a higher correlation of a presynaptic spike evoking a postsynaptic response. As ACh concentration increases, failures between synaptic connections increase, which shifts the map of reliable transmission in favor of lower correlation of a presynaptic spike inducing a postsynaptic response. Experimental studies that have attempted to characterize the effects of ACh on enhancing synaptic properties under in vivo-like conditions, in particular transmission failures are few and far between. However, a recent study examined ACh-induced effects on pairs of excitatory L23 PCs and inhibitory somatostatin-expressing neurons (putative MCs) in mouse visual cortex, which are predominantly mediated by weak, facilitating synapses [Urban-Ciecko et al., 2018]. The study, which undertook paired whole-cell recordings in vitro by mimicking in vivo-like conditions (high CCh and low Ca^{2+} levels in the extracellular recording medium), and also through endogenous ACh release by optogenetic stimulation in vivo, reported that synaptic transmission between these cell-types was marked with high failures, in the order of 70% on average [Urban-Ciecko et al., 2018]. Although, our framework cannot fully mimic in vivo states, predictions of average synaptic transmission failures for connections between L23 PCs and MCs at high ACh concentrations (Figure 4D; about 75% at 200 μM) are consistent with experimental findings. Indeed, our results need to be further validated through targeted experiments. However, the predicted non-linear change in transmission failure rates of all synaptic connections as a function of varying ACh levels is rather striking despite an assumption of homogeneous ACh-mediated effects on both excitatory and inhibitory synapses.

ACh modulation of network activity

It is thought that ACh enhances arousal and vigilance in primary sensory cortices by altering the signal-to-noise ratio of incoming synaptic input [Minces et al., 2017]. However, it remains unclear how the differential regulation of neuronal and synaptic physiology by ACh, specifically the modulation

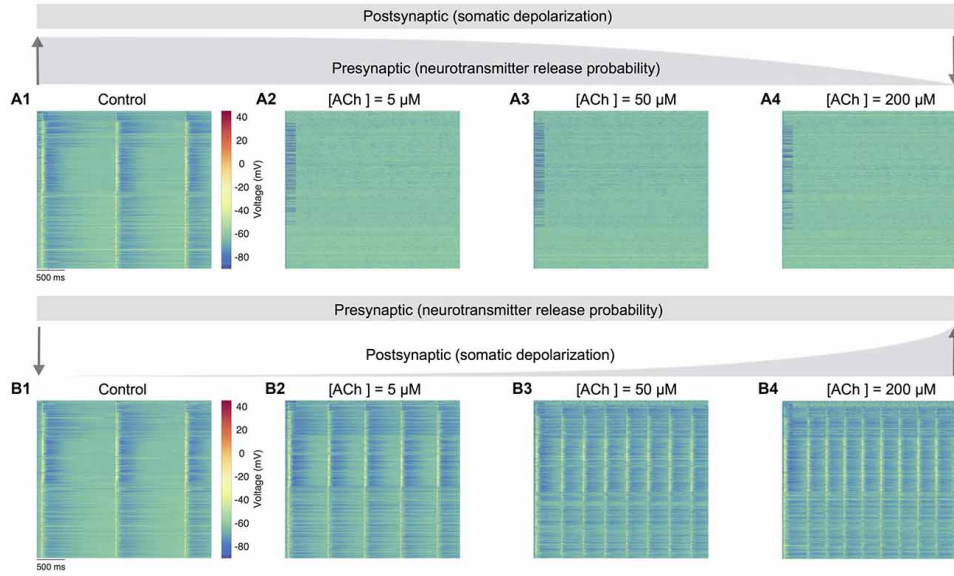


Figure 3.7: Figure 5 - Predicting only the pre- and postsynaptic effects of ACh on network activity. (A1) Voltage raster of 1000 randomly sampled neurons across layers 1–6 with neurotransmitter release probability and somatic depolarization values resembling the control condition. (A2) Same as A1, but with constant somatic depolarization and neurotransmitter release probability resembling $[ACh] = 5 \mu M$. (A3) Same as A1, but with constant somatic depolarization and neurotransmitter release resembling probability $[ACh] = 50 \mu M$. (A4) Same as A1, but with constant somatic depolarization and neurotransmitter release probability resembling $[ACh] = 200 \mu M$. Upward and downward arrows depict the changing gradient of neurotransmitter release probability. (B1) Voltage raster of 1000 randomly sampled neurons across layers 1–6 with neurotransmitter release probability and somatic depolarization values resembling the control condition. (B2) Same as in B1, but with constant neurotransmitter release probability and somatic depolarization resembling $[ACh] = 5 \mu M$. (B3) Same as in B1, but with constant neurotransmitter release probability and somatic depolarization resembling $[ACh] = 50 \mu M$. (B4) Same as in B1, but with constant neurotransmitter release probability and somatic depolarization resembling $[ACh] = 200 \mu M$. Downward and upward arrows depict the changing gradient of somatic depolarization.

of feedforward excitatory and feedback inhibitory transmission, influences the emergence of neocortical network activity. Previous work has shown that failure of synaptic transmission leads to a suppression of firing rate oscillations and network synchrony [Rosenbaum et al., 2014]. In the next set of simulations, we investigated the impact of the ACh-induced changes on the physiology of 31000 neurons and 1941 morphology-specific synaptic connections in collectively shaping the dynamics of neocortical microcircuitry. We incorporated phenomenological models of ACh control of neuronal and synaptic physiology into a validated digital model reconstruction of neocortical microcircuitry [Markram et al., 2015] and explored how ACh-induced effects on local cells and synapses modulate global network activity.

To enable a direct comparison with experimental data obtained from cortical slices on the impact of ACh on cellular excitability and synaptic transmission, we created a virtual slice (with a thickness of $231\ \mu\text{m}$; see “Methods,” section) to explore neocortical network activity for a range of ACh concentrations (see “Methods,” section). We simulated spontaneous activity in the virtual slice by applying tonic background depolarization (see “Methods,” section) and found that in the control condition without any extracellular ACh, neocortical network activity exhibited low-frequency ($1.7\ \text{Hz}$), highly synchronous bursts of oscillatory behavior (Figure 3F, top left) akin to previous reports of regular rhythmic activity during slow-wave sleep [Steriade et al., 1993, Sanchez-Vives and McCormick, 2000, Reyes, 2003]. ACh concentrations at 5 and $50\ \mu\text{M}$ further diminished the frequency of synchronous oscillatory network activity (Figure 3F, top right and bottom right). At ACh levels of $200\ \mu\text{M}$, slow oscillatory bursts of synchronous network activity were superseded by irregular asynchronous activity, resembling active waking states (Figure 3F, bottom right). The transition from synchronous to asynchronous neocortical states occurred at $75\ \mu\text{M}$. Interestingly, we found that a change in $50\ \mu\text{M}$ of ACh can switch neocortical dynamics from the synchronous to asynchronous state, divulging two distinct network activity regimes. The mechanisms giving rise to this sharp transition of network activity from synchrony to asynchrony are very likely due to alterations brought about by diverse ACh-induced changes in cellular excitability, physiology of 1941 synaptic connections and transmission failure rates, and highly correlated excitatory synaptic conductance changes across 31000 neurons that are almost completely abolished by uncorrelated inhibition.

Next, we gauged the effects of perturbing only presynaptic (neurotransmitter release probability) or postsynaptic (somatic depolarization) parameters in regulating spontaneous network activity (Figure 5). An extensive parameter sweep of all modeled presynaptic and postsynaptic mechanisms

is beyond the scope of this study. We therefore, undertook simple manipulations to explore the impact on network dynamics under two conditions: (1) only the neurotransmitter release probability was gradually changed as before (see “ACh Control of Synaptic Physiology,” section; Figure 3C) to solely simulate the specific presynaptic effects of ACh, but the postsynaptic mechanism achieved through somatic depolarization was fixed at a value matching the control condition in the absence of ACh (see Figures 3A,B); and (2) only the somatic depolarization was gradually varied as above (see “ACh Modulation of Neuronal Physiology,” section; see Figures 3A,B) to exclusively mimic the postsynaptic effects of ACh, but the presynaptic effects attained by changing neurotransmitter release probability was kept constant, again at a value matching the control condition in the absence of ACh (see Figure 3C).

In the first set of simulations, we manipulated only the presynaptic parameter, corresponding to the effects of varying ACh levels exclusively on the neurotransmitter release probability. Expectedly, network activity was highly synchronous at high release probability of all synapses analogous to an absence of ACh in the control case (Figure 5A1). However, continuously altering only the presynaptic parameter through a gradual decrease of neurotransmitter release probability pushed network activity much faster towards asynchrony. Surprisingly, asynchronous network activity remained persistent across changes to presynaptic neurotransmitter release probability resembling low to high ACh levels as before (Figures 5A2–A4). In the next set of simulations, we altered only the postsynaptic parameter reflecting the impact of changing ACh levels specifically on cellular excitability, which was achieved by gradually changing the amount of current required for somatic depolarization as before. In these simulations, the presynaptic parameter was unchanged throughout, and fixed at a high release probability matching the control case. Indeed, it was not surprising that network activity was again synchronous at high release probability and low depolarization levels (Figure 5B1). However, a gradual increase in somatic depolarization levels resulted in network activity becoming more synchronous with an increase in the frequency of oscillatory bursts (Figures 5B2–B4). Modifying only the presynaptic release probability but keeping postsynaptic somatic depolarization unchanged seems to suggest that the effects of ACh on cellular excitability are essential to gradually, but not abruptly transition network activity from synchrony to asynchrony. An exhaustive analysis of the functional implications of such a sharp transition in network activity is not attempted here. However, from a global standpoint, this sudden shift from synchrony to robust asynchrony could suggest that altered ACh release might lead to sleep disruption, which might result in a failure of memory consolidation [Hasselmo, 1999, Power, 2004]. On the other hand, modifying

only the postsynaptic depolarization but maintaining a constant presynaptic release probability causes strong, recurrent network activity with a heightened occurrence of oscillatory bursts. This manipulation suggests that the simultaneous effects of an increase in ACh-induced depolarization, which is balanced with a mirroring decrease in neurotransmitter release probability, is crucial to transition network activity from synchrony to asynchrony—for example, in enabling the changeover from non-rapid eye movement (nREM) to REM sleep or waking [Steriade, 2004]. Although this warrants further investigation, our preliminary predictions are consistent with previous work showing that a breakdown in the presynaptic effects of ACh could lead to epileptiform-like activity in the neocortex [Schwartzkroin, 1994].

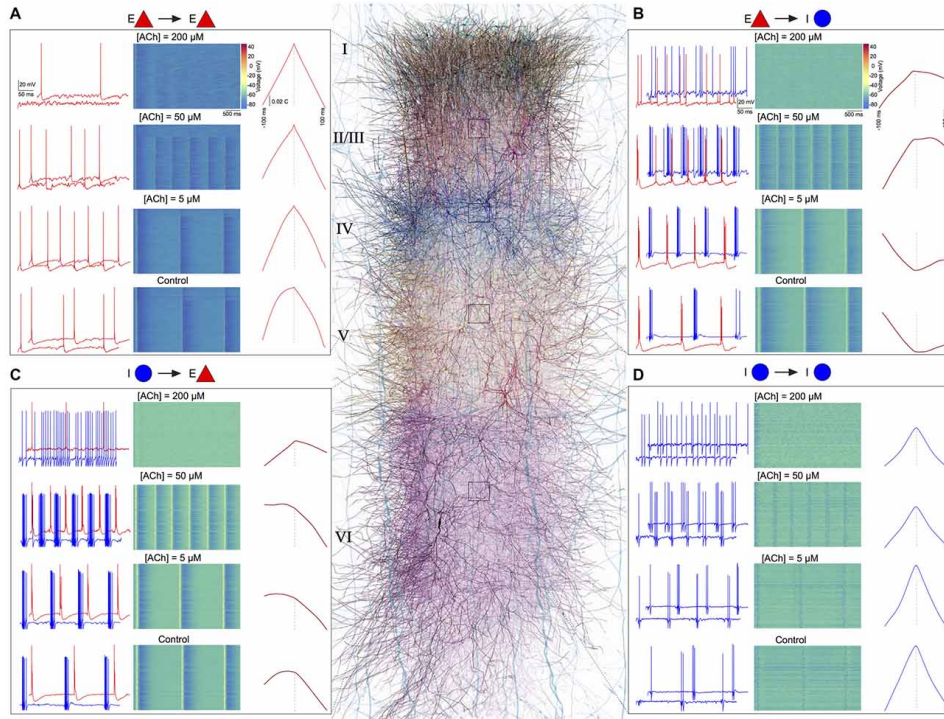


Figure 3.8: Figure 6 - ACh shapes spike-spike cross-correlations. (A) Left: spontaneous spiking activity in a randomly chosen pair of E-E (L23 PC-L23 PC) neurons at different ACh levels. Middle: voltage raster for all L23 PCs at different ACh levels. Right: spike-time cross correlations for 10000–20000 randomly sampled pairs of L23PCs at different ACh levels. (B) same as in A, but for E-I neurons (L4 PC-L4 Nest basket cell (NBC)) (C) same as in A, but for I-E neurons (L5 NBC-L5 thick-tufted layer 5 pyramidal cell (TTPC)) (D) Same as in A, but for I-I neurons (L6 MC-L6 Martinotti cell (MC)).

Finally, we investigated the effect of ACh concentrations in shaping spike-time cross-correlations for pairs of neurons—E-E (L23 PC-L23 PC; Figure 6A), E-I (L4 PC-L4 NBC; Figure 6B), I-E (L5 NBC-L5 TTPC; Figure 6C), and I-I (L6 MC-L6 MC; Figure 6D). We observed a striking diversity in the average cross-correlation profiles for different pairs of neurons compris-

ing these populations, which was computed as the mean spike-time cross-correlation from 10000 to 20000 randomly sampled pairs. At the outset, correlations differed in their temporal profiles (Figures 6A–D). Upon closer examination of these correlation profiles, in particular with the peak lag (delay to peak) and the median lag (delay of the median) revealed that they differed significantly between all examined populations (Figures 6A–D). For example, between pairs of excitatory neurons, the cross-correlations at different ACh concentrations were similar to auto-correlations, with a very small range in peak lag values (Figure 6A) in comparison to the cross-correlations between excitatory and inhibitory neurons (Figure 6B). Our preliminary results predict that ACh release from subcortical structures, such as the NBM, powerfully modulates neocortical activity giving rise to a spectrum of network activity ranging from one extreme where low ACh levels bring about synchronous activity, to another, where high ACh concentrations lead to asynchrony. Our results are broadly consistent with studies employing optogenetic approaches that associate nREM sleep states with low ACh levels and wakefulness or REM sleep with high ACh concentrations [Lee and Dan, 2012, Chen et al., 2015]. We have previously demonstrated that extracellular calcium (Ca^{2+}) regulates the emergence of synchronous and asynchronous network activity in the neocortex [Markram et al., 2015]. Based on these preliminary predictions, we hypothesize that neuromodulators, such as ACh, provide a complementary functional mechanism in the neocortex, similar to a “push-pull” switch, where the interplay of low ACh and high Ca^{2+} pushes network state towards synchronous activity, whereas high ACh and low Ca^{2+} levels pulls network activity towards asynchrony. We propose that ACh orchestrates neocortical dynamics by generating a spectrum of network activity—where a regime of correlated firing in neurons causes synchronous activity that could modulate functions such as coincidence detection, response selection and binding, and asynchronous activity could promote encoding of new information boosted by heightened attention to incoming sensory input.

3.2.5 Discussion

This study presents a first-draft implementation of a data-driven framework, which unifies the phenomenological effects of the regulation of local cellular excitability and synaptic physiology by neuromodulators into a data-driven digital model of neocortical microcircuitry to predict their global impact on the emergence of spontaneous network activity, without any parameter tweaking. As a first foray into exploring the utility of this framework, we integrated biological data on how ACh controls the electrical and synaptic properties of cell-types in the rodent neocortex and derived preliminary insights into how a range of ACh levels generated a spectrum of network activity. Numerous computational models have been proposed to predict cholin-

ergic regulation of network dynamics [Hasselmo, 1993, Hasselmo, 1995, Hasselmo, 2006, Fellous and Linster, 1998, Tiesinga et al., 2001, Stiefel et al., 2009, Fink et al., 2011, Fink et al., 2013]. However, most of these models have been implemented to specifically replicate distinct behavioral roles of ACh, such as in learning and memory, or by specifically tuning model parameters to match a particular network-level phenomenon. To the best of our knowledge, our data-driven framework, is probably the first bottom-up effort to model cholinergic effects on local cells and synapses and predict emergent global network dynamics, without any parameter tweaking to replicate specific forms of network activity. Our framework, which is an extension of a rigorously validated, detailed biological model of neocortical microcircuitry could, therefore, serve as a substrate to develop hypotheses on the cellular and synaptic mechanisms by which ACh controls network dynamics. Emerging experimental state-of-the-art suggests that ACh exerts a divergent control of neocortical neurons and synapses. The effects of ACh on the vast majority of neurons and synapses in the neocortex remains unknown. However, the advent of optogenetics to interrogate the cell-type specific effects of ACh combined with a data-driven computational framework, such as the one presented here holds promise in filling knowledge gaps and accelerating our understanding of the complex spatiotemporal actions of ACh in the neocortex. Although our framework can already provide preliminary insights into ACh regulation of neocortical states by bridging cellular, synaptic and network levels, it is still a first-draft and lacks numerous biological details on the anatomy and physiology of ACh innervation of neocortical layers and neurons. Indeed, in this first-draft implementation, we assumed that the dose-dependent activation profile of ACh is homogeneous on excitatory and inhibitory cell-types and their synaptic connections, which is a gross generalization. For example, recent work reports that ACh inhibits L4 spiny neurons through muscarinic receptors, as against persistent excitation of L23 and L5 PCs [Eggermann and Feldmeyer, 2009, Dasgupta et al., 2018] and could have contrasting effects on sub-types of PCs located in the same neocortical layer and region [Joshi et al., 2016, Baker et al., 2018]. As the next step to refine the biological accuracy and specificity of our framework, we plan to systematically incorporate physiological data on cholinergic varicosities, receptor localization and kinetics of ACh receptors, and specific ACh-induced effects on neuronal and synaptic function of an assortment of neocortical cell-types. A methodical integration of biological data on neuromodulatory control of neocortical cells and synapses into the unifying framework will enable the identification of the unknowns, reconciliation of disparate datasets, and prediction of their general organizing principles. Additionally, our framework not only allows further investigation on the role of ACh in regulating neocortical dynamics but can also be applicable to hypothesize and predict the function of other major neuromodulators—noradrenaline, dopamine, serotonin and histamine—that influence

the emergence of network activity. In conclusion, we propose the framework as a complementary resource to existing experimental and theoretical approaches to advance our understanding of how neuromodulatory systems differentially regulate the activity of a diversity of neurons and synapses and sculpt neocortical network activity.

3.3 Extending the framework to other neuromodulators

3.3.1 Dopamine

Dopamine is likely the most well-known neuromodulator because of its powerful actions on behavior [Tritsch and Sabatini, 2012]. DA release has been extensively studied in subcortical areas such as the VTA, the striatum and the midbrain where it is associated to movement initiation and execution, but also to the regulation of cognitive processes such as motivation and learning, reward prediction error and many others [Schultz, 2007]. Dopaminergic functions can be inferred from behavioral deficits: experimentally-induced lesions to the striatum and the consequential loss of dopaminergic neurons result in severe dysfunctions similar to those associated to Parkinson’s disease (PD). Moreover, DA is involved in various psychiatric conditions such as schizophrenia, depression, ADHD and OCD [Grace, 2016, Koo et al., 2010], and dopaminergic agonists are psychotomimetic drugs. Dopaminergic projections in rodents brains can be subdivided in two main pathways: the mesostriatal pathway that mostly projects to the striatum, and the mesocorticolimbic pathway that targets preferentially motor regions in the frontal lobe, the anterior cingulate cortex and rhinal cortices [Descarries et al., 1987]. Compared to motor regions, sensory cortices receive a much sparser dopaminergic innervation, and not many studies have explored the role of DA in sensory processing [Jacob and Nienborg, 2018].

DA transmission is accomplished by its binding to five different receptor subtypes, D_1R to D_5R receptors, and can occur both via synaptic release from DA varicosities and volumetric transmission through the formation of a network of extra synaptic receptor complexes [Borroto-Escuela et al., 2018]. Many studies have investigated the distribution of DA receptors (DRs) and their putative juxtaposition with DA terminals and concluded that short-distance volumetric transmission is the major mode of dopaminergic release, given the frequent lack of co-localization between DRs immunoreactive structures and DA varicosities. However, there exist also evidence to the contrary: some authors have observed that up to 25% of DA varicosities are in close contact with the D_4 dopaminergic receptors, which are mainly localized in L2 and L3 of sensory cortices, suggesting that synaptic transmission

of DA also exists [Rivera et al., 2008]. Points of contact between tyrosine hydroxylase (TH) immunoreactive terminals and post-synaptic structures have potentially been overlooked, similarly to ACh synapses [Takács et al., 2013, Uchigashima et al., 2016]. Neuromodulatory synapses are difficult to find with traditional methods, but the presence of neuroligin-2 (a type of synaptic adhesion protein) might be a novel indicator of the presence of heterologous dopaminergic synapses. Even though dopaminergic receptors are not clustered on the post-synaptic sites in this case, such heterologous contacts might be an expedient to increase the specificity of dopaminergic modulation by securing dopamine release sites to dopamine-sensing targets. Moreover, short-latency dopaminergic transmission has been observed [Beckstead et al., 2004, Mylius et al., 2015] both in the cortex and subcortical structures. Therefore, dopaminergic release likely reflects a mixture of spatiotemporal dynamics.

The effects of DA on neocortical cells have been investigated mainly in the prefrontal regions [Cousineau et al., 2020, Gao and Goldman-Rakic, 2003, Gorelova et al., 2002, Zhong et al., 2020] and so have been the network effects of DA release. Behaviorally, selective stimulation of DA neurons in the VTA induces a transition from anesthetized to awake state and suggests a role for DA modulation in behavioral arousal; moreover, inhibition of DA inputs suppresses wakefulness, even in the presence of relevant salient stimuli [Eban-Rothschild et al., 2016, Monti and Monti, 2007, Taylor et al., 2016]. However, DA is known to impact the activity of associative and sensory cortices, even though the mechanisms haven’t been elucidated yet. In particular, bath-application of $10\ \mu M$ dopamine in medial entorhinal cortex (mEC) slices suppresses UP states via the activation of D1Rs. This suggests that DA has inhibitory effects on cortical slow oscillations [Mayne et al., 2013]. Moreover, pairing VTA stimulation with auditory stimuli of a particular tone increases the selectivity of neural responses to those frequencies in auditory cortex, and enhances long-range coherence of neural discharge between primary and secondary auditory areas. Thus, there emerges a need to fill the gaps in the current knowledge and assess the effects of dopaminergic release on network activity of sensory areas.

3.3.2 Serotonin

5-hydroxy-tryptophan (5-HT) is a naturally occurring monoamine with complex and multi-faceted biological functions [Iriti, 2013]; it is commonly known as the ‘happiness molecule’ because of its notorious mood-regulating effects [Celada et al., 2013]. Most of the endogenously produced serotonin is located in the gastro-intestinal tract (GI tract), but it is also synthesized in the brain stem at the level of the dorsal and median raphe nuclei (DR and MR) [Berger et al., 2009]. Other than regulating GI motility, 5-HT is

known to be involved in a plethora of functions in the CNS resulting from its widespread innervation of the cortical mantle, such as the regulation of mood, appetite, sleep, sexuality, cognition, learning and social behaviors. 5-HT is also at the heart of several neurochemical theories of the pathophysiology of psychiatric disorders (namely depression, OCD, autism, and others). The role of 5-HT in brain function and disorder has been investigated extensively, but despite decades of research, its nature remains elusive [Marazziti, 2017].

Projections from brain-stem serotonin-producing clusters are topographically organized, suggesting that 5-HT release in the cortex is not merely broadcasted in a diffuse manner, and that it involves at least some degree of specificity [Jacob and Nienborg, 2018]. Serotonergic projections to primary sensory cortices include visual, auditory, somatosensory and olfactory areas and share the typical structure of neuromodulatory varicose-displaying axons. Given that only a small proportions of the axonal varicosities established specialized synaptic contacts, 5-HT is traditionally thought to be released in a volumetric manner [Descarries et al., 2010], but the matter is still being debated. For instance, in subcortical nuclei such as the SN pars reticulata (SNpr) almost all serotonergic release sites establish synaptic contacts, while in the pars compacta (SNpc) and in the DR volumetric and synaptic transmission co-exist [De-Miguel and Trueta, 2005]. However, a substantial body of evidence of 5-HT being released synaptically in the neocortex is hard to find, even though some studies have documented rapid 5-HT actions in sensory areas [Lottem et al., 2016, Roerig et al., 1997].

Serotonin acts on a wide array of receptors, classified from 5-HT₁ to 5-HT₇ types comprising a total of 14 subtypes [Nichols and Nichols, 2008]. Intriguingly, most subtypes are metabotropic receptors that are located extrasynaptically, and only the 5-HT₃ subtype mediates rapid excitatory synaptic transmission [Sharp and Barnes, 2020]. Moreover, 5-HT can be co-released with glutamate, thus ulteriorly complicating the issue of serotonin release. The effects of 5-HT release on neocortical cell types have mostly been studied in executive, fronto-striatal circuits [Puig et al., 2015], but some results have also been obtained in sensory and associative cortices [Athilingam et al., 2017, de Filippo et al., 2021, Foehring et al., 2002, Lee et al., 2010]. The repercussions of the 5-HT modulation of neocortical neurons include inhibitory effects on spontaneous firing activity and the suppression of slow oscillations; intriguingly, 5-HT modulation spares sensory-driven responses [Lottem et al., 2016]. Taken together, the evidence suggests that serotonergic release affects the spontaneous activity of sensory areas by modulating membrane properties of neocortical cell types, but does not impact sensory-evoked network activity. Thus, considering that the evidence in favor of

synaptic 5-HT release is weak, it is reasonable to hypothesize that serotonin cannot affect sensory responses because it acts on a slow time scale. This implies that its predominant transmission modality might be volumetric, but additional research is required to clarify the relative contributions of wired vs volumetric 5-HT release.

Chapter 4

Modelling the neuromodulation of neural microcircuits: a multi-scale framework to investigate the effects of cholinergic release

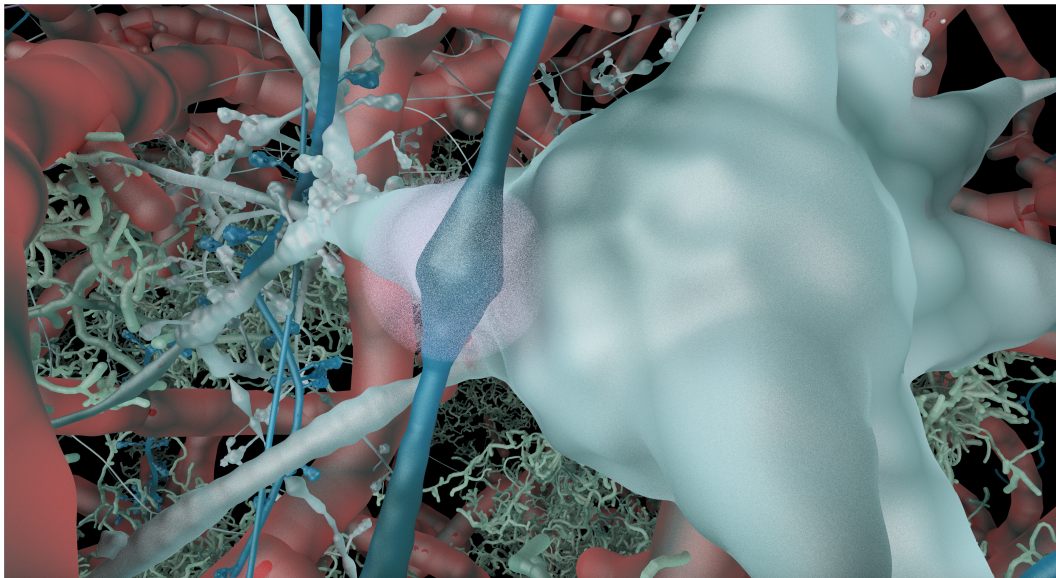


Figure 4.1: Visualization of neuromodulatory release in the neocortex

4.1 Influence of neuromodulatory systems in the hindlimb representation in the developing somatosensory cortex of the rat

Cristina Colangelo, Alberto Muñoz, Alberto Antonietti, Alejandro Antón-Fernández, Armando Romani, Joni Herttuainen, Henry Markram, Javier DeFelipe and Srikanth Ramaswamy

(to be submitted in 2022)

4.1.1 Abstract

The vast majority of cortical synapses are found in the neuropil which is implicated in multiple and diverse functions underlying brain computation. Unraveling the organizing principles of the cortical neuropil requires an intricate characterization of synaptic connections established by excitatory and inhibitory axon terminals, of intrinsic and extrinsic origin and from ascending projections that govern the function of cortical microcircuits through the release of neuromodulators either through point-to-point chemical synapses or diffuse volume transmission. The hindlimb representation of the somatosensory cortex (HLS1) of two-week old Wistar rats has served as a model system to dissect the microcircuitry of neurons and their synaptic connections. In the present study, we quantified the fiber length per cortical volume and the density of varicosities for catecholaminergic, serotonergic and cholinergic neuromodulatory systems in the cortical neuropil using immunocytochemical staining and stereological techniques. Acquired data were integrated into a computational modeling framework to reconcile the specific modalities and predict the effects of neuromodulatory release in shaping neocortical network activity. We predict that ACh and DA and 5-HT desynchronize cortical activity by inhibiting slow oscillations (delta range), and that 5-HT triggers faster oscillations (theta). Moreover, we found that high levels ($>40\%$) of neuromodulatory volumetric transmission (VT) are sufficient to induce network desynchronization, but also that combining volume release with synaptic inputs leads to more robust and stable effects, and lower levels of VT are needed to achieve the same outcome (10%).

Keywords: Acetylcholine (ACh), Dopamine (DA), Serotonin (5-HT), Choline Acetyl Transferase (ChAT), Tyrosine Hydroxylase (TH), ascending modulatory systems, point-to-point chemical synapses, synaptic transmission, volume transmission, cortical models, simulations

4.1.2 Introduction

Knowledge of the principal organization of the neocortex requires the characterization of the finest details of the complexity of the cortical neuropil. This includes the characterization of the density and distribution of the synaptic junctions most of which (90-98%), in the cerebral cortex, are established in the neuropil [DeFelipe, 1999]. Ascending cholinergic, catecholaminergic and serotonergic regulatory systems made by intricate networks of varicose fibers, participate in the control of cortical microcircuits both through synaptic contacts (“classical” point-to-point chemical synapses), and non-synaptic diffuse or volume transmission processes and affect cortical states, functions and development [Mechawar et al., 2002]. The hindlimb representation of the somatosensory cortex (HLS1) of the two-week old Wistar rats represent an excellent model to characterize the organizational principles of neocortical microcircuits due to its accessibility and the availability of detailed anatomical, molecular and physiological experimental data on its cellular and synaptic organization. In the last years it has received much attention within the framework of the Blue Brain Project (<http://bluebrain.epfl.ch/> and <https://cajalbbp.es/>) [Markram et al., 2015]. Modeling the influence that ascending modulatory systems exert on cortical microcircuitry requires a detailed assessment of the density and distribution of cholinergic, catecholaminergic and serotonergic fibers and varicosities. In the present, study we have estimated their densities and laminar distribution patterns using immunostaining and stereological techniques. Furthermore, to extend our characterization of the neuromodulatory innervation of the developing rodent neocortex, we use computational methods to digitally reconstruct dopaminergic, serotonergic and cholinergic virtual fibers in a detailed, biologically accurate model of the cortical column [Markram et al., 2015]. Our algorithmic approach to reconstruct neuromodulatory innervation leverages experimental datasets to predict missing biological information such as the relative proportions of targeted neurons or the number of contacts established by each neuromodulatory fiber. We subsequently simulate the activation of ACh, DA and 5-HT projections to model the synaptic and volumetric release of neuromodulators in the neocortical sensory microcircuit, and predict a desynchronizing effect on the network. We found that volumetric and synaptic release of neuromodulators have synergistic effects and lead to more robust desynchronizing effects when combined, rather than on their own. Moreover, we predict that ACh, DA inhibit slow oscillations, whereas 5-HT additionally brings about faster oscillatory activity. Overall, we propose a framework to integrate what is known about synaptic and non-synaptic transmission to attempt to reconcile conflicting reports in the literature and direct experimental research to answering long-standing questions about the nature of neuromodulatory release.

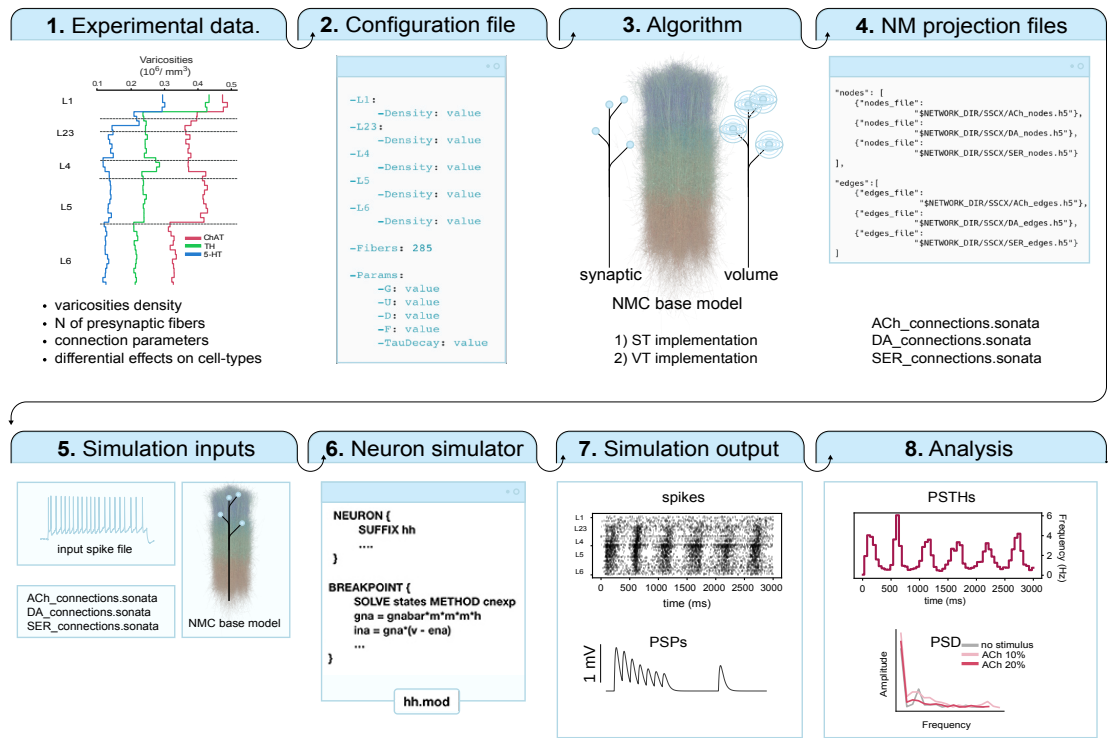


Figure 4.2: Modelling workflow. ST, synaptic transmission; VT, volumetric transmission; NMC neural microcircuit; PSP post synaptic potential; PSTH, peri-stimulus time histogram; PSD, power spectral density

4.1.3 Materials and methods

Animals

Wistar rats (n=11, aged 14 days) were sacrificed by administering a lethal intraperitoneal injection of sodium pentobarbital (40 mg/kg), and they were then perfused intracardially with saline solution followed by 4% paraformaldehyde in 0.1 M phosphate buffer (PB), pH 7.4. All experiments were approved by the local ethics committee of the Spanish National Research Council (CSIC) and performed in accordance with the guidelines established by the European Union regarding the use and care of laboratory animals (Directive 2010/63/EU). Brains were removed and post-fixed by immersion in the same fixative for 7h at 4°C. For the quantification of the serotonergic, catecholaminergic and cholinergic fibers, after post-fixation, six brains (Rabb6-Rabb11) were cryoprotected in 30% sucrose solution in PB until they sank, frozen in dry ice and cut in the coronal plane with a sliding freezing microtome. In all cases, 50 μ m-thick sections extending in the antero-posterior axis from the anterior commissure to the rostral limit of the hippocampal formation and including the hindlimb representation area of the primary somatosensory cortex [Paxinos and Watson, 2007] were processed for immunocytochemistry.

Immunocytochemistry

The sections were rinsed in PB and to block non-specific antibody binding they were preincubated for 1 h at room temperature in a stock solution containing 3% normal serum of the species in which the secondary antibodies was raised (Vector Laboratories, Burlingame, CA) in PB with Triton X-100 (0.25%). After preincubation, sections were incubated for 48 h at 4 °C in the same stock solution containing rabbit anti-serotonin (1:1000, Diasorin, Italy), mouse-anti-Tyrosine hydroxylase (TH, 1:1000, Diasorin) or goat-anti choline acetyl transferase (Chat, 1: 1000, Santa Cruz CA, USA). Sections were then rinsed in PB and incubated in anti-rabbit, anti-mouse, or anti-goat biotinylated secondary antibodies (1:200; Vector Laboratories, Burlingame, CA). After rinsing in PB, a first set of sections were processed for immunofluorescence being incubated for 2 h at room temperature in Alexa 488-coupled Streptavidin (1:200; Molecular Probes, Eugene, OR, USA). Sections were rinsed and stained with DAPI to reveal borders between layers and cytoarchitectonic areas. The sections were then washed in PB, mounted in antifade mounting medium (Invitrogen/Molecular Probes, Eugene, OR) and studied by conventional fluorescence and confocal microscopy (Zeiss, 710). For confocal microscopy, stripes through the layers of the hindlimb primary somatosensory cortex were scanned from every animal. Z sections were recorded at 0,45 μ m intervals through separate channels using a 40x oil-immersion lens (NA=1,3). Subsequently, ZEN software (Zeiss) was used to

construct composite images from each optical series by combining the images recorded through the different channels. Adobe Photoshop CS4 software was used to generate the figures (Adobe Systems Inc., San Jose, CA). For DAB immunostaining, a second set of sections were processed using the Vectastain ABC immunoperoxidase kit (Vector). Antibody labeling was visualized with 0.05% 3,3'-diaminobenzidine tetrahydrochloride (Sigma, St Louis, MO) and 0.01% hydrogen peroxide. The sections were rinsed in PB and mounted on siliconized glass slides. After attachment, sections were lightly Nissl-stained with thionin, dehydrated, cleared with xylene, and cover slipped. Controls were included in all the immunocytochemical procedures, either by replacing the primary antibodies with preimmune goat serum in some sections, by omitting the secondary antibodies, or by replacing the secondary antibody with an inappropriate secondary antibody. No significant immunolabeling was detected under these control conditions.

Estimation of fiber length

The fiber length and density of varicosities of the catecholaminergic, serotonergic and cholinergic systems, DAB-immunostained through the depth of the tissue, were stereologically estimated in every cortical layer using respectively the space ball probe (dissector height of 11-18 μm) and the optical fractionator tool (dissector height of 11 μm in all cases) of Stereo Investigator software (StereoInvestigator 7.0, MicroBright Field Inc. Vermont, USA) following previous studies [Mouton et al., 2002]. An oil immersion x100 objective (NA 1,35) on a BX51 Olympus microscope equipped with a Prior motorized stage and a JVC video camera was used. The light Nissl staining of every immunostained section helped to distinguish areal and layer limits and to trace the contour lines corresponding to the individual cortical layers within the hindlimb cortex with the aid of an x20 objective. For each cortical layer, type of immunostaining and animal, the number of sampling sites performed and the number sections used was determined by the constrain of maintaining the coefficient of error below 0.09 [Gundersen, 1988]. The fiber length and density of varicosities were corrected for shrinkage as brain tissue shrinks during processing. To estimate the shrinkage in our samples we measured the surface area and thickness of the sections using Adobe Photoshop and Stereo Investigator software respectively before and after tissue processing either for immunoperoxidase or immunofluorescence. The surface area after processing was divided by the value before processing to obtain an area shrinkage factor (p2) of 0.89. In addition, the obtained linear shrinkage factor in the z-axis (pZ) was 0.28. Therefore, the volume shrinkage factor (p3=p2.pZ) was 0.25.

Statistical analysis

To estimate possible differences in the length, density values obtained in the different cortical layers, a non-parametric test was performed and correction for multiple comparisons was applied. First, we used Friedman’s test and we found that length and varicosity densities differed across layers; post-hoc analysis (Conover’s test) was later performed to compare all layers for the three neuromodulatory systems. Bonferroni’s correction was applied to account for multiple comparisons. To assess the statistical significance of the PSD analysis results, we used a paired T-student test.

Neural microcircuit model

The previously existing model on which we base the entire simulation pipeline has been continuously refined through the years. In this study we use an updated version of the neocortical microcircuit replica and it is our duty to report the changes that have taken place since the last published version. We refer to this new updated version as V7 and to the previously published one as V6 [Markram et al., 2015]. The majority of the reconstructed morphologies that are used for the V7 are the same as the ones used in V6. Additional morphologies include data from in-vivo reconstructions and in-vitro reconstructions. Furthermore, pyramidal cells morphologies were objectively classified with methods from algebraic topology based in topological descriptors of the dendritic morphologies for pyramidal cells [Kanari et al., 2018], that led to the identification of 17 types of PCs in the rat somatosensory cortex [Kanari et al., 2019]. The electrical models and the data they’re based on have not changed and thus remain the same as in V6. The whole synaptic workflow, that is starting from sparse literature data and ending with the characterization of all viable synaptic pathways was modified as per [Ecker et al., 2020]. The v6 model included both a hexagonal microcircuit as well as an atlas-based circuit: the latest release further developed the atlas-aware circuit building pipeline in order to build the circuits in a curved-space volume.

Synaptic model of neuromodulatory release

To build a model of neuromodulatory release we used an in-house tool described in [Markram et al., 2015] that was developed to model projections to the neocortical microcircuit in a way that satisfies experimental constraints. Data about the density of synaptic boutons, or, more specifically in our case, neuromodulatory varicosities is used to constrain the generation of new synaptic release sites in the model, that is, we instantiate a layer-wise varicosity density profile in the model, that matches the experimentally measured density. The neuromodulatory projections approach happens in 3 major steps: sample, assign to fiber and parameter selection.

- *Sample*: all morphological segments contained in every layer are pooled; from this distribution, random segments are repeatedly sampled and new synaptic release sites (sRS) are placed at their centers in order to match the experimental constraints. Drawing is performed with replacement (i.e., a segment could be drawn more than once). The probability of drawing a given segment is proportional to its length (where longer segments would be drawn more often).
- *Assign to fiber*: a set of ‘fibers’ is given as input to the whole process. These are set of vectors with starting positions and directions. The tool creates straight synthetic fibers: in the v7 circuit used for this study these begin in L6 and point straight up through all the layers. The parameter ‘number of fibers’ can be estimated or directly constrained from experimental data. The distances between the newly instantiated sRS and the fibers are used to compute a Gaussian that determines the probability of being picked, and using this probability, a fiber is associated to each segment, or ‘mapped’. Given that we do not directly model the subcortical nuclei from which the projections originate, the fibers are activated via an artificially injected spike train of the desired frequency and duration.
- *Parameter selection*: in this step, we select the parameters that are better suited to mimic neuromodulatory connections. Our model of synaptic connections follows a conductance-based approach and comprises several parameters. We redirect the reader to [Markram et al., 2015], for an exhaustive description. In the following paragraph we will focus on describing how we constrained the connection parameters from literature reported data.

We reasoned that since the reported number of cholinergic neurons in the rat nucleus basalis of Meynert (NBM) is 7312 [Miettinen et al., 2002] and the NBM projects mainly to S1 [Chaves-Coira et al., 2018, Chaves-Coira et al., 2016] then there would be $7132/26 = 283$ fibers projecting to our reconstructed microcircuit, because the entire S1 area is 26 times bigger. Similarly, we assigned $2651 / 26 = 102$ fibers to the dopaminergic system, based on cell-counts obtained in the rat ventral tegmental area (VTA) [Nair-Roberts et al., 2008] and estimations of the number of VTA neurons that project to S1 [Aransay et al., 2015]. Lastly, we computed the number of serotonergic fibers; 11500 serotonergic cell bodies have been counted in the dorsal raphe (DR) according to Descarries and others, and only 12% project to the S1 region [Descarries et al., 1982, Wilson and Molliver, 1991]. That is $1380/26 = 53$ 5-HT fibers for the O1 circuit. The values obtained seem to fall within reasonable ranges, considering the estimated density of each neuromodulatory system, but nevertheless they rest on assumptions that have not been proven. We refer the reader to the Discussion section

ChAT	Pyramidal cells	Interneurons	Reference
L1		EPSP (and spiking activity)	[Arroyo et al., 2012] (p20-40 mice SSC) optogenetics
L1		EPSC	[Hay et al., 2016] (p25 mice); [Bennett et al., 2012] (adult mice) ; optogenetics
L2/3	IPSC barrage	EPSP (BPCs)	[Arroyo et al., 2012] (p20-40 mice SSC) optogenetics
L2/3		SOM increase FF; PV reduced FF	[Chen et al., 2015] (mouse v1) optogenetics
L4	IPSP		[Meir et al., 2018] (adult mice SSC) optogenetics
L5	EPSP or IPSP		[Hedrick and Waters, 2015] (mouse V1)optogenetics
L5	EPSP or IPSP		[Joshi et al., 2016] (p24 mouse A1) optogenetics
L6	EPSC		[Hay et al., 2016] (p25 mice) ; [Verhoog et al., 2016] (mouse PFC) optogenetics

Table 4.1: Summarized literature reported cell-type specific effects of cholinergic release. Inclusion criteria privilege studies performed a) by means of optogenetic stimulation of subcortical nuclei as a method to evoke neuromodulator release; b) in the somatosensory areas of the rodent neocortex c) in developing brains. When this is not applicable (i.e., data is missing) data was taken from studies using electrical stimulation of subcortical nuclei or bath-application of neuromodulators as methods to evoke neuromodulator release.

where we list the most important assumptions. Parameters for the synaptic dynamics of the new neuromodulatory connections were drawn from experimental distributions representative of the synaptic types (s-types) discussed in [Markram et al., 2015] (Tables 4.4, 4.5 and 4.6), except for the offset decay time constants (DTC). The DTCs of NM connections were constrained with the aid of literature reported values: we refer the reader to Tables 4.4, 4.5 and 4.6.

Volumetric model of neuromodulatory release

Our model of volumetric neuromodulatory transmission relies upon the implementation of the synaptic model explained above. To model VT, we first take the experimentally recorded varicosity density profile and we instanti-

TH	Pyramidal cells	Interneurons	Reference
L1		depolarization	[Zhou and Hablitz, 1999] adult rat PFC (Bath application of DA (30–100 μM))
L2/3	hyperpolarization or depolarization	increase excitability of PV-FS	[Zhong et al., 2020] (3w rats PFC in low Ca); [Zhou and Hablitz, 1999] adult rat PFC (Bath application of DA (30–100 μM))
L2/3		increase excitability of FS and depolarization	[Gorelova et al., 2002] (40 μM DA, rat PFC)
L4	hyperpolarization or depolarization	increase excitability of FS and depolarization	[Gorelova et al., 2002] (40 μM DA, rat PFC); [Zhou and Hablitz, 1999] (adult rat PFC)
L5	increase excitability via D1r (or sometimes decrease via D2r)	increase excitability of PV-FS	[Radnikow and Feldmeyer, 2018] (rodents PFC); [Zhong et al., 2020] (3w rats PFC); [Gao and Goldman-Rakic, 2003] (ferret PFC)
L5		increase excitability of FS and depolarization;	[Gorelova et al., 2002] (40 μM DA, rat PFC); [Zhou and Hablitz, 1999] (adult rat PFC)
L6	increase excitability		[Radnikow and Feldmeyer, 2018] (rodents PFC); [Zhou and Hablitz, 1999] (adult rat PFC)

Table 4.2: Summarized literature reported cell-type specific effects of dopaminergic release. Inclusion criteria privilege studies performed a) by means of optogenetic stimulation of subcortical nuclei as a method to evoke neuromodulator release; b) in the somatosensory areas of the rodent neocortex c) in developing brains. When this is not applicable (i.e., data is missing) data was taken from studies using electrical stimulation of subcortical nuclei or bath-application of neuromodulators as methods to evoke neuromodulator release.

5-HT	Pyramidal cells	Interneurons	Reference
L1		5-HT _{2A} R mediated excitatory responses	[Foehring et al., 2002] (immature rat SSC)
L1		slow-spiking interneurons are excited by 5-HT _{3A} R	[Lee et al., 2010] (juvenile SSC)
L2/3		SOM neurons are excited via 5-HT _{2A} R	[De Filippo et al., 2020] (C57BL6 mice (6 to 10 weeks), olfactory cortex)
L2/3		PV neurons are excited by 5-HT	[Puig et al., 2010, Athilingam et al., 2017]
L2/3		predominance of 5-HT _{1A} R mediated inhibitions in FS neurons	[Puig and Gullledge, 2011] (DR electrical stimulation)
L2/3		5-HT _{2A} R mediated excitatory responses	[Foehring et al., 2002] (immature rat SSC)
L5	5-HT _{1A} R mediated inhibitory responses in 2/3 of pyramidal neurons		[Puig, 2004] (rat mPFC, young adult)
L5	inhibited by 5-HT application		[Avesar and Gullledge, 2012] (3-weeks to 8-months-old C57BL6 mice PFC)

Table 4.3: Summarized literature reported cell-type specific effects of serotonergic release. Inclusion criteria privilege studies performed a) by means of optogenetic stimulation of subcortical nuclei as a method to evoke neuromodulator release; b) in the somatosensory areas of the rodent neocortex c) in developing brains. When this is not applicable (i.e., data is missing) data was taken from studies using electrical stimulation of subcortical nuclei or bath-application of neuromodulators as methods to evoke neuromodulator release.

ACh	L5PCs, L6PCs	L23PCs, L4PCs	L1 IINs	L23 prox tar- geting IINs
Synaptic DTC	241.2 \pm 15.5 ms	241.2 \pm 15.5 ms	241.2 \pm 15.5 ms	241.2 \pm 15.5 ms
Volumetric DTC	342.2 \pm 147.2 ms	342.2 \pm 147.2 ms	608.6 \pm 109.7 ms	608.6 \pm 109.7 ms
G	0.31 \pm 0.11 nS	0.66 \pm 0.15 nS	0.3 \pm 0.11 nS	1.4 \pm 1.6 nS
U	0.5 \pm 0.011	0.3 \pm 0.043	0.86 \pm 0.048	0.23 \pm 0.093
D	670 \pm 9.3 ms	1300 \pm 280 ms	670 \pm 9.1 ms	600 \pm 350 ms
F	17 \pm 2.8 ms	2.2 \pm 1.9 ms	17 \pm 2.7 ms	33 \pm 20 ms
s-type	E2	I2	E2	I3

Table 4.4: ACh connections parameters. DTC: decay time constant of the PSC; G: synaptic conductance; U: time constant of synaptic depression; F: time constant of synaptic facilitation; s-type: synaptic type according to [Markram et al., 2015]

ACh	L5PCs, L6PCs	L23PCs, L4PCs	L1 IINs	PV-FS all lay- ers
Synaptic DTC	241.2 \pm 15.5 ms	241.2 \pm 15.5 ms	241.2 \pm 15.5 ms	241.2 \pm 15.5 ms
Volumetric DTC	400 \pm 100 ms	400 \pm 100 ms	400 \pm 100 ms	400 \pm 100 ms
G	0.31 \pm 0.11 nS	0.66 \pm 0.15 nS	0.3 \pm 0.11 nS	0.31 \pm 0.11 nS
U	0.5 \pm 0.011	0.3 \pm 0.043	0.86 \pm 0.048	0.22 \pm 0.093
D	670 \pm 9.3 ms	1300 \pm 280 ms	670 \pm 9.1 ms	390 \pm 240 ms
F	17 \pm 2.8 ms	2.2 \pm 1.9 ms	17 \pm 2.7 ms	300 \pm 240 ms
s-type	E2	I2	E2	E1

Table 4.5: DA connections parameters. DTC: decay time constant of the PSC; G: synaptic conductance; U: time constant of synaptic depression; F: time constant of synaptic facilitation; s-type: synaptic type according to [Markram et al., 2015]

ACh	L5PCs, L6PCs	L1 IINs	L23 proximal targeting IINs	L23 distal targeting IINs
Synaptic DTC	241.2 \pm 15.5 ms	241.2 \pm 15.5 ms	241.2 \pm 15.5 ms	241.2 \pm 15.5 ms
Volumetric DTC	342.2 \pm 147.2 ms	342.2 \pm 147.2 ms	608.6 \pm 109.7 ms	608.6 \pm 109.7 ms
G	0.66 \pm 0.15 nS	0.3 \pm 0.11 nS	1.4 \pm 1.6 nS	0.3 \pm 0.11 nS
U	0.3 \pm 0.043 ms	0.86 \pm 0.048 ms	0.23 \pm 0.093 ms	0.09 \pm 0.062ms
D	1200 \pm 280 ms	670 \pm 9.1 ms	600 \pm 350 ms	140 \pm 110 ms
F	2.2 \pm 1.9 ms	17 \pm 2.7 ms	33 \pm 20 ms	670 \pm 430 ms
s-type	I2	E2	241.2 \pm I3	E1

Table 4.6: 5-HT connections parameters. DTC: decay time constant of the PSC; G: synaptic conductance; U: time constant of synaptic depression; F: time constant of synaptic facilitation; s-type: synaptic type according to [Markram et al., 2015]

ate new release sites (RS) in order to match this density. Then, every RS is taken as the center of a sphere of radius R_{\max} , which is the sphere of influence of volume transmission (thus the RS becomes a volumetric RS, or vRS). We chose $R_{\max} = 5 \mu m$ for ACh (Figure 4) as was computed by Borden and colleagues, because it was recorded in rodent neocortical brain areas, as opposed to other values obtained in the mEC or the retina, which nevertheless are in a similar range [Borden et al., 2020, Jing et al., 2018, Sethuramanujam et al., 2021]. Dopaminergic transients have also been measured by means of a synthetic catecholamine nanosensor which revealed DA hotspots with a median size of $2 \mu m$ [Beyene et al., 2019] so we instantiated $R_{\max} = 2 \mu m$ for DA connections, even though this data was recorded in the striatal region. Serotonin’s volumetric influence was estimated by [Bunin and Wightman, 1998] who recorded serotonergic extrasynaptic transmission via carbon fiber microelectrodes in the rat DR; thus, we selected $R_{\max} = 3 \mu m$ for 5-HT signals. Subsequently all morphological segments within the sphere are sampled and a new conductance is instantiated in a random position along each segment. In this case the vRS is the source of the NM signal, and the segment where the new conductance is placed is the target. Still, these two do not coincide like in the synaptic implementation of NM release. Thus, we developed a way to mimic the one-source-to-many-targets characteristic of VT. The new volumetric connections are parametrized similarly to the synaptic ones (see above). The conductance values in this case are scaled according to the distance from the vRS. Specifically, we determine a scaling factor whose value ranges from 1 to 0.1 and is inversely proportional to the distance from the vRS. We refer the reader again to Tables 4.4, 4.5 and 4.6

for a more specific description of the DTC values used to parametrize the kinetics of VT.

Microcircuit

Our in-silico neuromodulation model was implemented in a digital microcircuit consisting of a connected network of 31 346 neurons, 8 million connections, and 37 million synapses. The network was arranged in a columnar volume $462 \times 400 \mu\text{m}$ wide and $2082 \mu\text{m}$ deep. In this configuration, depth axes were mutually parallel, and columnar surfaces were coplanar. The cell morphologies populating the circuit were obtained from 3D reconstructions of biocytin-stained neurons from juvenile rat hindlimb somatosensory cortex, while the placement, connectivity, and electrophysiological properties of each cell was determined algorithmically and constrained by sparse data derived from experiments and literature. See [Markram et al., 2015] for additional details concerning microcircuit construction and composition. Models and circuit data are freely available for download at: <https://bbp.epfl.ch/nmc-portal/downloads>

Network simulations

Simulations were conducted using proprietary software based on the NEURON simulation environment. Data were output in the form of binary files containing spike times sampled every 0.1 ms for each neuron in the network. Extracellular calcium and potassium concentrations were modeled by considering their phenomenological effects on neurotransmitter release probability and somatic depolarization, respectively. These values were adjusted to most closely mimic an in vivo-like network state, corresponding (empirically) to extracellular calcium and potassium concentrations of 1.7 mM, and 5.0 mM ($\sim 95\%$ somatic firing threshold), respectively. Simulations of ascending neuromodulatory inputs were performed near the transition from the synchronous to the asynchronous state, in order to set the initial state of the network to a substantially synchronized activity pattern. In the control case our microcircuit is oscillating at ~ 2 Hz, a condition that we use to approximate an inactivated brain state. Every simulation was repeated 30 times with different seeds (tied to random number generators that we use in our simulation pipelines) to reproduce trial variability, and a power density analysis was performed to evaluate the frequency contents of the oscillatory activity of our simulated network of neurons. The stimulus to the neuromodulatory projections was delivered as single-pulse or train stimulation of frequencies ranging from 5 to 30 Hz. In order to recruit different proportions of ascending inputs we selected varying percentages (from 10 to 100%) of the ‘virtual’ afferent fibers. The stimulus was delivered at $t=2000$ ms; the single pulse stimulus had a frequency of 150 Hz and a duration of 10 ms and

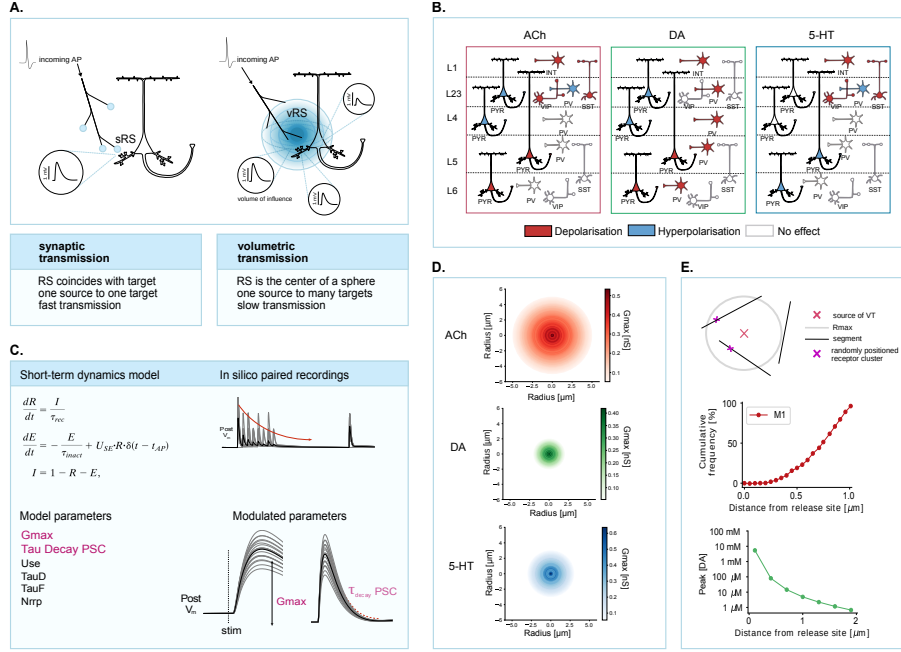


Figure 4.3: Implementation of volumetric vs synaptic release A) Schematics illustrating the differential implementation of volumetric vs synaptic transmission. sRS, synaptic release site; vRS, volumetric release site. B) Schematics illustrating the data gathered in Tables 4.1, 4.2, 4.3 on the effects of neuromodulator release on a given target that was used to parametrize the neuromodulatory synaptic inputs to neocortical cells. The schema represents the main cell types in the neocortex. Abbreviations: PYR, pyramidal cell; INT, interneuron; SOM, somatostatin-positive cells; PV, pv-positive cells. C) Implementation of the synaptic model. Left: equations describing the Tsodyks-Markram model of synaptic short-term dynamics (above) and list of model parameters (below). Right: example of an in silico paired-recording experiment (excitatory, depressing connection) (above), and schematics illustrating the parameters that are modulated in order to mimic neuromodulatory effects. G_{max} maximal conductance; $\tau_{Decay PSC}$, decay time constant of the post-synaptic current; Use , utilization of synaptic efficacy; τ_D , time constant of depression; τ_F , time constant of facilitation; $NRRP$ number of readily-released pool vesicles. D) Implementation of the volumetric transmission model for the three neuromodulatory systems. Left: Graphs illustrating the distance-dependent change in G_{max} . Right: first, from above: schematic illustrating the spherical sampling portion of the algorithm developed to model volumetric transmission (VT). Second, partial validation of the VT model for ACh release (data from [Yamasaki et al., 2010]). Third, partial validation of the VT model for DA release (data from [Courtney and Ford, 2014]).

Layers	ChAT fibers length ($\mu m/1000$ μm^3)	ChAT fibers var (var/1000 μm^3)	TH fibers length ($\mu m/1000$ μm^3)	TH fibers var (var/1000 μm^3)	5-HT fibers length ($\mu m/1000$ μm^3)	5-HT fibers var (var/1000 μm^3)
L1	7.31 \pm 1.16	0.48 \pm 0.09	5.37 \pm 0.97	0.42 \pm 0.18	0.74 \pm 0.16	0.30 \pm 0.09
L2	9.49 \pm 2.53	0.39 \pm 0.06	3.90 \pm 0.69	0.24 \pm 0.04	0.56 \pm 0.11	0.22 \pm 0.06
L3	9.27 \pm 2.28	0.37 \pm 0.05	3.57 \pm 0.63	0.24 \pm 0.06	0.20 \pm 0.04	0.14 \pm 0.01
L4	11.72 \pm 1.3	0.37 \pm 0.03	4.93 \pm 0.37	0.28 \pm 0.03	0.14 \pm 0.05	0.12 \pm 0.02
L5	9.55 \pm 2.27	0.42 \pm 0.07	3.39 \pm 0.39	0.24 \pm 0.01	0.11 \pm 0.04	0.14 \pm 0.02
L6	10.64 \pm 2.1	0.33 \pm 0.09	3.20 \pm 0.26	0.21 \pm 0.05	0.13 \pm 0.04	0.12 \pm 0.02

Table 4.7: Fiber length and densities of the three projection systems Fiber length and density of varicosities of cholinergic, catecholaminergic, and serotonergic regulatory systems in HLS1 at P14. Measured data were corrected for shrinkage and refer to the total volume of cortical layers.

the train stimulus was applied for 2000 ms.

Supercomputing

A 2-rack Intel supercomputer using dual socket, 2.3 GHz, 18 core Xeon SkyLake 6140 CPUs, with a total of 120 nodes, 348 GB of memory, and 46 TB of DRAM was used to run the simulations and carry out analysis.

Simulation outputs analysis

All code for analysis was written in the Python programming language. To estimate the power of the signal at different frequencies, we performed a power spectrum density analysis (PSD) by calculating firing rate frequencies and subsequently applying the Welch transformation. The estimation was performed on the first 1000 ms time interval after the stimulus delivery. To compute the delta power we specifically selected the 2 Hz frequencies.

4.1.4 Results

Cholinergic fibers

In addition to sparsely distributed ChAT-immunoreactive (ir) neuronal cell bodies distributed from layers 2 to 6, ChAT immunostaining revealed the presence of an intricate network of varicose fibers across all cortical layers of the rat P14 HLS1 (Fig. 1 and Table 4.7). Unfortunately, at a distance from the cell body, ChAT-ir positive processes emanating from the cell body of cortical cholinergic neurons could not be distinguished from the surrounding

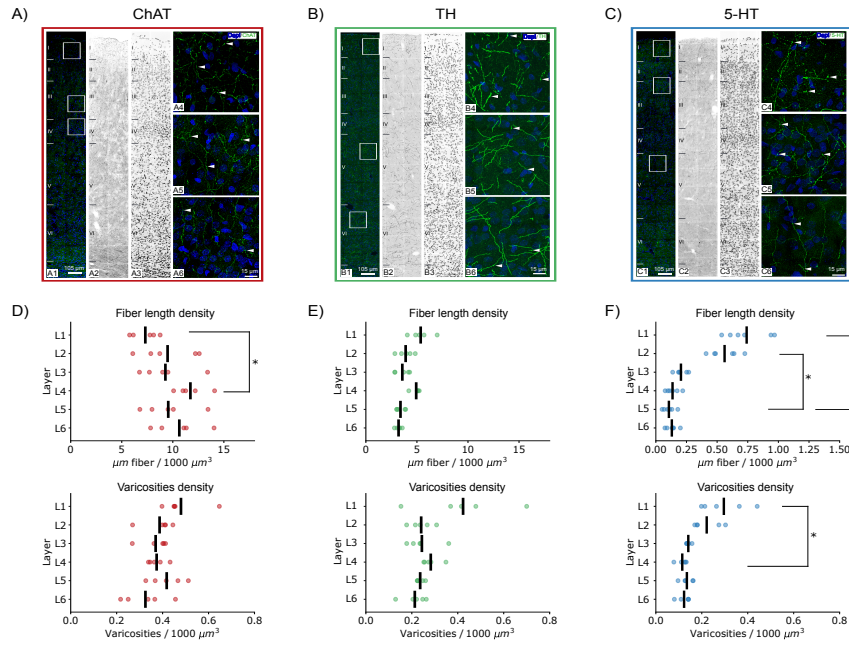


Figure 4.4: ChAT, TH and 5-HT immunoreactivity A) confocal stack projection image, corresponding to a cortical thickness of 14 μm , showing the distribution of ChAT-immunoreactive fibers (green) in the different layers, as revealed by DAPI staining (blue), of the P14 rat hindlimb somatosensory cortex. A2) and A3) show respectively, in monochrome images, ChAT immunostaining and DAPI staining. Squared zones in A are shown at higher magnification in A4-A5-A6. Arrow heads point to fiber varicosities. B) same as in A) but for TH-immunoreactive fibers C) same as in A) but for 5-HT-immunoreactive fibers D) Graph showing the mean values obtained in the HLS1 of the five P14 rats analyzed for the density of fibers (above) and the density of varicosities (below) for the cholinergic system. E) same as in D) but for the catecholaminergic system F) same as in D) but for the serotonergic system

positive elements, most of which are known to originate in the basal forebrain [Mechawar et al., 2000]. Fibers throughout cortical layers were apparently oriented in all directions but in layers 1 and 6 fibers with an orientation parallel to the pial surface were frequently found. The density of cholinergic fibers was relatively homogeneous throughout cortical thickness and laminar differences were statistically significant only between layers 1 and 4 (P-value = 0.048) (Fig. 1). Fiber varicosities were also homogeneously found with no significant differences between the different cortical layers (Fig. 1).

Catecholaminergic fibers

Immunocytochemistry for tyrosine hydroxylase (TH), the rate-limiting catecholamine synthesizing enzyme, revealed the presence of groups of aspiny non-pyramidal neurons. According to previous studies [Kosaka et al., 1987], these cells are distributed in all cortical layers, although they are most abundant in layers 2–3. The processes arising from this neuronal population might therefore contribute to the TH-ir fibers quantified in the present study (Fig. 1 and Table 4.7). In addition, TH-ir fibers are considered to label mainly dopaminergic fibers in the cerebral cortex [Lewis et al., 1988, Martin and Spühler, 2013, Sesack et al., 1998], although the possibility that our results include noradrenergic fibers and boutons, mainly labeled with dopamine- β hydroxylase [Latsari et al., 2002], cannot be excluded. In the rat HLS1 neocortex layers 1 and 4 had the highest density of TH-ir fibers, followed by layers 2 and 3, whereas the density was lowest in layers 5 and 6 (Fig. 1). However, no statistical differences were found between layers in the density of TH-ir fibers. The density of TH-ir varicosities followed a similar laminar distribution pattern although no statistical differences were found between layers (Fig. 1).

Serotonergic fibers

Immunocytochemistry for serotonin (5-HT) revealed the presence of numerous 5-HT-ir fibers through all cortical layers (Fig. 1 and Table 4.7). No immunoreactive cell bodies were found, as expected. A higher density of serotonergic fibers was found in supragranular layers, in layer 1 and 2, compared to layer 5 (p-values respectively 0.007 and 0.035) (Fig. 1). Fibers in layers 1 and 6 showed a preferential horizontal orientation parallel to the pial surface whereas in other layers fibers oriented in all spatial orientations but with a radial orientation were frequently found. Fibers with varicosities were also found in all cortical layers and the density of varicosities tended to be higher in superficial rather than in infragranular layers (Fig. 1), but a statistically significant difference was found only between L1 and L4 (p-value: 0.048).

Comparison of the three ascending neuromodulatory systems

The present observations indicate that in terms of fiber length the cholinergic system constitutes the densest neuromodulatory system of the three systems studied, followed by the catecholaminergic fiber system, with the serotonergic system showing the lowest density of fibers. These differences were significant when averaging data from all cortical layers and also in each cortical layer separately (Fig 1). Regarding fiber varicosities, that represent the presumed sites of transmitter release, the density of cholinergic varicosities corresponded to 1.4 times the density of varicosities of catecholaminergic varicosities and 2.3 times to the number of serotonin axon varicosities. Finally, the density of catecholaminergic varicosities was 1.6 higher than that of serotonergic varicosities.

In silico predictions about the organization of neuromodulatory input

We implemented two full sets of neuromodulatory projections that work only with ST and VT respectively. The model allows us to combine the two in the desired proportions, or to only use one projection system at a time. To extend our assessment of the influence of neuromodulatory systems we used the varicosity density profiles across the six neocortical layers to digitally reconstruct cholinergic, dopaminergic and serotonergic inputs to the hindlimb region of the rat somatosensory cortex and to obtain quantitative anatomical predictions about the columnar targets of the three neuromodulatory innervation systems. Specifically, we estimate the total number of neurons innervated by each projection system, the number of post-synaptic cells contacted by each fiber and the most contacted cell types (Figure 3). Overall, we estimated that each cholinergic fiber targets 301.0 ± 493.6 neurons with 336.6 ± 567.4 synaptic RS, while each cortical neuron receives 4.2 ± 2.7 fibers with 4.7 ± 3.3 synaptic RS. In the case of volumetric transmission, we calculated that each ACh fiber contacts up to 7104.4 ± 4581.0 neurons. The most contacted excitatory cell type is the TPC:A in L23, while the most contacted inhibitory cell-type is the LBC in L23. Moreover, we predict that each TH immuno-positive fiber targets 521.4 ± 852.2 neurons with 631.4 ± 1063.4 synaptic RS, while each cortical neuron receives 2.7 ± 1.6 fibers with 3.3 ± 2.3 synaptic RS. In the VT implementation each TH fiber targets 4377.7 ± 3982.9 neurons. The most densely innervated cell-type is the L23 TPC:A while in terms of inhibitory cells the most contacted type is the LBC in L6. Each 5-HT fiber targets 365.7 ± 566.7 neurons with 458.2 ± 740.0 synaptic RS and each neurons receives 2.0 ± 1.1 fibers with 2.5 ± 1.7 synaptic RS. In the VT case serotonergic contacts reach 3463.2 ± 2605.1 neurons. The most contacted excitatory neuron is the TPC:A in L5 and the most contacted interneuron is the L23 LBC. For a more refined

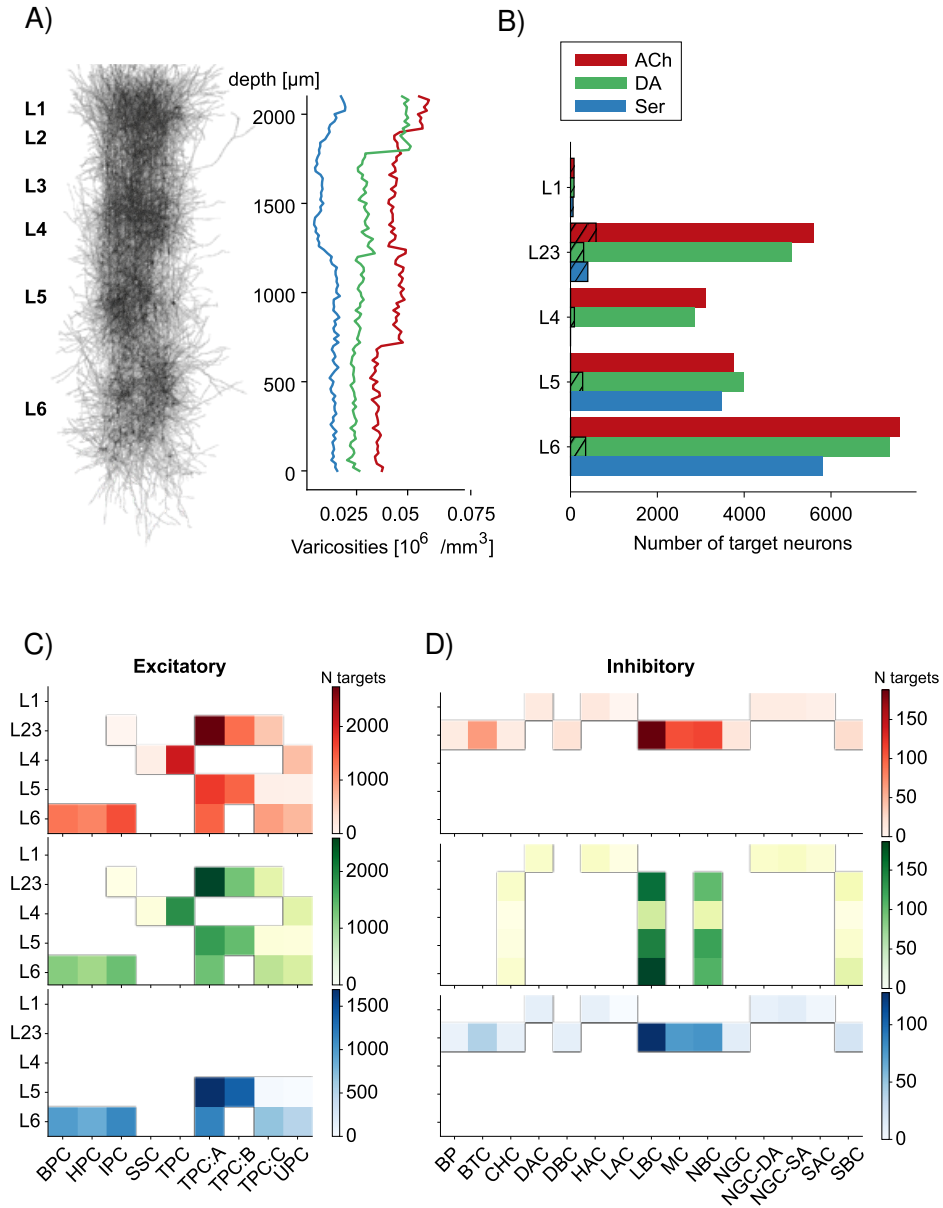


Figure 4.5: In silico predictions of neuromodulatory innervation All data is representative of a single column in our in silico neocortical microcircuit. A) From left to right: in silico Golgi stain microphotograph of a cortical column; in silico neuromodulatory varicosities densities. B) Histograms showing the distribution of the number of post-synaptic targets contacted by each neuromodulatory fiber, for the three neuromodulatory systems. Striped bars represent inhibitory cell-types C) Heatmap of the proportion of excitatory morphological types contacted by each projection system. D) Heatmap of the proportion of inhibitory morphological types contacted by each projection system.

breakdown of the proportions of cell-types innervated by the three systems see panel C in Figure 3. Next, we tested whether our virtual neuromodulatory projection systems can be activated to induce network effects reported in the literature. We reasoned that albeit sparse, if properly connected and parametrized, neuromodulatory fibers should elicit a modulation of network activity.

Simulating cholinergic network effects

Optogenetic activation of ChAT-positive neurons in the basal forebrain (BF) is known to produce a desynchronizing effect on the activity of neurons in sensory cortices [Lee and Dan, 2012, Pinto et al., 2013], even though exactly how this is achieved remains unclear. We therefore gathered and integrated data about the effects of optogenetic cholinergic BF neurons stimulation on neocortical cell types residing in sensory cortices, to simulate the activation of cholinergic projections in our detailed model of a neocortical column. As reported in Table 4.1 and Figure 4, in our implementation, cholinergic inputs depolarize L1 interneurons, L23 distal-targeting interneurons and L5 - L6 pyramidal cells (PCs), and instead have a hyperpolarizing effect on L23 - L4 PCs and L23 proximal-targeting interneurons. The remaining cell-types are not targeted by our ACh connections because cholinergic stimuli in a physiologically relevant range (achieved via optogenetic tools or relatively low concentrations of ACh agonists, i.e., not greater than 100 μM) fail to elicit a response in deeper layers inhibitory interneurons [Arroyo et al., 2012, Obermayer et al., 2018]. For a more detailed explanation of the parameters used for simulations, we redirect the reader to Table 4.4. First, we simulated the all-synaptic activation of the whole cholinergic projection system at increasingly higher stimulation rates (5, 10, 15, 20, 25, 30 Hz) to model progressively higher levels of ACh release. Cholinergic ST inputs significantly reduce the delta component of the power spectrum of network activity (at 20 Hz ST we observe a 49% reduction with respect to control; $p\text{-value} = 0.18 \times 10^{-30}$); moreover, this reduction tends to be larger as the stimulation frequency increases. For all subsequent simulations of cholinergic inputs, we therefore chose to mimic the firing frequencies used in optogenetics experiments (around 20 Hz) which in turn imitate the synchronous spiking of cholinergic neurons in the BF [Hedrick and Waters, 2015, Obermayer et al., 2018].

Predicting ACh release kinetics

The dynamics of ACh release have not been elucidated yet, likely because they can be influenced by a variety of factors. ACh can be released tonically or phasically, via volume or synaptic transmission, and it can be subjected to fast clearing from the extracellular space because of the activity of catalytic

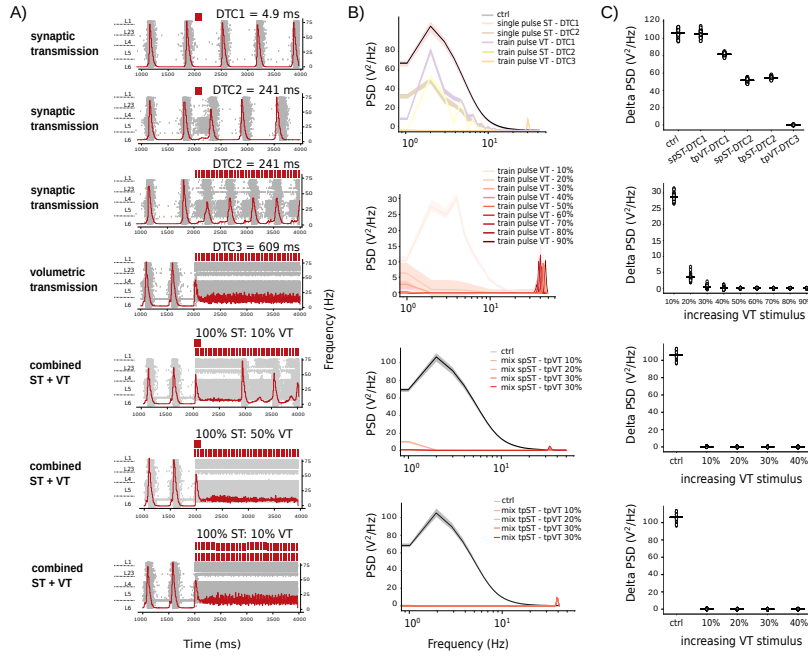


Figure 4.6: ACh network effects Simulated network effects during the progressive activation of the virtual neuromodulatory projection systems. Timing of cholinergic, dopaminergic and serotonergic manipulation is shown as colored vertical bars on top of the plots. Simulation time is 4000 ms, and projections activation occurs at $t=2000$ ms and stops at $t=4000$ ms. A) Cholinergic effects; raster plots and superimposed frequency histograms. ST: synaptic transmission; VT: volumetric transmission. DTC: decay time constant of the PSC B) time-frequency representation plots. C) Graph showing only the delta (1.5 -3 Hz) range power for every simulated condition. sp: single pulse; tp: train pulse.

enzymes such as cholinesterases [Coppola et al., 2016, Lysakowski et al., 1989]. The literature reported values for the offset decay kinetics of ACh currents range across several orders of magnitude [Arroyo et al., 2012, Hay et al., 2016, Nelson and Mooney, 2016a]. To reconcile the conflicting reports, we simulated the cholinergic modulation of network activity as if it were 1) completely synaptic 2) wholly mediated by volumetric transmission and by varying the input type (phasic or tonic stimulation) and the kinetic parameters assigned to the connections to check the subsequent network effects. We designed a stimulus to mimic the phasic activation of cholinergic ascending fibers (a single-pulse, high frequency stimulus) and one to simulate a more tonic stimulation (a 20 Hz train of pulses) as was done experimentally by [Hay et al., 2016]. In order to select an appropriate volume of influence for the neuromodulatory volumetric signal we searched for studies reporting the spatial extent of neuromodulatory transients; often these are quite recent studies that leverage recently developed genetically-encoded-fluorescent sensors. To instantiate the ACh VT model, we assigned a value of 5 microns to the R_{\max} parameter (see Methods and Figure 4), which was kept fixed for all simulations of volumetric cholinergic release, as reported by [Borden et al., 2020]. The DTC values (Table 4.4) are important to determine the transmission timeline in both synaptic and volumetric release. While neuromodulatory ST is known to act on rapid timescales (i.e., the ms range), VT works with significantly longer transmission delays (hundreds of milliseconds) [Agnati et al., 2006, Arroyo et al., 2012]. Nevertheless, synaptically mediated cholinergic currents with a slower decay have been observed as well [Hay et al., 2016]. We therefore used some of the experimentally obtained DTC values and combined them with the other conditions in order to predict which set of parameters leads to a more substantial effect on network activity. We found that specific combinations of input type – transmission mode – and kinetic parameters are required to fully desynchronize the microcircuit (Fig. 5). Specifically, when ACh is released synaptically in our model, a 10 ms pulse can impact network activity only when the connections are assigned a slow enough decay kinetics (~ 200 ms), while no effect can be observed when a faster kinetic is at play (~ 5 ms). A 20 Hz train of pulses is even more impactful and leads to a prolonged desynchronization of network activity. However, the strongest desynchronization occurs when in our model ACh is released volumetrically (99% reduction; $p\text{-value}=9.09 \times 10^{-40}$). In this case, if a train stimulation is coupled to even slower decay kinetic values (~ 600 ms), activation of cholinergic fibers leads to a complete cessation of slow oscillatory phenomena, and network activity shifts to a much faster and entirely desynchronized regime as can be seen in Figure 5. In our simulations cholinergic stimuli bring about a significant decrease of the delta band (0.5 - 3 Hz) power that is not due to a mere change in the mean firing frequencies of the neurons in the network that are receiving the stimuli. Therefore, all subsequent simulations implementing

the VT model were assigned a DTC of 608.6 ± 109.7 ms [Hay et al., 2016] while for the simulations implementing the ST model, we used $\text{DTC} = 241.2 \pm 15.5$ ms [Nelson and Mooney, 2016b].

Relative contributions of synaptic and volumetric release

We showed that the VT implementation of cholinergic release dramatically desynchronized microcircuit activity while the ST implementation had a smaller effect on the reduction of slow oscillations. We therefore wondered what would happen if we activated the two systems simultaneously while manipulating the amount of input received. We performed an in-silico experiment where we only simulated cholinergic VT and activated increasing proportions of the afferent projections, thus simulating progressively higher levels of cholinergic release. For example, activating 10% of the projections in our model means that 28/283 source neurons are firing at 20 Hz. As can be seen in (Figure 5) we found that at least 50% of the VT projections have to be activated to completely desynchronize network activity. However, if we add synaptic release (100% of the fibers activated and firing at a 20 Hz frequency), lower levels of VT are sufficient to induce full network desynchronization (as low as 10% of VT), suggesting that the two modalities might work synergistically to evoke network states transitions. We kept testing this hypothesis, and performed another experiment where we activated progressively higher levels of VT while simultaneously simulating ST, this time by activating the ST projections with a high-frequency single pulse stimulation. Low levels of VT caused a complete desynchronization of microcircuit activity, that was however shorter in duration (~ 1 s) (Figure 5). The longer-lasting shift in network activity (comparable to results obtained with a tonic stimulation, ~ 3 s) could be still rescued by recruiting higher levels of VT, once again suggesting that VT and ST might work together in a diversity of contexts.

Simulating dopaminergic network effects

Dopamine is known to modulate arousal and promote wakefulness in living animals [Taylor et al., 2016], and to have effects on neocortical cell types [Bassant et al., 1990, Gonzalez-Islas and Hablitz, 2003, Gorelova et al., 2002]. However, VTA inputs to sensory cortices have not been extensively described (as opposed to inputs to the prefrontal cortex), nor has their impact on network activity (unlike behavioral effects). For lack of better options, we used data about the effects on neocortical cell types elicited by bath application of dopaminergic agonists, mostly obtained in the prefrontal cortex, to parametrize the newly added dopaminergic synapses. As reported in Table 4.2 and Figure 4, in our model, dopaminergic inputs depolarize L1 interneurons, all-layers proximal-targeting interneurons and pyramidal cells in L5

and L6. Pyramidal cells in L23 and L4 are instead inhibited by DA. We chose not to target the remaining cell-types because of lack of literature-reported effects. For a more detailed explanation of the parameters used for simulations, we redirect the reader to the Methods section of this paper and to Table 4.6. We implemented both the all-synaptic (ST) and the all-volumetric (VT) model of dopaminergic release, for which we used a $R_{\max} = 2 \mu m$. The DTCs values were constrained through literature-reported values [ST: 220 ± 41 ms [Condon et al., 2021]; VT: 0.4 ± 0.1 s [Courtney and Ford, 2014]]. First, we simulated the all-synaptic activation of the dopaminergic projection system at increasingly higher stimulation rates (5, 10, 15, 20, 25, 30 Hz) to model progressively higher levels of dopamine release. As shown in Figure 6 dopaminergic ST inputs significantly reduce the delta component of the power spectrum of network activity (26% reduction, $p\text{-value}=1.04 \times 10^{-21}$). For all subsequent simulations of dopaminergic inputs, we chose a firing frequency of 20 Hz, again to be aligned with optogenetic stimulations experiments [Brunk et al., 2019, Taylor et al., 2016]. Then we simulated an all-volumetric activation of dopaminergic projections and we found that VT transmission has a higher impact on network synchrony than ST: the delta power is reduced of 85% when 100% of the DA fibers are stimulated ($p\text{-value}=1.05 \times 10^{-26}$). Furthermore, we did another experiment where we activated an increasingly higher proportion of inputs (10%, 20%, 30% up to 90% of the projections) thus simulating progressively increasing recruitment of neuromodulatory fibers. Dopaminergic inputs do not lead to a complete desynchronization of network activity, but the effect on slow oscillations seems to increase linearly with the number of fibers recruited. We also combined ST (100% fibers) with increasing amounts of VT (10, 20, 30 ... 90 % fibers) and found that when the two systems are activated simultaneously, low levels of VT are sufficient to induce complete desynchronisation in network activity (100% reduction); the effect remains stable at higher levels of VT.

Simulating serotonergic network effects

A substantial body of evidence suggests a causal relationship between 5-HT levels and cortical activity [Grandjean et al., 2019, Harris and Thiele, 2011, Lee and Dan, 2012, Puig et al., 2010]; optogenetic stimulation of the DR reduces low frequency power in the cortex thus promoting desynchronization. However, these results are mostly obtained in prefrontal areas, and the role of 5-HT projections to the SSCX is not clear to date. To test whether this holds true for the somatosensory cortex as well, we parametrized the serotonergic connections as reported in experiments where 5-HT was bath-applied (see Table 4.3). As reported in Figure 4, serotonergic inputs hyperpolarize lower layers (L4 and L5) pyramidal cells and L23 PV interneurons, but have excitatory effects on L23 VIP and SST interneurons, and (as for

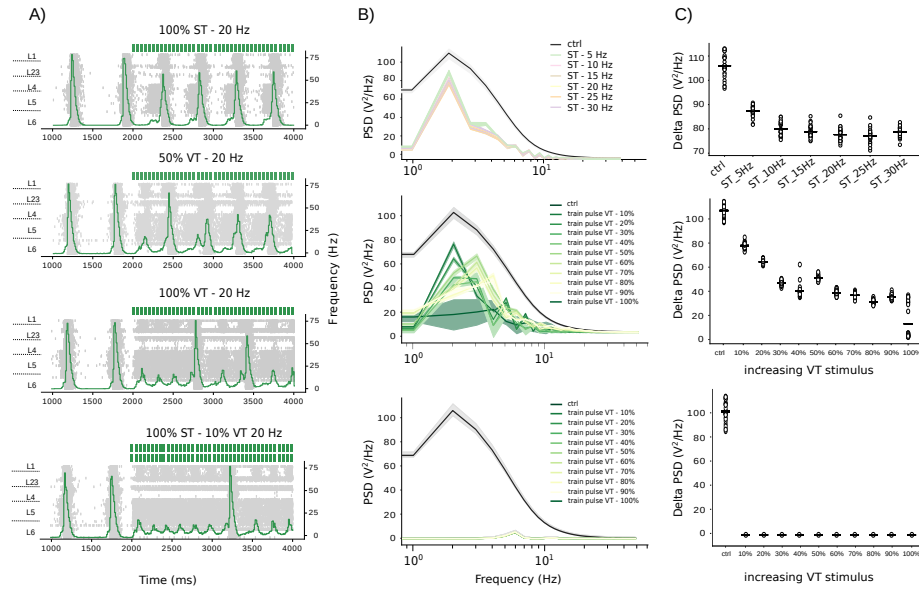


Figure 4.7: DA network effects Simulated network effects during the progressive activation of the virtual dopaminergic projection systems. Timing of simulated optogenetic dopamine release is shown as colored vertical bars on top of the plots. Simulation time is 4000 ms, and projections activation occurs at $t=2000$ ms and stops at $t=4000$ ms. A) Dopaminergic effects; raster plots and superimposed frequency histograms. ST: synaptic transmission; VT: volumetric transmission; Ctrl: control condition. B) time-frequency representation plots. C) Graph showing only the delta (1.5 -3 Hz) range power for every simulated condition.

most neuromodulators) they depolarize all L1 interneurons. We chose not to target the remaining cell-types because of lack of literature-reported effects. For a more detailed explanation of the parameters used for simulations, we redirect the reader to the Methods section of this paper and to Table 4.7. We implemented both the all-synaptic (ST) and the all-volumetric (VT) model of 5-HT release, for which we used a $R_{\max} = 3 \mu m$. The DTCs values were constrained through literature-reported values (we assigned ST and VT the same value for lack of better data: 0.44 ± 0.3 s; (Courtney and Ford, 2016)). First, we simulated the all-synaptic activation of 5-HT fibers with progressively increasing stimulation frequencies (5, 10, 15, 20, 25, 30 Hz) to check the effect on slow oscillations. We found that 5-HT inputs reduce the delta component of network oscillations (80% reduction, $p\text{-value}=1.6 \times 10^{-37}$) and shift the power spectrum towards higher-frequency components; while the reduction of the 2 Hz peak is drastic, an increase in oscillation frequency is also evident, as can be seen in the raster plots in Figure 7. For all subsequent simulations of 5-HT release we used a train of pulses at 20 Hz (again, to fall in line with optogenetics experiments such as in (Lottem et al., 2016)). The effect on 2 Hz oscillations is even larger when we simulate an all-volumetric implementation of 5-HT release (reduction of 99% $p\text{-value}=2.6 \times 10^{-40}$), and it increases with the number of fibers stimulated (again, we simulated the activation of 10%, 20% ... up to 100% of the fibers). The VT model of serotonergic inputs also predicts an increase in higher-frequency oscillations (the theta range) and brings about a significant desynchronization of network activity. We also tried coupling the ST and VT models (where we activated 100% of ST inputs, and increasing percentages of VT release) and found that when the two release modes are combined, low levels (10%) of VT are sufficient to induce a complete desynchronization of network activity (100% reduction).

4.1.5 Discussion

Anatomy of neuromodulatory Systems

In the present, study we have estimated their densities and laminar distribution patterns using immunostaining and stereological techniques. The data are compared to previous data generated in our laboratory using FIB/SEM and Espina software that allow the identification and quantification of virtually all cortical synapses in long series of images that represent a 3D sample of cortical neuropil [Merchan-Pérez, 2009, Santuy et al., 2018]. Previous studies in different cortical regions and species have examined the developmental maturation of the rat cortical innervation by the networks of cholinergic, catecholaminergic and serotonergic fibers [Descarries and Mechawar, 2000, Dori et al., 1996, Kalsbeek et al., 1988, Latsari et al., 2002, Lidov and Molliver, 1982, Mechawar and Descarries, 2001, Mechawar et al., 2002, Ver-

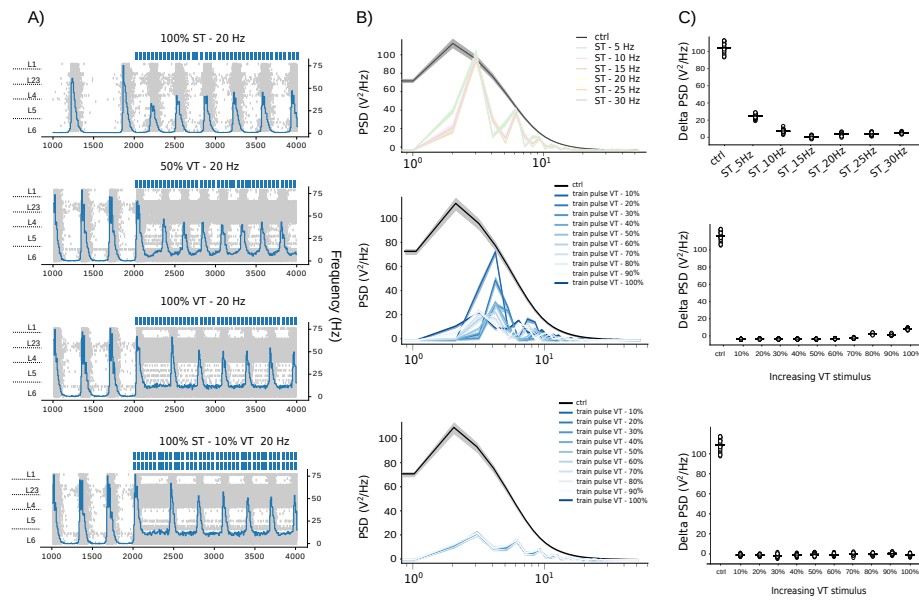


Figure 4.8: 5-HT network effects Simulated network effects during the progressive activation of the virtual serotonergic projection systems. Timing of simulated optogenetic serotonin release is shown as colored vertical bars on top of the plots. Simulation time is 4000 ms, and projections activation occurs at $t=2000$ ms and stops at $t=4000$ ms. A) 5-HT effects; raster plots and superimposed frequency histograms. ST: synaptic transmission; VT: volumetric transmission; Ctrl: control condition. B) time-frequency representation plots. C) Graph showing only the delta (1.5 -3 Hz) range power for every simulated condition.

ney et al., 1984]. These studies suggested that the pronounced effects that these regulatory systems exert on the morphology and physiology of maturing cortical neurons are both through synaptic and non-synaptic connections. They reported regional specificity throughout the neocortex and progressive changes over postnatal development in fiber length, branching patterns, number of varicosities and percentage of varicosities that form synaptic contacts. To get a deeper insight in the organization of the cortical neuropil in the different cortical layers of the HLS1 of two-week old rats, in the present study we have also estimated the fiber length per cortical volume and the density of varicosities of catecholaminergic, serotonergic and cholinergic systems, using immunocytochemical and stereological techniques. Our combined experimental and modeling approach demonstrates that the cholinergic projection system prevails over other neuromodulatory systems in the cerebral cortex and contacts by far the largest number of post-synaptic targets in each neocortical layer. The second most prevalent type of neuromodulatory innervation is the TH-positive fiber system. Dopaminergic fibers are generally thought to be present mostly in the frontal areas [Jacob and Nienborg, 2018] while only sparsely innervating the sensory cortices [Aransay et al., 2015]. Our findings confirm previous results concerning the presence of TH staining in the developing somatosensory cortex (Descarries et al., 1987). Anatomical studies in different rodent species have identified substantial serotonergic projections from the raphe nuclei to early sensory areas including the somatosensory cortex [Jacob and Nienborg, 2018]. 5-HT fiber density transiently increases in the neonatal rodent neocortex [D’Amato et al., 1987], and becomes more uniformly distributed after the third postnatal week. Here, we confirm that serotonergic fibers innervate the developing rodent neocortex and are more abundantly present in superficial rather than in deep layers. This preferential organization of serotonergic fibers and varicosities could reflect the fact that a large, developmentally distinct category of inhibitory interneurons that also expresses the 5HT_{3a}R is concentrated in supragranular layers. This population is heterogeneous and includes all of the VIP expressing neurons, as well as an equally numerous subgroups of neurons that do not express VIP and includes neurogliaform cells [Rudy et al., 2011]. The preferential innervation of L1 seems to be a key feature of neuromodulatory projections to the somatosensory cortex: given the relative scarcity of cell bodies in layer 1 it is reasonable to hypothesize that they would be contacted by a large number of fibers, in order to maximize the probability of receptor activation. To gain a better insight of the organization of neuromodulatory systems we also developed a structural model of cholinergic, dopaminergic and serotonergic innervation of the sensory cortex. Our goal here was to generate predictions of quantities that are hardly measurable in real-life settings such as the number of neurons contacted by each neuromodulatory axon, the number of synapses established by each fiber and the proportions of innervated

cell-types.

Physiology of neuromodulatory systems

Neuromodulators are traditionally thought to act with low spatial precision throughout the cortex, but recent lines of evidence suggest that they also exhibit fast modes of signaling [Kalmbach et al., 2012, Obermayer et al., 2018, Poorthuis et al., 2013] and that neuromodulatory axons establish specialized synaptic contacts [Nelson and Mooney, 2016b, Takács et al., 2013, Turrini et al., 2001]. In rodent neocortex reports of the percentage of varicosities that establish synaptic contacts are conflicting and values range from 14% to 66% [Colangelo et al., 2019]. Some authors argue that cholinergic synapses might be difficult to find with traditional methods, and propose novel ways to identify cholinergic synapses; Takacs et al for instance observed that cholinergic contact sites in rodent neocortex were strongly labeled with neuroligin-2 and they did not resemble typical synapses, suggesting that cholinergic fibers establish more synaptic connections than it was recognized previously. More in general, a body of anatomical evidence suggests that cholinergic synapses exist, with apposition of pre and post synaptic sites, although they might not account for all ACh release sites [Disney and Higley, 2020, Turrini et al., 2001]. Evidence in favor of cholinergic volumetric transmission, such as the presence of extrasynaptic receptors and slowly decaying current kinetics [Descarries and Mechawar, 2000, Hay et al., 2016, Yamasaki et al., 2010] has also been reported. According to Hay et al, both synaptic and diffuse cholinergic transmission occur in the neocortex depending on the regime of BF neurons. Thus, even though fast point-to-point modulation of synaptic transmission has been repeatedly demonstrated in the rodent neocortex [Kalmbach et al., 2012], the possibility that neuromodulatory systems exert their action via volume transmission as well cannot be excluded. Incidentally, whilst en passant axonal boutons of cholinergic neurons of subcortical provenance can mediate volume transmission broadly in the cortex, acetylcholinesterase (AChE) restricts the diffusion of ACh by enzymatic hydrolysis after its release [Sarter et al., 2009]. Thus, slow and diffuse cholinergic transmission in the cortex is likely to be spatially and temporally constrained by the catalytic power of AChE, other than by the localization and density of cholinergic receptors. It is reasonable to hypothesize that neuromodulatory activity likely reflects a mixture of spatiotemporal dynamics [Muñoz and Rudy, 2014]; however, the relative contributions of the two transmission modalities remain unclear. In this study, we implemented a model of neuromodulatory release that accounts for volumetric and synaptic transmission to investigate the dynamics of cholinergic release in sensory cortices. Additionally, we extend our framework to include other neuromodulators, such as DA and 5-HT, that have not been so extensively studied in the somatosensory cortex of the rat. We show that cholinergic projections

modulate the activity of the simulated microcircuit by decreasing slow oscillations (delta oscillations) and by desynchronizing network activity (Figure 5). In particular we show that high levels of volumetric transmission are sufficient to fully and persistently desynchronize the microcircuit, but they are not necessary: when VT is coupled to ST, we observe a synergic effect and lower levels of VT suffice to achieve the same network effect. Moreover, we show that conflicting reports about the magnitude of the DTC in cholinergic induced PSCs can be reconciled via *in silico* experiments performed within our framework, and so can the cell-type specific effects of cholinergic release. No amount of validation can prove a model right, but within its domain of validity our model allowed us to put to the test the underlying hypothesis (i.e. the data that we used to constrain the model). The literature about the cell-type specific cholinergic modulation of membrane properties is quite conflicting. For example, there is no clear agreement on the effects exerted by ACh on pyramidal neurons, nor on basket cells (PV-FS interneurons). Some papers report inhibitory effects, others excitatory or biphasic, or (sometimes paradoxically) a lack of effect [Eggermann and Feldmeyer, 2009, Gullledge and Stuart, 2005, Hedrick and Waters, 2015, Joshi et al., 2016, Obermayer et al., 2018, Xiang et al., 1998b]. The same is true for measurements of transmission features such as the DTC, or the firing frequency of cholinergic cells of subcortical provenance. Because our model replicates well-established emergent phenomena such as the desynchronizing effect of cholinergic release reported in the literature [Alitto and Dan, 2013, Pinto et al., 2013], we can be confident that it captures at least some essential properties of the system being modeled. Less is known about the activation of the DA and 5-HT modulatory systems and their effects on sensory microcircuits. Most of the data is recorded in prefrontal regions or in subcortical modulatory regions such as the striatum and the DR [Courtney and Ford, 2014, Gonzalez-Islas and Hablitz, 2003, Puig et al., 2010], so it's harder to validate the results of our model. However, the presence of both DA and 5-HT varicosities and receptors has been reported in the rodent sensory cortex [Bao et al., 2001, D'Amato et al., 1987, Descarries et al., 1987]. We decided to extend the assessment of the influence of these neuromodulatory systems in otherwise previously unexplored conditions, i.e., in somatosensory regions. We simulated the effects of endogenous DA release and we found that synaptic transmission alone induces a significant decrease in the delta power (30%) of microcircuit oscillatory activity; VT however is much more impactful in that it has an even stronger effect of slow oscillations. Combining dopaminergic VT and ST leads to complete network desynchronization. It is interesting to notice here that the desynchronization induced by DA is not as long-lasting as seen in the ACh case even though the train stimulation is equivalent. 5-HT volumetric and synaptic inputs also drastically reduce the delta component of network oscillations and cooperate to bring about complete network desynchronization. Addi-

tionally, serotonergic release induces a shift in the power spectrum towards higher-frequency components (5-8 Hz).

Modelling assumptions

When modeling, one is necessarily simplifying from ground truth. These simplifications are based on assumptions, where as long as the assumption holds true, the corresponding simplification does not limit the validity of the model. Consequently, in order to assess the validity of a model it is paramount to be aware of the assumptions it is based on. In the next paragraph we will describe three main types of assumptions that our model is based upon.

One is the "inherited assumption", that occurs whenever a model is built on top another existing model. The new model inherits all relevant assumptions of the base model. For example, our algorithm to reconstruct neuromodulatory innervation inherits the assumptions relating to neuronal composition, placements and morphology from the underlying neocortical column model.

The second type is the data/structuring assumption: that is, an assumption that acts on how the model is parameterized, i.e., how data is turned into parameters. In this modelling study, after placing additional synapses in our NCX model to match the distribution profile observed experimentally, we assigned synaptic features based on literature reports gathered in Tables 4.1, 4.2, 4.3. We developed an algorithm that assigns excitatory or inhibitory synaptic parameters based on the post-synaptic morphological type (m-type) contacted by our virtual projection systems. We assumed that synapses of subcortical provenance will display forms of short-term dynamics similar to the well-known dynamics of neocortical synapses [Markram et al., 2015] and that they would be governed by similar principles. Moreover, we assume that organizational principles extracted for specific cell-types hold true in more general cases and we apply them to broader target classes. For example, if we find that ACh depolarizes L5 pyramidal cells we extend this observation to a broader category, i.e., L5 excitatory cells. Additionally, we compute the number of fibers for each neuromodulatory projection system based on rough estimations of the number of presynaptic cells in the underlying subcortical neuromodulatory region. This assumption has limited validity in many ways. First, we are assuming that NM projections originate from a specific nucleus in the subcortical modulatory region (in particular: the NBM for ACh, the DR for 5-HT and the VTA for DA) and we are disregarding the possibility that some proportion of the connections can arise from other less relevant or less studied nuclei. While it is true that these nuclei are the main sources of neuromodulatory inputs, the possibility that

other nuclei are also involved cannot be excluded. Second, we assume that the innervation of the S1 region is homogeneous in all its subregions, while there may be differences in the innervation of specific areas.

Third, we report modelling assumptions, that is all the assumptions at the very core of the model itself. For instance, we assume that the slow oscillatory activity of our simulated microcircuit (yielded by a specific set of parameters) can mimic the inactivated / synchronized brain state typical of SWS states (see Methods section – Neural microcircuit model). The other modelling assumptions revolve around the VT implementation. Information such as the concentration of the neurotransmitter in the extracellular matrix, and the dynamics of the release in terms of diffusion kinetics is central to understand the spatiotemporal constraints of VT. However, neither the effective concentration of neuromodulators in the extracellular space, nor the rates of their diffusion/degradation are known and an accurate knowledge of the spatiotemporal limits of diffuse neuromodulator release is still lacking = [Coppola et al., 2016], mostly because of technological limitations. In our model, we assume that the extracellular matrix has no influence on volumetric transmission, and we do not specifically model the action of catalytic enzymes like cholinesterases. Additionally, we sample a spherical volume around the VT release site and assume transmission isotropy. A list of assumptions can be complete only when the following conditions are met: the infinite set of all conceivable models has to be considered, and then each assumption, combined with ground truth data, rules out a part of that set. Then, the proposed model is the only one remaining that is consistent with the ground truth data. The theoretical goal of having a complete list of assumptions is therefore unachievable, for the simple reason that the space of all conceivable models is most likely impossible to describe, but it provides a useful thought framework.

4.1.6 Conclusions and future directions

Our goal here was to integrate sparse experimental datasets and provide a way to generate predictions about the influences of three distinct neuromodulatory systems in the somatosensory cortex. Through our modelling efforts we sought to provide a framework to investigate the long-standing issue of the relative importance of volumetric vs point-to-point synaptic transmission. Our results show that the two modalities have cooperative effects and we propose that one key feature of network transitions between synchrony and asynchrony regimes is the co-occurrence of volumetric and synaptic neuromodulatory transmission. Predictably, our model has limitations, several of which we have already listed in the assumptions section. To mention a few others, we do not account for the action of other neuromodulators in the cortex (Disney, 2021), which are likely to influence the context in

which ACh, DA and 5-HT work, nor we take into consideration the effects that these three neuromodulators have on each other and on their own activity. ACh is known to be involved in feedback regulation of cholinergic release via presynaptic axonal autoceptors for instance, and neuromodulators can be co-released with other peptides or transmitters [Granger et al., 2017, Saunders et al., 2015]. The framework we built to model neuromodulatory transmission can be updated as we gather new data and move forward in our understanding of neuromodulatory systems.

Chapter 5

Discussion and concluding remarks

The goal of this thesis was to develop a computational framework to integrate multiscale data on the effects of neuromodulatory release in the neocortex and predict the fine-grain mechanisms shaping the modulation of cortical states. This thesis addresses the need to turn the understanding of the brain into a more tractable issue, generating novel ways and approaches to investigate the multi-scale and complex nature of neuromodulatory processes.

After an initial review of the state-of-the-art of literature, I presented a collaborative, proof-of-concept paper that shows that it is indeed possible, and potentially very advantageous, to build a multi-level model of the chemical modulation of neocortical microcircuit activity. I then augmented this framework with biologically plausible models of neuromodulatory release. To this end, I present an original study with ACh as a use case and describe how I extended the framework to other neuromodulators, such as DA and 5-HT. Beginning with experimental datasets on the layer-wise neuromodulatory varicosity density profiles and data about the effects of neuromodulatory release on neocortical cell-types, we reconstructed ACh, DA and 5-HT projections to the rat somatosensory cortex, and simulated the effects of their activation. More specifically, we implemented two distinct models of neuromodulatory release, in an attempt to address the long-standing debate on the nature of volumetric vs synaptic transmissions of neuromodulators. Contrary to traditional beliefs, we found that one modality does not prevail upon the other: volumetric and synaptic transmission act in a synergistic fashion to desynchronize cortical microcircuits. While volumetric transmission alone is sufficient to impact network activity, the combination of synaptic and volumetric inputs produces a dramatic and much more stable effect, for all three neuromodulatory systems examined. Thanks to our model

we show that desynchronization of network activity is achieved through a marked inhibition of the spontaneously generated slow oscillatory activity that characterizes inactivated brain states. Overall, my thesis suggests a departure from the dogma that neuromodulators are released prevalently through a single transmission modality. My work predicts that there is no direct correspondence between tonic activity and volume transmission, and phasic activity and synaptic transmission. Supported by these findings, I propose that volume and synaptic transmission of neuromodulators co-exist in the rodent neocortex, and act concomitantly on cortical microcircuits to ultimately reconfigure global brain states.

It goes without saying that a model cannot perfectly represent the system taken into consideration, and the utility of a simulation is limited by the quality of the underlying data and assumptions. In the previous chapter I have extensively described the assumptions that constrain the model of neuromodulatory release, but the list is virtually impossible to complete. Despite these shortcomings, we can be confident that our model captures at least some of the essential properties of neuromodulatory innervation, because it replicates well-known emergent phenomena. Furthermore, I'd like to highlight that the framework I have built is a first version of a reconstruction that can be augmented and refined as more data is obtained.

The goal of this thesis is to develop a first draft implementation of neuromodulatory effects to guide experimental research. Having summarized the known effects of cholinergic release on neuronal activity in the somatosensory cortex, and having identified the gaps in the current knowledge is one of the major contributions of the thesis to the advancement of the field of cortical neuromodulation. Gathering and integrating sparse information about the effects of neuromodulation is a daunting task requiring meticulous data acquisition and curation. Computational models and simulation-based approaches provide ways to integrate existing knowledge and emerged as an answer to the growing necessity to make sense of sparse datasets in the literature. Modelling approaches turn the scientific investigation cycle into an iterative process: with each iteration, knowledge can be gained and the interpretation and validation of the data can change. Managing such a process poses a number of organizational and technical challenges: data that is scattered across multiple systems and repositories needs to be discovered and organized coherently. Data can be collected from multiple sources, potentially revealing inconsistencies across different workflows, raising the need to strictly track data provenance. Furthermore, data may need to be transformed, reshaped or generalized. Thus, collecting and integrating experimental datasets for the purpose of model-building is an exercise in data management, classification and transformation. Another important

aspect that needs to be highlighted is that summarizing all the established knowledge into a coherent framework allows the identification of knowledge gaps in the literature. Confirming previously obtained results is of paramount importance when trying to make sense of neuroscientific phenomena, but differences in experimental setups, methods and workflows can produce inconsistent observations and duplication of effort across research groups should be avoided. What is instead needed is a way to consolidate high-quality information and shed light on what is still missing in order to achieve a more complete perspective of the problem. For instance, I would argue that in order to get a more comprehensive view of the effects of ACh on neocortical cell-types (assuming that we can agree on what cell-types are) we should focus on using identical methodologies across different laboratories and apply them to a large number of cell types, rather than constantly repeating slightly different experiments focusing on the major cell-types in the neocortex. For instance, the state-of-the-art literature comprises dozens of scientific research papers all focusing on elucidating the effects of ACh on pyramidal cells in layer 5, without generating true consensus on what the effects are. The lack of agreement is likely attributable to subtle but important differences in how the data is collected but also to the species, age of the animal, brain area and agonist type being used. Agreeing on methodologies and experimental protocols could potentially aid with dissipating the recurrent conflicting results in the field. Furthermore, endlessly duplicating experiments about the effects of ACh on major cell-types overshadows the need to perform these experiments on the remaining cell-types in the neocortex. Similarly, focusing on describing the actions of one neuromodulator in a given system cannot provide a complete understanding of how the system is being modulated: neuromodulators interact recursively to produce desired behavioral outcomes and their actions cannot be studied in isolation. In the following paragraph I will provide a list of what I believe are the main knowledge gaps in the neuromodulation field with the objective of providing direction for future experimental avenues. These suggestions are framed in the context of studying the neuromodulation of rodent somatosensory circuitry, but they can be extended to the investigation of other model systems.

- Effects of neuromodulators on neocortical cell types
 - Characterize the effects of increasing bath-applied concentrations of neuromodulators on major classes of inhibitory interneurons (PV, VIP, SOM) across cortical layers
 - Characterize the effects of optogenetically released neuromodulators on major types of excitatory and inhibitory interneurons across cortical layers and assess differential effects evoked by progressively increasing fiber stimulation frequencies

- Effects of neuromodulators on neocortical connections
 - Characterize effects of increasing bath-applied concentrations of neuromodulators on inhibitory connections in the neocortex
 - Characterize effects of optogenetically released neuromodulators on inhibitory connections in the neocortex and assess differential effects evoked by progressively increasing fiber stimulation frequencies
- Network effects of neuromodulators
 - Establish network effects of DA and 5-HT on sensory cortices
- Volumetric influence of neuromodulatory release
 - Measure or estimate radius of influence of 5-HT volumetric release
 - Measure or estimate decay kinetics of 5-HT and DA transients
 - Measure extrasynaptic neuromodulatory receptor concentration densities as a function of distance from neuromodulatory release sites
 - Measure neuromodulator concentration as a function of distance from neuromodulatory release (absolute concentrations are tricky to measure, relative concentrations would suffice)
- Characterization of neuromodulatory-releasing subcortical nuclei
 - Estimate number of neuromodulatory releasing neurons in subcortical areas such as the BF, the DR and the VTA
 - Characterize firing rates of neuromodulatory neurons in physiological contexts
 - Perform retrograde tracing experiments from specific cortical areas to estimate the portion of neuromodulatory neurons actually innervating those areas

Measuring the concentration of neuromodulatory compounds has constituted a challenge for neuroscientists mainly because of technological caveats: microdialysis methods are limited by aspects such as the temporal resolution and the size of sampling probes. That is why it is crucial to come up with methods to estimate such quantities. One way in which this could be achieved is by mapping the effects of optogenetically-evoked neuromodulatory inputs, which is a relatively more physiological way of activating neuromodulatory release, to the effects of bath-applied known neuromodulator concentrations. Establishing such a relationship would allow to relate firing frequencies of subcortical neuromodulatory-releasing neurons to the applied dose of neuromodulators, thus creating a way to predict their physiological extracellular concentration. Optogenetic activation of subcortical nuclei however is not a quintessential model of physiological neuromodulatory release. Low infection efficiency of channelrhodopsin2 (CHR2) containing viral vectors, the unknown spatial distribution of cholinergic axons being activated and other factors such as poor light penetration into brain tissue potentially confound results obtained with these methods [Kalmbach et al., 2012]. At the same time, bath-application of neuromodulatory agonists in brain slices is not guaranteed to be a valid model of neuromodulatory release either. The use of non-hydrolysable analogs and even more importantly the timeline of these kind of experiments are likely to lead to receptor desensitization as a consequence of agonist overexposure. Traditional bath-application methods elicit a tonic stimulation of the system, which might not reflect physiological activation of neuromodulatory stimuli; nevertheless these are the only techniques that allow us to control for the concentration being applied. I therefore propose to make the most of this advantage and collect data about the effects of increasing neuromodulatory bath-application and optogenetic stimulation with the aim of comparing the outcomes of the two methodologies.

Neuromodulation is a complex phenomenon to describe, because of its multi-faceted nature; many authors have attempted to clearly define neuromodulatory processes [Disney, 2021] by virtue of different aspects. A compelling definition of neuromodulation put forward by Katz in 1999, concerns the fact that a neuromodulator is a molecule that is neither excitatory nor inhibitory, but that can be involved in a form of neurotransmission. While it is very hard to predict the ultimate effect of a neuromodulator on a given cell-type in experimental settings, I believe that in the context of modelling, it is important to integrate different datasets in order to have the best estimate of the effect of a modulator on neuronal properties. Overall, the outputs of neuromodulatory actions depend on the specific receptor subtypes involved in the response which are concentrated on the post-synaptic membrane of the receiving neuron. Therefore, even though the same neu-

romodulator can have excitatory or inhibitory effects on cells, if data about receptor expression on specific cell-types is available, it could be in theory possible to predict the effect on the post-synaptic side. For instance, it is known that ACh tends to generate excitatory responses via M1-M3Rs or nAChRs mediated pathways, and inhibitory responses through M2-M4 like receptors. At the same time, the distribution of the different kinds of receptor populations vary across cell-types: for instance, excitatory cells in L4 mainly express the M2-M4 subpopulation [Eggermann et al., 2014], and are therefore more likely to generate hyperpolarising responses to the application of a cholinergic stimulus. The effects of ACh on ion channels and metabotropic G-protein coupled receptors have been widely studied, but to-date a comprehensive view of how ACh regulates the physiology of multiple ion channels is still lacking. ACh stimuli can elicit biphasic currents [Gulledge et al., 2007] because it can bind to receptors capable of generating diametrically opposing effects. Nevertheless, ACh will produce a net effect on membrane excitability, which will in turn affect E/I balance and generate network effects. Thus, I reasoned that it would be more useful to model the overall effects of ACh on neuronal excitability and check for emergent properties of network activity. In order to model the effects of neuromodulators on ion channels and specific currents it is essential to first have an underlying model of subcellular activity which represents yet another level of biological organization. According to Dasari and colleagues [Dasari et al., 2017], cholinergic biphasic (inhibitory and excitatory) responses work as complementary mechanisms regulating rapid calcium recycling from intracellular stores. This unifying view, originally proposed to explain the heterogeneity of cholinergic responses in pyramidal neurons, could serve as the basis of an integrative model of the subcellular actions of ACh, allowing a deeper understanding of the nuanced and interactive effects that neuromodulators exert on different ion channels and receptors.

To understand neuromodulation means to appreciate its formidable complexity and at the same time grasp its essential mechanisms. Questions such as " what are the fundamental properties of neuromodulation? " and "which level of detail should we aim for when modelling neuromodulation?" therefore naturally arise. If neuromodulatory phenomena are essentially gain-tuning mechanisms of neural microcircuits [Disney, 2021], it could be argued that to use point-neuron models to demonstrate the network effects of neuromodulatory release may suffice, and the level of details present in the NMC model is not necessarily needed to produce the same results. While that may be true for the synaptic implementation of neuromodulatory release, the same cannot be said about the volumetric model. Point neuron models lack spatial extent by definition, while the detailed neuron models used in the NMC replica have complex morphological properties. The

model of diffuse neuromodulatory release that we developed relies entirely upon an algorithm that samples the spatial surroundings of the volumetric release site and assigns differential connection parameters and conductance values to the newly instantiated targets of neuromodulatory innervation. Therefore, it wouldn't be possible to apply the same algorithm to a network of point neuron models, because the sampling subspace would be basically empty. Our detailed model of somatosensory microcircuitry serves as an ideal candidate to study both the structural and functional characteristics of neuromodulatory release.

Bibliography

- [Agnati et al., 2006] Agnati, L. F., Leo, G., Zanardi, A., Genedani, S., Rivera, A., Fuxe, K., and Guidolin, D. (2006). Volume transmission and wiring transmission from cellular to molecular networks: history and perspectives. *Acta Physiologica*, 187(1-2):329–344. _eprint: <https://onlinelibrary.wiley.com/doi/pdf/10.1111/j.1748-1716.2006.01579.x>.
- [Albuquerque et al., 2000] Albuquerque, E. X., Pereira, E. F., Mike, A., Eisenberg, H. M., Maelicke, A., and Alkondon, M. (2000). Neuronal nicotinic receptors in synaptic functions in humans and rats: physiological and clinical relevance. *Behavioural Brain Research*, 113(1-2):131–141.
- [Alger et al., 2014] Alger, B. E., Nagode, D. A., and Tang, A.-H. (2014). Muscarinic cholinergic receptors modulate inhibitory synaptic rhythms in hippocampus and neocortex. *Frontiers in Synaptic Neuroscience*, 6.
- [Alitto and Dan, 2013] Alitto, H. J. and Dan, Y. (2013). Cell-type-specific modulation of neocortical activity by basal forebrain input. *Frontiers in Systems Neuroscience*, 6.
- [Alkondon and Albuquerque, 2004] Alkondon, M. and Albuquerque, E. X. (2004). The nicotinic acetylcholine receptor subtypes and their function in the hippocampus and cerebral cortex. In *Progress in Brain Research*, volume 145, pages 109–120. Elsevier.
- [Alkondon et al., 1999] Alkondon, M., Pereira, E. F. R., Eisenberg, H. M., and Albuquerque, E. X. (1999). Choline and Selective Antagonists Identify Two Subtypes of Nicotinic Acetylcholine Receptors that Modulate GABA Release from CA1 Interneurons in Rat Hippocampal Slices. *The Journal of Neuroscience*, 19(7):2693–2705.
- [Anaclet et al., 2015] Anaclet, C., Pedersen, N. P., Ferrari, L. L., Venner, A., Bass, C. E., Arrigoni, E., and Fuller, P. M. (2015). Basal forebrain control of wakefulness and cortical rhythms. *Nature Communications*, 6(1).

- [Aoki and Kabak, 1992] Aoki, C. and Kabak, S. (1992). Cholinergic terminals in the cat visual cortex: ultrastructural basis for interaction with glutamate-immunoreactive neurons and other cells. *Visual Neuroscience*, 8(3):177–191.
- [Aransay et al., 2015] Aransay, A., Rodríguez-López, C., García-Amado, M., Clascá, F., and Prensa, L. (2015). Long-range projection neurons of the mouse ventral tegmental area: a single-cell axon tracing analysis. *Frontiers in Neuroanatomy*, 9:59.
- [Arroyo et al., 2012] Arroyo, S., Bennett, C., Aziz, D., Brown, S. P., and Hestrin, S. (2012). Prolonged Disynaptic Inhibition in the Cortex Mediated by Slow, Non- $\alpha 7$ Nicotinic Excitation of a Specific Subset of Cortical Interneurons. *Journal of Neuroscience*, 32(11):3859–3864.
- [Artinian et al., 2001] Artinian, L. R., Ding, J. M., and Gillette, M. U. (2001). Carbon Monoxide and Nitric Oxide: Interacting Messengers in Muscarinic Signaling to the Brain’s Circadian Clock. *Experimental Neurology*, 171(2):293–300.
- [Athilingam et al., 2017] Athilingam, J. C., Ben-Shalom, R., Keeshen, C. M., Sohal, V. S., and Bender, K. J. (2017). Serotonin enhances excitability and gamma frequency temporal integration in mouse prefrontal fast-spiking interneurons. *eLife*, 6:e31991.
- [Avesar and Gulledge, 2012] Avesar, D. and Gulledge, A. T. (2012). Selective serotonergic excitation of callosal projection neurons. *Frontiers in Neural Circuits*, 6.
- [Bailey et al., 2010] Bailey, C. D. C., Biasi, M. D., Fletcher, P. J., and Lambe, E. K. (2010). The Nicotinic Acetylcholine Receptor $\alpha 5$ Subunit Plays a Key Role in Attention Circuitry and Accuracy. *Journal of Neuroscience*, 30(27):9241–9252.
- [Baker et al., 2018] Baker, A. L., O’Toole, R. J., and Gulledge, A. T. (2018). Preferential cholinergic excitation of corticopontine neurons. *The Journal of Physiology*, pages n/a–n/a.
- [Bao et al., 2001] Bao, S., Chan, V. T., and Merzenich, M. M. (2001). Cortical remodelling induced by activity of ventral tegmental dopamine neurons. *Nature*, 412(6842):79–83.
- [Bassant et al., 1990] Bassant, M. H., Ennouri, K., and Lamour, Y. (1990). Effects of iontophoretically applied monoamines on somatosensory cortical neurons of unanesthetized rats. *Neuroscience*, 39(2):431–439.

- [Bazhenov et al., 2002] Bazhenov, M., Timofeev, I., Steriade, M., and Sejnowski, T. J. (2002). Model of Thalamocortical Slow-Wave Sleep Oscillations and Transitions to Activated States. *Journal of Neuroscience*, 22(19):8691–8704.
- [Bear and Singer, 1986] Bear, M. F. and Singer, W. (1986). Modulation of visual cortical plasticity by acetylcholine and noradrenaline. *Nature*, 320(6058):172–176.
- [Beaulieu and Somogyi, 1991] Beaulieu, C. and Somogyi, P. (1991). Enrichment of cholinergic synaptic terminals on GABAergic neurons and coexistence of immunoreactive GABA and choline acetyltransferase in the same synaptic terminals in the striate cortex of the cat. *The Journal of Comparative Neurology*, 304(4):666–680.
- [Beckstead et al., 2004] Beckstead, M. J., Grandy, D. K., Wickman, K., and Williams, J. T. (2004). Vesicular Dopamine Release Elicits an Inhibitory Postsynaptic Current in Midbrain Dopamine Neurons. *Neuron*, 42(6):939–946.
- [Bennett et al., 2012] Bennett, C., Arroyo, S., Berns, D., and Hestrin, S. (2012). Mechanisms Generating Dual-Component Nicotinic EPSCs in Cortical Interneurons. *Journal of Neuroscience*, 32(48):17287–17296.
- [Berger, 1929] Berger, H. (1929). Über das Elektrenkephalogramm des Menschen. *Archiv für Psychiatrie und Nervenkrankheiten*, 87(1):527–570.
- [Berger et al., 2009] Berger, M., Gray, J. A., and Roth, B. L. (2009). The Expanded Biology of Serotonin. *Annual Review of Medicine*, 60(1):355–366.
- [Bertrand, 2010] Bertrand, D. (2010). Neurocircuitry of the nicotinic cholinergic system. *Dialogues in Clinical Neuroscience*, 12(4):463–470.
- [Beyene et al., 2019] Beyene, A. G., Delevich, K., Del Bonis-O’Donnell, J. T., Piekarski, D. J., Lin, W. C., Thomas, A. W., Yang, S. J., Kosillo, P., Yang, D., Prounis, G. S., Wilbrecht, L., and Landry, M. P. (2019). Imaging striatal dopamine release using a nongenetically encoded near infrared fluorescent catecholamine nanosensor. *Science Advances*, 5(7):eaaw3108. Publisher: American Association for the Advancement of Science.
- [Blandina et al., 2004] Blandina, P., Efofudebe, M., Cenni, G., Mannaioni, P., and Passani, M. B. (2004). Acetylcholine, Histamine, and Cognition: Two Sides of the Same Coin. *Learning & Memory*, 11(1):1–8.
- [Borda et al., 1998] Borda, T., Genaro, A., Sterin-Borda, L., and Cremaschi, G. (1998). Involvement of endogenous nitric oxide signalling

- system in brain muscarinic acetylcholine receptor activation. *Journal of Neural Transmission*, 105(2-3):193–204.
- [Borden et al., 2020] Borden, P. M., Zhang, P., Shivange, A. V., Marvin, J. S., Cichon, J., Dan, C., Podgorski, K., Figueiredo, A., Novak, O., Tanimoto, M., Shigetomi, E., Lobas, M. A., Kim, H., Zhu, P., Zhang, Y., Zheng, W. S., Fan, C., Wang, G., Xiang, B., Gan, L., Zhang, G.-X., Guo, K., Lin, L., Cai, Y., Yee, A. G., Aggarwal, A., Bao, H., Lou, X., Chapman, E. R., Ford, C. P., Rees, D., Dietrich, D., Khakh, B. S., Dittman, J. S., Gan, W.-B., Koyama, M., Jayaraman, V., Cheer, J. F., Lester, H. A., Zhu, J. J., and Looger, L. (2020). A Fast Genetically Encoded Fluorescent Sensor for Faithful *in vivo* Acetylcholine Detection in Mice, Fish, Worms and Flies. SSRN Scholarly Paper ID 3554080, Social Science Research Network, Rochester, NY.
- [Borrito-Escuela et al., 2018] Borrito-Escuela, D. O., Perez De La Mora, M., Manger, P., Narváez, M., Beggiato, S., Crespo-Ramírez, M., Navarro, G., Wydra, K., Díaz-Cabiale, Z., Rivera, A., Ferraro, L., Tanganelli, S., Filip, M., Franco, R., and Fuxe, K. (2018). Brain Dopamine Transmission in Health and Parkinson’s Disease: Modulation of Synaptic Transmission and Plasticity Through Volume Transmission and Dopamine Heteroreceptors. *Frontiers in Synaptic Neuroscience*, 10:20.
- [Brombas et al., 2014] Brombas, A., Fletcher, L. N., and Williams, S. R. (2014). Activity-Dependent Modulation of Layer 1 Inhibitory Neocortical Circuits by Acetylcholine. *Journal of Neuroscience*, 34(5):1932–1941.
- [Brunk et al., 2019] Brunk, M. G. K., Deane, K. E., Kisse, M., Deliano, M., Vieweg, S., Ohl, F. W., Lippert, M. T., and Happel, M. F. K. (2019). Optogenetic stimulation of the VTA modulates a frequency-specific gain of thalamocortical inputs in infragranular layers of the auditory cortex. *Scientific Reports*, 9(1):20385. Number: 1 Publisher: Nature Publishing Group.
- [Bunin and Wightman, 1998] Bunin, M. A. and Wightman, R. M. (1998). Quantitative Evaluation of 5-Hydroxytryptamine (Serotonin) Neuronal Release and Uptake: An Investigation of Extrasynaptic Transmission. *Journal of Neuroscience*, 18(13):4854–4860. Publisher: Society for Neuroscience Section: ARTICLE.
- [Buzsaki et al., 1988] Buzsaki, G., Bickford, R. G., Ponomareff, G., Thal, L. J., Mandel, R., and Gage, F. H. (1988). Nucleus basalis and thalamic control of neocortical activity in the freely moving rat. *The Journal of Neuroscience: The Official Journal of the Society for Neuroscience*, 8(11):4007–4026.

- [Calabresi et al., 2006] Calabresi, P., Picconi, B., Parnetti, L., and Di Filippo, M. (2006). A convergent model for cognitive dysfunctions in Parkinson’s disease: the critical dopamine–acetylcholine synaptic balance. *The Lancet Neurology*, 5(11):974–983.
- [Callender and Newton, 2017] Callender, J. and Newton, A. (2017). Conventional protein kinase C in the brain: 40 years later. *Neuronal Signaling*, 1(2):NS20160005.
- [Carr and Surmeier, 2007] Carr, D. B. and Surmeier, D. J. (2007). M₁ Muscarinic Receptor Modulation of Kir2 Channels Enhances Temporal Summation of Excitatory Synaptic Potentials in Prefrontal Cortex Pyramidal Neurons. *Journal of Neurophysiology*, 97(5):3432–3438.
- [Castro-Alamancos and Gulati, 2014] Castro-Alamancos, M. A. and Gulati, T. (2014). Neuromodulators produce distinct activated states in neocortex. *The Journal of Neuroscience: The Official Journal of the Society for Neuroscience*, 34(37):12353–12367.
- [Cauli et al., 2004] Cauli, B., Tong, X.-K., Rancillac, A., Serluca, N., Lambolez, B., Rossier, J., and Hamel, E. (2004). Cortical GABA Interneurons in Neurovascular Coupling: Relays for Subcortical Vasoactive Pathways. *Journal of Neuroscience*, 24(41):8940–8949.
- [Celada et al., 2013] Celada, P., Puig, M. V., and Artigas, F. (2013). Serotonin modulation of cortical neurons and networks. *Frontiers in Integrative Neuroscience*, 7.
- [Chaves-Coira et al., 2016] Chaves-Coira, I., Barros-Zulaica, N., Rodrigo-Angulo, M., and Núñez, (2016). Modulation of Specific Sensory Cortical Areas by Segregated Basal Forebrain Cholinergic Neurons Demonstrated by Neuronal Tracing and Optogenetic Stimulation in Mice. *Frontiers in Neural Circuits*, 10.
- [Chaves-Coira et al., 2018] Chaves-Coira, I., Rodrigo-Angulo, M. L., and Nuñez, A. (2018). Bilateral Pathways from the Basal Forebrain to Sensory Cortices May Contribute to Synchronous Sensory Processing. *Frontiers in Neuroanatomy*, 12.
- [Chen et al., 2015] Chen, N., Sugihara, H., and Sur, M. (2015). An acetylcholine-activated microcircuit drives temporal dynamics of cortical activity. *Nature Neuroscience*, 18(6):892–902.
- [Christophe et al., 2002] Christophe, E., Roebuck, A., Staiger, J. F., Lavery, D. J., Charpak, S., and Audinat, E. (2002). Two Types of Nicotinic Receptors Mediate an Excitation of Neocortical Layer I Interneurons. *Journal of Neurophysiology*, 88(3):1318–1327.

- [Colangelo et al., 2019] Colangelo, C., Shichkova, P., Keller, D., Markram, H., and Ramaswamy, S. (2019). Cellular, Synaptic and Network Effects of Acetylcholine in the Neocortex. *Frontiers in Neural Circuits*, 13:24.
- [Condon et al., 2021] Condon, A. F., Robinson, B. G., Asad, N., Dore, T. M., Tian, L., and Williams, J. T. (2021). The residence of synaptically released dopamine on D2 autoreceptors. *Cell Reports*, 36(5):109465.
- [Constantinople and Bruno, 2011] Constantinople, C. and Bruno, R. (2011). Effects and Mechanisms of Wakefulness on Local Cortical Networks. *Neuron*, 69(6):1061–1068.
- [Coppola and Disney, 2018] Coppola, J. J. and Disney, A. A. (2018). Is There a Canonical Cortical Circuit for the Cholinergic System? Anatomical Differences Across Common Model Systems. *Frontiers in Neural Circuits*, 12.
- [Coppola et al., 2016] Coppola, J. J., Ward, N. J., Jadi, M. P., and Disney, A. A. (2016). Modulatory compartments in cortex and local regulation of cholinergic tone. *Journal of Physiology-Paris*, 110(1-2):3–9.
- [Couey et al., 2007] Couey, J. J., Meredith, R. M., Spijker, S., Poorthuis, R. B., Smit, A. B., Brussaard, A. B., and Mansvelder, H. D. (2007). Distributed Network Actions by Nicotine Increase the Threshold for Spike-Timing-Dependent Plasticity in Prefrontal Cortex. *Neuron*, 54(1):73–87.
- [Courtney and Ford, 2014] Courtney, N. A. and Ford, C. P. (2014). The Timing of Dopamine- and Noradrenaline-Mediated Transmission Reflects Underlying Differences in the Extent of Spillover and Pooling. *Journal of Neuroscience*, 34(22):7645–7656.
- [Cousineau et al., 2020] Cousineau, J., Lescouzères, L., Taupignon, A., Delgado-Zabalza, L., Valjent, E., Baufreton, J., and Le Bon-Jégo, M. (2020). Dopamine D2-Like Receptors Modulate Intrinsic Properties and Synaptic Transmission of Parvalbumin Interneurons in the Mouse Primary Motor Cortex. *eneuro*, 7(3):ENEURO.0081–20.2020.
- [Cremonesi et al., 2020] Cremonesi, F., Hager, G., Wellein, G., and Schürmann, F. (2020). Analytic performance modeling and analysis of detailed neuron simulations. *The International Journal of High Performance Computing Applications*, 34(4):428–449.
- [Dajas-Bailador and Wonnacott, 2004] Dajas-Bailador, F. and Wonnacott, S. (2004). Nicotinic acetylcholine receptors and the regulation of neuronal signalling. *Trends in Pharmacological Sciences*, 25(6):317–324.

- [Dale, 1914] Dale, H. H. (1914). The Action of Certain Esters and Ethers of Choline, and Their Relation to Muscarine. *Journal of Pharmacology and Experimental Therapeutics*, 6(2):147–190.
- [D’Amato et al., 1987] D’Amato, R. J., Blue, M. E., Largent, B. L., Lynch, D. R., Ledbetter, D. J., Molliver, M. E., and Snyder, S. H. (1987). Ontogeny of the serotonergic projection to rat neocortex: transient expression of a dense innervation to primary sensory areas. *Proceedings of the National Academy of Sciences*, 84(12):4322–4326.
- [Dani and Bertrand, 2007] Dani, J. A. and Bertrand, D. (2007). Nicotinic Acetylcholine Receptors and Nicotinic Cholinergic Mechanisms of the Central Nervous System. *Annual Review of Pharmacology and Toxicology*, 47(1):699–729.
- [Dasari et al., 2017] Dasari, S., Hill, C., and Gullledge, A. T. (2017). A unifying hypothesis for M1 muscarinic receptor signalling in pyramidal neurons. *The Journal of Physiology*, 595(5):1711–1723.
- [Dasgupta et al., 2018] Dasgupta, R., Seibt, F., and Beierlein, M. (2018). Synaptic Release of Acetylcholine Rapidly Suppresses Cortical Activity by Recruiting Muscarinic Receptors in Layer 4. *Journal of Neuroscience*, 38(23):5338–5350.
- [De Filippo et al., 2020] De Filippo, R., Rost, B. R., Stumpf, A., Cooper, C., Tukker, J. J., Harms, C., Beed, P., and Schmitz, D. (2020). Somatostatin interneurons activated by 5-HT_{2a} receptor suppress slow oscillations in medial entorhinal cortex. preprint, Neuroscience.
- [de Filippo et al., 2021] de Filippo, R., Rost, B. R., Stumpf, A., Cooper, C., Tukker, J. J., Harms, C., Beed, P., and Schmitz, D. (2021). Somatostatin interneurons activated by 5-HT_{2A} receptor suppress slow oscillations in medial entorhinal cortex. *eLife*, 10:e66960.
- [De-Miguel and Trueta, 2005] De-Miguel, F. F. and Trueta, C. (2005). Synaptic and Extrasynaptic Secretion of Serotonin. *Cellular and Molecular Neurobiology*, 25(2):297–312.
- [DeFelipe, 1999] DeFelipe, J. (1999). Estimation of the Number of Synapses in the Cerebral Cortex: Methodological Considerations. *Cerebral Cortex*, 9(7):722–732.
- [Delmas and Brown, 2005] Delmas, P. and Brown, D. A. (2005). Pathways modulating neural KCNQ/M (Kv7) potassium channels. *Nature Reviews. Neuroscience; London*, 6(11):850–62.

- [Descarries et al., 1987] Descarries, L., Lemay, B., Doucet, G., and Berger, B. (1987). Regional and laminar density of the dopamine innervation in adult rat cerebral cortex. *Neuroscience*, 21(3):807–824.
- [Descarries and Mechawar, 2000] Descarries, L. and Mechawar, N. (2000). Ultrastructural evidence for diffuse transmission by monoamine and acetylcholine neurons of the central nervous system. In *Progress in Brain Research*, volume 125 of *Volume Transmission Revisited*, pages 27–47. Elsevier.
- [Descarries et al., 2010] Descarries, L., Riad, M., and Parent, M. (2010). Ultrastructure of the Serotonin Innervation in the Mammalian Central Nervous System. In *Handbook of Behavioral Neuroscience*, volume 21, pages 65–101. Elsevier.
- [Descarries et al., 1982] Descarries, L., Watkins, K. C., Garcia, S., and Beaudet, A. (1982). The serotonin neurons in nucleus raphe dorsalis of adult rat: A light and electron microscope radioautographic study. *Journal of Comparative Neurology*, 207(3):239–254. eprint: <https://onlinelibrary.wiley.com/doi/pdf/10.1002/cne.902070305>.
- [Disney, 2021] Disney, A. A. (2021). Neuromodulatory Control of Early Visual Processing in Macaque. *Annual Review of Vision Science*, 7(1):181–199.
- [Disney et al., 2007] Disney, A. A., Aoki, C., and Hawken, M. J. (2007). Gain Modulation by Nicotine in Macaque V1. *Neuron*, 56(4):701–713.
- [Disney et al., 2006] Disney, A. A., Domakonda, K. V., and Aoki, C. (2006). Differential expression of muscarinic acetylcholine receptors across excitatory and inhibitory cells in visual cortical areas V1 and V2 of the macaque monkey. *The Journal of Comparative Neurology*, 499(1):49–63.
- [Disney and Higley, 2020] Disney, A. A. and Higley, M. J. (2020). Diverse Spatiotemporal Scales of Cholinergic Signaling in the Neocortex. *The Journal of Neuroscience*, 40(4):720–725.
- [Dori et al., 1996] Dori, I., Dinopoulos, A., Blue, M., and Parnavelas, J. (1996). Regional Differences in the Ontogeny of the Serotonergic Projection to the Cerebral Cortex. *Experimental Neurology*, 138(1):1–14.
- [Duque et al., 2000] Duque, A., Balatoni, B., Detari, L., and Zaborszky, L. (2000). EEG Correlation of the Discharge Properties of Identified Neurons in the Basal Forebrain. *Journal of Neurophysiology*, 84(3):1627–1635.
- [Eban-Rothschild et al., 2016] Eban-Rothschild, A., Rothschild, G., Giardino, W. J., Jones, J. R., and de Lecea, L. (2016). VTA dopaminergic

- gic neurons regulate ethologically relevant sleep–wake behaviors. *Nature Neuroscience*, 19(10):1356–1366.
- [Eccles et al., 1953] Eccles, J., Fatt, P., and Koketsu, K. (1953). Cholinergic and Inhibitory Synapses in a Central Nervous Pathway. *The Australian Journal of Science*, 16:50–54.
- [Eckenstein et al., 1988] Eckenstein, F. P., Baughman, R. W., and Quinn, J. (1988). An anatomical study of cholinergic innervation in rat cerebral cortex. *Neuroscience*, 25(2):457–474.
- [Ecker et al., 2020] Ecker, A., Romani, A., Sáray, S., Káli, S., Migliore, M., Falck, J., Lange, S., Mercer, A., Thomson, A. M., Muller, E., Reimann, M. W., and Ramaswamy, S. (2020). Data-driven integration of hippocampal CA1 synaptic physiology *in silico*. *Hippocampus*, 30(11):1129–1145.
- [Eggermann and Feldmeyer, 2009] Eggermann, E. and Feldmeyer, D. (2009). Cholinergic filtering in the recurrent excitatory microcircuit of cortical layer 4. *Proceedings of the National Academy of Sciences*, 106(28):11753–11758.
- [Eggermann et al., 2014] Eggermann, E., Kremer, Y., Crochet, S., and Petersen, C. H. (2014). Cholinergic Signals in Mouse Barrel Cortex during Active Whisker Sensing. *Cell Reports*, 9(5):1654–1660.
- [Elhusseiny and Hamel, 2000] Elhusseiny, A. and Hamel, E. (2000). Muscarinic—but Not Nicotinic—Acetylcholine Receptors Mediate a Nitric Oxide-Dependent Dilation in Brain Cortical Arterioles: A Possible Role for the M5 Receptor Subtype. *Journal of Cerebral Blood Flow & Metabolism*, 20(2):298–305.
- [Engelhardt et al., 2007] Engelhardt, J. v., Eliava, M., Meyer, A. H., Rozov, A., and Monyer, H. (2007). Functional Characterization of Intrinsic Cholinergic Interneurons in the Cortex. *Journal of Neuroscience*, 27(21):5633–5642.
- [Fanselow et al., 2008] Fanselow, E. E., Richardson, K. A., and Connors, B. W. (2008). Selective, State-Dependent Activation of Somatostatin-Expressing Inhibitory Interneurons in Mouse Neocortex. *Journal of Neurophysiology*, 100(5):2640–2652.
- [Fellous and Linster, 1998] Fellous, J.-M. and Linster, C. (1998). Computational Models of Neuromodulation. *Neural Computation*, 10(4):771–805.
- [Fink et al., 2011] Fink, C. G., Booth, V., and Zochowski, M. (2011). Cellularly-Driven Differences in Network Synchronization Propensity Are

- Differentially Modulated by Firing Frequency. *PLoS Computational Biology*, 7(5):e1002062.
- [Fink et al., 2013] Fink, C. G., Murphy, G. G., Zochowski, M., and Booth, V. (2013). A Dynamical Role for Acetylcholine in Synaptic Renormalization. *PLoS Computational Biology*, 9(3):e1002939.
- [Foehring et al., 2002] Foehring, R. C., Brederode, J. F. M. v., Kinney, G. A., and Spain, W. J. (2002). Serotonergic Modulation of Supragranular Neurons in Rat Sensorimotor Cortex. *Journal of Neuroscience*, 22(18):8238–8250. Publisher: Society for Neuroscience Section: ARTICLE.
- [Gao and Goldman-Rakic, 2003] Gao, W.-J. and Goldman-Rakic, P. S. (2003). Selective modulation of excitatory and inhibitory microcircuits by dopamine. *Proceedings of the National Academy of Sciences*, 100(5):2836–2841. Publisher: National Academy of Sciences Section: Biological Sciences.
- [Gericke et al., 2011] Gericke, A., Sniatecki, J. J., Mayer, V. G. A., Goloborodko, E., Patzak, A., Wess, J., and Pfeiffer, N. (2011). Role of M1, M3, and M5 muscarinic acetylcholine receptors in cholinergic dilation of small arteries studied with gene-targeted mice. *American Journal of Physiology - Heart and Circulatory Physiology*, 300(5):H1602–H1608.
- [Giacobini, 2003] Giacobini, E. (2003). Cholinergic function and Alzheimer’s disease. *International Journal of Geriatric Psychiatry*, 18(S1):S1–S5.
- [Gielow and Zaborszky, 2017] Gielow, M. R. and Zaborszky, L. (2017). The Input-Output Relationship of the Cholinergic Basal Forebrain. *Cell Reports*, 18(7):1817–1830.
- [Gil et al., 1997] Gil, Z., Connors, B. W., and Amitai, Y. (1997). Differential Regulation of Neocortical Synapses by Neuromodulators and Activity. *Neuron*, 19(3):679–686.
- [Gonzalez-Islas and Hablitz, 2003] Gonzalez-Islas, C. and Hablitz, J. J. (2003). Dopamine Enhances EPSCs in Layer II–III Pyramidal Neurons in Rat Prefrontal Cortex. *Journal of Neuroscience*, 23(3):867–875. Publisher: Society for Neuroscience Section: ARTICLE.
- [Gorelova et al., 2002] Gorelova, N., Seamans, J. K., and Yang, C. R. (2002). Mechanisms of Dopamine Activation of Fast-Spiking Interneurons That Exert Inhibition in Rat Prefrontal Cortex. *Journal of Neurophysiology*, 88(6):3150–3166. Publisher: American Physiological Society.

- [Grace, 2016] Grace, A. A. (2016). Dysregulation of the dopamine system in the pathophysiology of schizophrenia and depression. *Nature Reviews Neuroscience*, 17(8):524–532.
- [Grandjean et al., 2019] Grandjean, J., Corcoba, A., Kahn, M. C., Upton, A. L., Deneris, E. S., Seifritz, E., Helmchen, F., Mansuy, I. M., Mann, E. O., Rudin, M., and Saab, B. J. (2019). A brain-wide functional map of the serotonergic responses to acute stress and fluoxetine. *Nature Communications*, 10(1):350. Number: 1 Publisher: Nature Publishing Group.
- [Granger et al., 2016] Granger, A. J., Mulder, N., Saunders, A., and Sabatini, B. L. (2016). Cotransmission of acetylcholine and GABA. *Neuropharmacology*, 100:40–46.
- [Granger et al., 2017] Granger, A. J., Wallace, M. L., and Sabatini, B. L. (2017). Multi-transmitter neurons in the mammalian central nervous system. *Current Opinion in Neurobiology*, 45:85–91.
- [Granger et al., 2018] Granger, A. J., Wang, W., Robertson, K., El-Rifai, M., Zanello, A., Bistrong, K., Saunders, A., Chow, B., Nunez, V., Gu, C., and Sabatini, B. L. (2018). Target-specific co-transmission of acetylcholine and GABA from a subset of cortical VIP+ interneurons. *bioRxiv*.
- [Groleau et al., 2015] Groleau, M., Kang, J. I., Huppé-Gourgues, F., and Vaucher, E. (2015). Distribution and effects of the muscarinic receptor subtypes in the primary visual cortex. *Frontiers in Synaptic Neuroscience*, 7.
- [Gulledge et al., 2009] Gulledge, A. T., Bucci, D. J., Zhang, S. S., Matsui, M., and Yeh, H. H. (2009). M1 Receptors Mediate Cholinergic Modulation of Excitability in Neocortical Pyramidal Neurons. *Journal of Neuroscience*, 29(31):9888–9902.
- [Gulledge et al., 2007] Gulledge, A. T., Park, S. B., Kawaguchi, Y., and Stuart, G. J. (2007). Heterogeneity of Phasic Cholinergic Signaling in Neocortical Neurons. *Journal of Neurophysiology*, 97(3):2215–2229.
- [Gulledge and Stuart, 2005] Gulledge, A. T. and Stuart, G. J. (2005). Cholinergic Inhibition of Neocortical Pyramidal Neurons. *Journal of Neuroscience*, 25(44):10308–10320.
- [Gundersen, 1988] Gundersen, H. J. G. (1988). The nucleator. *Journal of Microscopy*, 151(1):3–21.
- [Gupta et al., 2000] Gupta, A., Wang, Y., and Markram, H. (2000). Organizing Principles for a Diversity of GABAergic Interneurons and Synapses in the Neocortex. *Science*, 287(5451):273–278.

- [Harris and Thiele, 2011] Harris, K. D. and Thiele, A. (2011). Cortical State and Attention. *Nature Reviews. Neuroscience*, 12(9):509–523.
- [Hasselmo, 1993] Hasselmo, M. E. (1993). Acetylcholine and Learning in a Cortical Associative Memory. *Neural Computation*, 5(1):32–44.
- [Hasselmo, 1995] Hasselmo, M. E. (1995). Neuromodulation and cortical function: modeling the physiological basis of behavior. *Behavioural Brain Research*, 67(1):1–27.
- [Hasselmo, 1999] Hasselmo, M. E. (1999). Neuromodulation: acetylcholine and memory consolidation. *Trends in Cognitive Sciences*, 3(9):351–359.
- [Hasselmo, 2006] Hasselmo, M. E. (2006). The role of acetylcholine in learning and memory. *Current Opinion in Neurobiology*, 16(6):710–715.
- [Hasselmo and Sarter, 2011] Hasselmo, M. E. and Sarter, M. (2011). Modes and Models of Forebrain Cholinergic Neuromodulation of Cognition. *Neuropsychopharmacology*, 36(1):52–73.
- [Hay et al., 2016] Hay, Y. A., Lambolez, B., and Tricoire, L. (2016). Nicotinic Transmission onto Layer 6 Cortical Neurons Relies on Synaptic Activation of Non- $\alpha 7$ Receptors. *Cerebral Cortex*, 26(6):2549–2562.
- [Hedrick and Waters, 2015] Hedrick, T. and Waters, J. (2015). Acetylcholine excites neocortical pyramidal neurons via nicotinic receptors. *Journal of Neurophysiology*, 113(7):2195–2209.
- [Henny and Jones, 2008] Henny, P. and Jones, B. E. (2008). Projections from basal forebrain to prefrontal cortex comprise cholinergic, GABAergic and glutamatergic inputs to pyramidal cells or interneurons. *European Journal of Neuroscience*, 27(3):654–670.
- [Heys and Hasselmo, 2012] Heys, J. G. and Hasselmo, M. E. (2012). Neuromodulation of Ih in Layer II Medial Entorhinal Cortex Stellate Cells: A Voltage-Clamp Study. *Journal of Neuroscience*, 32(26):9066–9072.
- [Heys et al., 2012] Heys, J. G., Schultheiss, N. W., Shay, C. F., Tsuno, Y., and Hasselmo, M. E. (2012). Effects of acetylcholine on neuronal properties in entorhinal cortex. *Frontiers in Behavioral Neuroscience*, 6.
- [Hilscher et al., 2017] Hilscher, M. M., Leão, R. N., Edwards, S. J., Leão, K. E., and Kullander, K. (2017). Chrna2-Martinotti Cells Synchronize Layer 5 Type A Pyramidal Cells via Rebound Excitation. *PLOS Biology*, 15(2):e2001392.
- [Hines and Carnevale, 1997] Hines, M. L. and Carnevale, N. T. (1997). The NEURON Simulation Environment. *Neural Computation*, 9(6):1179–1209.

- [Hines et al., 2008] Hines, M. L., Markram, H., and Schürmann, F. (2008). Fully implicit parallel simulation of single neurons. *Journal of Computational Neuroscience*, 25(3):439–448.
- [Hwang et al., 2005] Hwang, J.-I., Kim, H. S., Lee, J. R., Kim, E., Ryu, S. H., and Suh, P.-G. (2005). The Interaction of Phospholipase C- β 3 with Shank2 Regulates mGluR-mediated Calcium Signal. *Journal of Biological Chemistry*, 280(13):12467–12473.
- [Iriti, 2013] Iriti, M. (2013). Plant Neurobiology, a Fascinating Perspective in the Field of Research on Plant Secondary Metabolites. *International Journal of Molecular Sciences*, 14(6):10819–10821.
- [Izhikevich and Edelman, 2008] Izhikevich, E. M. and Edelman, G. M. (2008). Large-scale model of mammalian thalamocortical systems. *Proceedings of the National Academy of Sciences*, 105(9):3593–3598.
- [Jacob and Nienborg, 2018] Jacob, S. N. and Nienborg, H. (2018). Monoaminergic Neuromodulation of Sensory Processing. *Frontiers in Neural Circuits*, 12:51.
- [Jiang and Bajpayee, 2009] Jiang, M. and Bajpayee, N. S. (2009). Molecular Mechanisms of Go Signaling. *Neurosignals*, 17(1):23–41.
- [Jiang et al., 2013] Jiang, X., Wang, G., Lee, A. J., Stornetta, R. L., and Zhu, J. J. (2013). The organization of two new cortical interneuronal circuits. *Nature Neuroscience*, 16(2):210–218.
- [Jing et al., 2018] Jing, M., Zhang, P., Wang, G., Feng, J., Mesik, L., Zeng, J., Jiang, H., Wang, S., Looby, J. C., Guagliardo, N. A., Langma, L. W., Lu, J., Zuo, Y., Talmage, D. A., Role, L. W., Barrett, P. Q., Zhang, L. I., Luo, M., Song, Y., Zhu, J. J., and Li, Y. (2018). A genetically encoded fluorescent acetylcholine indicator for in vitro and in vivo studies. *Nature Biotechnology*.
- [Joshi et al., 2016] Joshi, A., Kalappa, B. I., Anderson, C. T., and Tzounopoulos, T. (2016). Cell-Specific Cholinergic Modulation of Excitability of Layer 5B Principal Neurons in Mouse Auditory Cortex. *Journal of Neuroscience*, 36(32):8487–8499.
- [Kalmbach et al., 2012] Kalmbach, A., Hedrick, T., and Waters, J. (2012). Selective optogenetic stimulation of cholinergic axons in neocortex. *Journal of Neurophysiology*, 107(7):2008–2019.
- [Kalsbeek et al., 1988] Kalsbeek, A., Voorn, P., Buijs, R. M., Pool, C. W., and Uylings, H. B. M. (1988). Development of the dopaminergic innervation in the prefrontal cortex of the rat. *The Journal of Comparative Neurology*, 269(1):58–72.

- [Kan et al., 2014] Kan, W., Adjobo-Hermans, M., Burroughs, M., Faibis, G., Malik, S., Tall, G. G., and Smrcka, A. V. (2014). M3 Muscarinic Receptor Interaction with Phospholipase C β 3 Determines Its Signaling Efficiency. *Journal of Biological Chemistry*, 289(16):11206–11218.
- [Kanari et al., 2018] Kanari, L., Dłotko, P., Scolamiero, M., Levi, R., Shillcock, J., Hess, K., and Markram, H. (2018). A Topological Representation of Branching Neuronal Morphologies. *Neuroinformatics*, 16(1):3–13.
- [Kanari et al., 2019] Kanari, L., Ramaswamy, S., Shi, Y., Morand, S., Meystre, J., Perin, R., Abdellah, M., Wang, Y., Hess, K., and Markram, H. (2019). Objective Morphological Classification of Neocortical Pyramidal Cells. *Cerebral Cortex*, 29(4):1719–1735.
- [Kassam et al., 2008] Kassam, S. M., Herman, P. M., Goodfellow, N. M., Alves, N. C., and Lambe, E. K. (2008). Developmental Excitation of Corticothalamic Neurons by Nicotinic Acetylcholine Receptors. *Journal of Neuroscience*, 28(35):8756–8764.
- [Katz and Miledi, 1973] Katz, B. and Miledi, R. (1973). The binding of acetylcholine to receptors and its removal from the synaptic cleft. *The Journal of Physiology*, 231(3):549–574.
- [Kawaguchi, 1997] Kawaguchi, Y. (1997). Selective cholinergic modulation of cortical GABAergic cell subtypes. *Journal of Neurophysiology*, 78(3):1743–1747. moruz.
- [Kawaguchi and Kubota, 1997] Kawaguchi, Y. and Kubota, Y. (1997). GABAergic cell subtypes and their synaptic connections in rat frontal cortex. *Cerebral Cortex*, 7(6):476–486.
- [Kennedy and Bullier, 1985] Kennedy, H. and Bullier, J. (1985). A double-labeling investigation of the afferent connectivity to cortical areas V1 and V2 of the macaque monkey. *The Journal of Neuroscience: The Official Journal of the Society for Neuroscience*, 5(10):2815–2830.
- [Kim et al., 2016] Kim, J.-H., Jung, A.-H., Jeong, D., Choi, I., Kim, K., Shin, S., Kim, S. J., and Lee, S.-H. (2016). Selectivity of Neuromodulatory Projections from the Basal Forebrain and Locus Ceruleus to Primary Sensory Cortices. *The Journal of Neuroscience*, 36(19):5314–5327.
- [Kimura et al., 1999] Kimura, F., Fukuda, M., and Tsumoto, T. (1999). Acetylcholine suppresses the spread of excitation in the visual cortex revealed by optical recording: possible differential effect depending on the source of input. *The European Journal of Neuroscience*, 11(10):3597–3609.

- [Kocharyan et al., 2008] Kocharyan, A., Fernandes, P., Tong, X.-K., Vaucher, E., and Hamel, E. (2008). Specific Subtypes of Cortical GABA Interneurons Contribute to the Neurovascular Coupling Response to Basal Forebrain Stimulation. *Journal of Cerebral Blood Flow & Metabolism*, 28(2):221–231.
- [Koo et al., 2010] Koo, M.-S., Kim, E.-J., Roh, D., and Kim, C.-H. (2010). Role of dopamine in the pathophysiology and treatment of obsessive-compulsive disorder. *Expert Review of Neurotherapeutics*, 10(2):275–290.
- [Kosaka et al., 1987] Kosaka, T., Kosaka, K., Hataguchi, Y., Nagatsu, I., Wu, J.-Y., Ottersen, O., Storm-Mathisen, J., and Hama, K. (1987). Catecholaminergic neurons containing GABA-like and/or glutamic acid decarboxylase-like immunoreactivities in various brain regions of the rat. *Experimental Brain Research*, 66(1).
- [Koukouli et al., 2017] Koukouli, F., Rooy, M., Tziotis, D., Sailor, K. A., O’Neill, H. C., Levenga, J., Witte, M., Nilges, M., Changeux, J.-P., Hoeffler, C. A., Stitzel, J. A., Gutkin, B. S., DiGregorio, D. A., and Maskos, U. (2017). Nicotine reverses hypofrontality in animal models of addiction and schizophrenia. *Nature Medicine*, 23(3):347–354.
- [Kringelbach and Deco, 2020] Kringelbach, M. L. and Deco, G. (2020). Brain States and Transitions: Insights from Computational Neuroscience. *Cell Reports*, 32(10):108128.
- [Krnjević, 2004] Krnjević, K. (2004). Synaptic mechanisms modulated by acetylcholine in cerebral cortex. In *Progress in Brain Research*, volume 145, pages 79–93. Elsevier.
- [Kruglikov and Rudy, 2008] Kruglikov, I. and Rudy, B. (2008). Perisomatic GABA Release and Thalamocortical Integration onto Neocortical Excitatory Cells Are Regulated by Neuromodulators. *Neuron*, 58(6):911–924.
- [Latsari et al., 2002] Latsari, M., Dori, I., Antonopoulos, J., Chiotelli, M., and Dinopoulos, A. (2002). Noradrenergic innervation of the developing and mature visual and motor cortex of the rat brain: A light and electron microscopic immunocytochemical analysis. *The Journal of Comparative Neurology*, 445(2):145–158.
- [Lee et al., 2010] Lee, S., Hjerling-Leffler, J., Zagha, E., Fishell, G., and Rudy, B. (2010). The Largest Group of Superficial Neocortical GABAergic Interneurons Expresses Ionotropic Serotonin Receptors. *Journal of Neuroscience*, 30(50):16796–16808.
- [Lee and Dan, 2012] Lee, S.-H. and Dan, Y. (2012). Neuromodulation of Brain States. *Neuron*, 76(1):209–222.

- [Lester et al., 2010] Lester, D. B., Rogers, T. D., and Blaha, C. D. (2010). Acetylcholine-Dopamine Interactions in the Pathophysiology and Treatment of CNS Disorders: Dopamine-Acetylcholine Interactions in CNS Disorders. *CNS Neuroscience & Therapeutics*, 16(3):137–162.
- [Letzkus et al., 2011] Letzkus, J. J., Wolff, S. B. E., Meyer, E. M. M., Tovote, P., Courtin, J., Herry, C., and Lüthi, A. (2011). A disinhibitory microcircuit for associative fear learning in the auditory cortex. *Nature*, 480(7377):331–335.
- [Levey et al., 1987] Levey, A. I., Hallanger, A. E., and Wainer, B. H. (1987). Cholinergic nucleus basalis neurons may influence the cortex via the thalamus. *Neuroscience Letters*, 74(1):7–13.
- [Levey et al., 1991] Levey, A. I., Kitt, C. A., Simonds, W. F., Price, D. L., and Brann, M. R. (1991). Identification and localization of muscarinic acetylcholine receptor proteins in brain with subtype-specific antibodies. *The Journal of Neuroscience: The Official Journal of the Society for Neuroscience*, 11(10):3218–3226.
- [Levy et al., 2008] Levy, R. B., Reyes, A. D., and Aoki, C. (2008). Cholinergic modulation of local pyramid–interneuron synapses exhibiting divergent short-term dynamics in rat sensory cortex. *Brain Research*, 1215:97–104.
- [Lewis et al., 1988] Lewis, D. A., Foote, S. L., Goldstein, M., and Morrison, J. H. (1988). The dopaminergic innervation of monkey prefrontal cortex: a tyrosine hydroxylase immunohistochemical study. *Brain Research*, 449(1-2):225–243.
- [Lidov and Molliver, 1982] Lidov, H. G. and Molliver, M. E. (1982). An immunohistochemical study of serotonin neuron development in the rat: Ascending pathways and terminal fields. *Brain Research Bulletin*, 8(4):389–430.
- [Lin et al., 2015] Lin, S.-C., Brown, R. E., Shuler, M. G. H., Petersen, C. C. H., and Kepecs, A. (2015). Optogenetic Dissection of the Basal Forebrain Neuromodulatory Control of Cortical Activation, Plasticity, and Cognition. *Journal of Neuroscience*, 35(41):13896–13903.
- [Ling and Benardo, 1999] Ling, D. S. F. and Benardo, L. S. (1999). Restrictions on Inhibitory Circuits Contribute to Limited Recruitment of Fast Inhibition in Rat Neocortical Pyramidal Cells. *Journal of Neurophysiology*, 82(4):1793–1807.
- [Little, 1998] Little, M.D., J. (1998). Combined Nicotinic and Muscarinic Blockade in Elderly Normal Volunteers: Cognitive, Behavioral, and Physiologic Responses. *Neuropsychopharmacology*, 19(1):60–69.

- [Loewi, 1924] Loewi, O. (1924). Über humorale Übertragbarkeit der Herznervenwirkung: V. Mitteilung. Die Übertragbarkeit der negativ chronotrophen und dromotropen Vaguswirkung. *Pflügers Archiv für die Gesamte Physiologie des Menschen und der Tiere*, 204(1):629–640.
- [Lott et al., 2016] Lott, E., Lorincz, M. L., and Mainen, Z. F. (2016). Optogenetic Activation of Dorsal Raphe Serotonin Neurons Rapidly Inhibits Spontaneous But Not Odor-Evoked Activity in Olfactory Cortex. *Journal of Neuroscience*, 36(1):7–18.
- [Lysakowski et al., 1989] Lysakowski, A., Wainer, B. H., Bruce, G., and Hersch, L. B. (1989). An atlas of the regional and laminar distribution of choline acetyltransferase immunoreactivity in rat cerebral cortex. *Neuroscience*, 28(2):291–336.
- [Mancarci et al., 2017] Mancarci, B. O., Toker, L., Tripathy, S. J., Li, B., Rocco, B., Sibille, E., and Pavlidis, P. (2017). Cross-Laboratory Analysis of Brain Cell Type Transcriptomes with Applications to Interpretation of Bulk Tissue Data. *eneuro*, 4(6):ENEURO.0212–17.2017.
- [Marazziti, 2017] Marazziti, D. (2017). Understanding the role of serotonin in psychiatric diseases. *F1000Research*, 6:180.
- [Marchi and Grilli, 2010] Marchi, M. and Grilli, M. (2010). Presynaptic nicotinic receptors modulating neurotransmitter release in the Central Nervous System: Functional interactions with other coexisting receptors. *Progress in Neurobiology*, 92(2):105–111.
- [Marder, 2012] Marder, E. (2012). Neuromodulation of Neuronal Circuits: Back to the Future. *Neuron*, 76(1):1–11.
- [Markram et al., 1997] Markram, H., Lübke, J., Frotscher, M., Roth, A., and Sakmann, B. (1997). Physiology and anatomy of synaptic connections between thick tufted pyramidal neurones in the developing rat neocortex. *The Journal of Physiology*, 500(2):409–440.
- [Markram et al., 2015] Markram, H., Muller, E., Ramaswamy, S., Reimann, M., Abdellah, M., Sanchez, C., Ailamaki, A., Alonso-Nanclares, L., Antille, N., Arsever, S., Kahou, G., Berger, T., Bilgili, A., Buncic, N., Chalmourda, A., Chindemi, G., Courcol, J.-D., Delalandre, F., Delattre, V., Druckmann, S., Dumusc, R., Dynes, J., Eilemann, S., Gal, E., Gevaert, M., Ghobril, J.-P., Gidon, A., Graham, J., Gupta, A., Haenel, V., Hay, E., Heinis, T., Hernando, J., Hines, M., Kanari, L., Keller, D., Kenyon, J., Khazen, G., Kim, Y., King, J., Kisvarday, Z., Kumbhar, P., Lasserre, S., Le Bé, J.-V., Magalhães, B., Merchán-Pérez, A., Meystre, J., Morrice, B., Muller, J., Muñoz-Céspedes, A., Muralidhar, S., Muthurasa, K.,

- Nachbaur, D., Newton, T., Nolte, M., Ovcharenko, A., Palacios, J., Pastor, L., Perin, R., Ranjan, R., Riachi, I., Rodríguez, J.-R., Riquelme, J., Rössert, C., Sfyarakis, K., Shi, Y., Shillcock, J., Silberberg, G., Silva, R., Tauheed, F., Telefont, M., Toledo-Rodriguez, M., Tränkler, T., Van Geit, W., Díaz, J., Walker, R., Wang, Y., Zaninetta, S., DeFelipe, J., Hill, S., Segev, I., and Schürmann, F. (2015). Reconstruction and Simulation of Neocortical Microcircuitry. *Cell*, 163(2):456–492.
- [Markram et al., 2004] Markram, H., Toledo-Rodriguez, M., Wang, Y., Gupta, A., Silberberg, G., and Wu, C. (2004). Interneurons of the neocortical inhibitory system. *Nature Reviews Neuroscience*, 5(10):793–807.
- [Martin and Spühler, 2013] Martin, K. A. C. and Spühler, I. A. (2013). The fine structure of the dopaminergic innervation of area 10 of macaque prefrontal cortex. *European Journal of Neuroscience*, 37(7):1061–1071.
- [Mathes and Thompson, 1996] Mathes, C. and Thompson, S. (1996). The nitric oxide/cGMP pathway couples muscarinic receptors to the activation of Ca²⁺ influx. *The Journal of Neuroscience*, 16(5):1702–1709.
- [Mayne et al., 2013] Mayne, E. W., Craig, M. T., McBain, C. J., and Paulsen, O. (2013). Dopamine suppresses persistent network activity via D1-like dopamine receptors in rat medial entorhinal cortex. *European Journal of Neuroscience*, 37(8):1242–1247. eprint: <https://onlinelibrary.wiley.com/doi/pdf/10.1111/ejn.12125>.
- [McCormick, 1992] McCormick, D. A. (1992). Cellular mechanisms underlying cholinergic and noradrenergic modulation of neuronal firing mode in the cat and guinea pig dorsal lateral geniculate nucleus. *The Journal of Neuroscience: The Official Journal of the Society for Neuroscience*, 12(1):278–289.
- [McCormick and Prince, 1985] McCormick, D. A. and Prince, D. A. (1985). Two types of muscarinic response to acetylcholine in mammalian cortical neurons. *Proceedings of the National Academy of Sciences*, 82(18):6344–6348.
- [McCormick and Prince, 1986] McCormick, D. A. and Prince, D. A. (1986). Mechanisms of action of acetylcholine in the guinea-pig cerebral cortex in vitro. *The Journal of Physiology*, 375(1):169–194.
- [Mechawar et al., 2000] Mechawar, N., Cozzari, C., and Descarries, L. (2000). Cholinergic innervation in adult rat cerebral cortex: A quantitative immunocytochemical description. *Journal of Comparative Neurology*, 428(2):305–318.

- [Mechawar and Descarries, 2001] Mechawar, N. and Descarries, L. (2001). The cholinergic innervation develops early and rapidly in the rat cerebral cortex: a quantitative immunocytochemical study. *Neuroscience*, 108(4):555–567.
- [Mechawar et al., 2002] Mechawar, N., Watkins, K. C., and Descarries, L. (2002). Ultrastructural features of the acetylcholine innervation in the developing parietal cortex of rat. *The Journal of Comparative Neurology*, 443(3):250–258.
- [Meir et al., 2018] Meir, I., Katz, Y., and Lampl, I. (2018). Membrane Potential Correlates of Network Decorrelation and Improved SNR by Cholinergic Activation in the Somatosensory Cortex. *The Journal of Neuroscience*, 38(50):10692–10708.
- [Merchan-Pérez, 2009] Merchan-Pérez, A. (2009). Counting synapses using FIB/SEM microscopy: a true revolution for ultrastructural volume reconstruction. *Frontiers in Neuroanatomy*, 3.
- [Mesulam et al., 1992] Mesulam, M.-M., Hersh, L. B., Mash, D. C., and Geula, C. (1992). Differential cholinergic innervation within functional subdivisions of the human cerebral cortex: A choline acetyltransferase study. *The Journal of Comparative Neurology*, 318(3):316–328.
- [Metherate, 2004] Metherate, R. (2004). Nicotinic Acetylcholine Receptors in Sensory Cortex. *Learning & Memory*, 11(1):50–59.
- [Metherate et al., 1992] Metherate, R., Cox, C., and Ashe, J. (1992). Cellular bases of neocortical activation: modulation of neural oscillations by the nucleus basalis and endogenous acetylcholine. *The Journal of Neuroscience*, 12(12):4701–4711.
- [Metherate and Weinberger, 1990] Metherate, R. and Weinberger, N. M. (1990). Cholinergic modulation of responses to single tones produces tone-specific receptive field alterations in cat auditory cortex. *Synapse*, 6(2):133–145.
- [Miettinen et al., 2002] Miettinen, R. A., Kalesnykas, G., and Koivisto, E. H. (2002). Estimation of the Total Number of Cholinergic Neurons Containing Estrogen Receptor- α in the Rat Basal Forebrain. *Journal of Histochemistry & Cytochemistry*, 50(7):891–902. Publisher: Journal of Histochemistry & Cytochemistry.
- [Minces et al., 2017] Minces, V., Pinto, L., Dan, Y., and Chiba, A. A. (2017). Cholinergic shaping of neural correlations. *Proceedings of the National Academy of Sciences*, 114(22):5725–5730.

- [Monti and Monti, 2007] Monti, J. M. and Monti, D. (2007). The involvement of dopamine in the modulation of sleep and waking. *Sleep Medicine Reviews*, 11(2):113–133.
- [Moruzzi and Magoun, 1949] Moruzzi, G. and Magoun, H. (1949). Brain stem reticular formation and activation of the EEG. *Electroencephalography and Clinical Neurophysiology*, 1(1-4):455–473.
- [Mouton et al., 2002] Mouton, P. R., Gokhale, A. M., Ward, N. L., and West, M. J. (2002). Stereological length estimation using spherical probes. *Journal of Microscopy*, 206(1):54–64.
- [Mrzljak et al., 1995] Mrzljak, L., Pappy, M., Leranth, C., and Goldman-Rakic, P. S. (1995). Cholinergic synaptic circuitry in the macaque prefrontal cortex. *The Journal of Comparative Neurology*, 357(4):603–617.
- [Mrzljak et al., 1993] Mrzljak, L., Levey, A. I., and Goldman-Rakic, P. S. (1993). Association of m1 and m2 muscarinic receptor proteins with asymmetric synapses in the primate cerebral cortex: morphological evidence for cholinergic modulation of excitatory neurotransmission. *Proceedings of the National Academy of Sciences of the United States of America*, 90(11):5194–5198.
- [Muñoz and Rudy, 2014] Muñoz, W. and Rudy, B. (2014). Spatiotemporal specificity in cholinergic control of neocortical function. *Current Opinion in Neurobiology*, 26:149–160.
- [Mylius et al., 2015] Mylius, J., Happel, M. F. K., Gorkin, A. G., Huang, Y., Scheich, H., and Brosch, M. (2015). Fast transmission from the dopaminergic ventral midbrain to the sensory cortex of awake primates. *Brain Structure and Function*, 220(6):3273–3294.
- [Nair-Roberts et al., 2008] Nair-Roberts, R., Chatelain-Badie, S., Benson, E., White-Cooper, H., Bolam, J., and Ungless, M. (2008). Stereological estimates of dopaminergic, GABAergic and glutamatergic neurons in the ventral tegmental area, substantia nigra and retrorubral field in the rat. *Neuroscience*, 152(4-2):1024–1031.
- [Nashmi and Lester, 2006] Nashmi, R. and Lester, H. A. (2006). CNS localization of neuronal nicotinic receptors. *Journal of Molecular Neuroscience*, 30(1-2):181–184.
- [Nelson and Mooney, 2016a] Nelson, A. and Mooney, R. (2016a). The Basal Forebrain and Motor Cortex Provide Convergent yet Distinct Movement-Related Inputs to the Auditory Cortex. *Neuron*, 90(3):635–648.

- [Nelson and Mooney, 2016b] Nelson, A. and Mooney, R. (2016b). The Basal Forebrain and Motor Cortex Provide Convergent yet Distinct Movement-Related Inputs to the Auditory Cortex. *Neuron*, 90(3):635–648.
- [Newman et al., 2012] Newman, E. L., Gupta, K., Climer, J. R., Monaghan, C. K., and Hasselmo, M. E. (2012). Cholinergic modulation of cognitive processing: insights drawn from computational models. *Frontiers in Behavioral Neuroscience*, 6.
- [Nguyen et al., 1995] Nguyen, Q., Sapp, D. W., Van Ness, P. C., and Olsen, R. W. (1995). Modulation of GABAA receptor binding in human brain by neuroactive steroids: Species and brain regional differences. *Synapse*, 19(2):77–87.
- [Nichols and Nichols, 2008] Nichols, D. E. and Nichols, C. D. (2008). Serotonin Receptors. *Chemical Reviews*, 108(5):1614–1641.
- [Obermayer et al., 2018] Obermayer, J., Heistek, T. S., Kerkhofs, A., Goriounova, N. A., Kroon, T., Baayen, J. C., Idema, S., Testa-Silva, G., Couey, J. J., and Mansvelder, H. D. (2018). Lateral inhibition by Martinotti interneurons is facilitated by cholinergic inputs in human and mouse neocortex. *Nature Communications*, 9(1):4101.
- [Obermayer et al., 2017] Obermayer, J., Verhoog, M. B., Luchicchi, A., and Mansvelder, H. D. (2017). Cholinergic Modulation of Cortical Microcircuits Is Layer-Specific: Evidence from Rodent, Monkey and Human Brain. *Frontiers in Neural Circuits*, 11.
- [Pawlak, 2010] Pawlak, V. (2010). Timing is not everything: neuromodulation opens the STDP gate. *Frontiers in Synaptic Neuroscience*, 2.
- [Picciotto et al., 2012] Picciotto, M., Higley, M., and Mineur, Y. (2012). Acetylcholine as a Neuromodulator: Cholinergic Signaling Shapes Nervous System Function and Behavior. *Neuron*, 76(1):116–129.
- [Pinto et al., 2013] Pinto, L., Goard, M. J., Estandian, D., Xu, M., Kwan, A. C., Lee, S.-H., Harrison, T. C., Feng, G., and Dan, Y. (2013). Fast modulation of visual perception by basal forebrain cholinergic neurons. *Nature Neuroscience*, 16(12):1857–1863.
- [Poorthuis et al., 2013] Poorthuis, R. B., Bloem, B., Schak, B., Wester, J., de Kock, C. P. J., and Mansvelder, H. D. (2013). Layer-Specific Modulation of the Prefrontal Cortex by Nicotinic Acetylcholine Receptors. *Cerebral Cortex*, 23(1):148–161.
- [Poorthuis et al., 2014] Poorthuis, R. B., Enke, L., and Letzkus, J. J. (2014). Cholinergic circuit modulation through differential recruitment of neo-

- cortical interneuron types during behaviour. *The Journal of Physiology*, 592(19):4155–4164.
- [Poorthuis et al., 2018] Poorthuis, R. B., Muhammad, K., Wang, M., Verhoog, M. B., Junek, S., Wrana, A., Mansvelder, H. D., and Letzkus, J. J. (2018). Rapid Neuromodulation of Layer 1 Interneurons in Human Neocortex. *Cell Reports*, 23(4):951–958.
- [Power, 2004] Power, A. E. (2004). Slow-wave sleep, acetylcholine, and memory consolidation. *Proceedings of the National Academy of Sciences*, 101(7):1795–1796.
- [Puig, 2004] Puig, M. V. (2004). Modulation of the Activity of Pyramidal Neurons in Rat Prefrontal Cortex by Raphe Stimulation In Vivo: Involvement of Serotonin and GABA. *Cerebral Cortex*, 15(1):1–14.
- [Puig and Gullledge, 2011] Puig, M. V. and Gullledge, A. T. (2011). Serotonin and Prefrontal Cortex Function: Neurons, Networks, and Circuits. *Molecular Neurobiology*, 44(3):449–464.
- [Puig et al., 2015] Puig, M. V., Gullledge, A. T., Lambe, E. K., and Gonzalez-Burgos, G. (2015). Editorial: Neuromodulation of executive circuits. *Frontiers in Neural Circuits*, 9.
- [Puig et al., 2010] Puig, M. V., Watakabe, A., Ushimaru, M., Yamamori, T., and Kawaguchi, Y. (2010). Serotonin Modulates Fast-Spiking Interneuron and Synchronous Activity in the Rat Prefrontal Cortex through 5-HT1A and 5-HT2A Receptors. *Journal of Neuroscience*, 30(6):2211–2222.
- [Radnikow and Feldmeyer, 2018] Radnikow, G. and Feldmeyer, D. (2018). Layer- and Cell Type-Specific Modulation of Excitatory Neuronal Activity in the Neocortex. *Frontiers in Neuroanatomy*, 12.
- [Ramaswamy et al., 2018] Ramaswamy, S., Colangelo, C., and Markram, H. (2018). Data-Driven Modeling of Cholinergic Modulation of Neural Microcircuits: Bridging Neurons, Synapses and Network Activity. *Frontiers in Neural Circuits*, 12.
- [Ramaswamy et al., 2015] Ramaswamy, S., Courcol, J.-D., Abdellah, M., Adaszewski, S. R., Antille, N., Arsever, S., Atenekeng, G., Bilgili, A., Brukau, Y., Chalimourda, A., Chindemi, G., Delalondre, F., Dumusc, R., Eilemann, S., Gevaert, M. E., Gleeson, P., Graham, J. W., Hernandez, J. B., Kanari, L., Katkov, Y., Keller, D., King, J. G., Ranjan, R., Reimann, M. W., Rössert, C., Shi, Y., Shillcock, J. C., Telefont, M., Van Geit, W., Villafranca Diaz, J., Walker, R., Wang, Y., Zaninetta, S. M., DeFelipe, J., Hill, S. L., Muller, J., Segev, I., Schürmann, F.,

- Muller, E. B., and Markram, H. (2015). The neocortical microcircuit collaboration portal: a resource for rat somatosensory cortex. *Frontiers in Neural Circuits*, 9.
- [Rasmusson, 2000] Rasmusson, D. (2000). The role of acetylcholine in cortical synaptic plasticity. *Behavioural Brain Research*, 115(2):205–218.
- [Reimann et al., 2015] Reimann, M. W., King, J. G., Muller, E. B., Ramaswamy, S., and Markram, H. (2015). An algorithm to predict the connectome of neural microcircuits. *Frontiers in Computational Neuroscience*, 9.
- [Reyes et al., 1998] Reyes, A., Lujan, R., Rozov, A., Burnashev, N., Somogyi, P., and Sakmann, B. (1998). Target-cell-specific facilitation and depression in neocortical circuits. *Nature Neuroscience*, 1(4):279–285.
- [Reyes, 2003] Reyes, A. D. (2003). Synchrony-dependent propagation of firing rate in iteratively constructed networks in vitro. *Nature Neuroscience*, 6(6):593–599.
- [Rivera et al., 2008] Rivera, A., Peñafiel, A., Megías, M., Agnati, L., López-Téllez, J., Gago, B., Gutiérrez, A., de la Calle, A., and Fuxe, K. (2008). Cellular localization and distribution of dopamine D4 receptors in the rat cerebral cortex and their relationship with the cortical dopaminergic and noradrenergic nerve terminal networks. *Neuroscience*, 155(3):997–1010.
- [Roerig et al., 1997] Roerig, B., Nelson, D. A., and Katz, L. C. (1997). Fast Synaptic Signaling by Nicotinic Acetylcholine and Serotonin 5-HT₃ Receptors in Developing Visual Cortex. *The Journal of Neuroscience*, 17(21):8353–8362.
- [Rosenbaum et al., 2014] Rosenbaum, R., Zimnik, A., Zheng, F., Turner, R. S., Alzheimer, C., Doiron, B., and Rubin, J. E. (2014). Axonal and synaptic failure suppress the transfer of firing rate oscillations, synchrony and information during high frequency deep brain stimulation. *Neurobiology of Disease*, 62:86–99.
- [Rudy et al., 2011] Rudy, B., Fishell, G., Lee, S., and Hjerling-Leffler, J. (2011). Three groups of interneurons account for nearly 100% of neocortical GABAergic neurons. *Developmental Neurobiology*, 71(1):45–61.
- [Runfeldt et al., 2014] Runfeldt, M. J., Sadovsky, A. J., and MacLean, J. N. (2014). Acetylcholine functionally reorganizes neocortical microcircuits. *Journal of Neurophysiology*, 112(5):1205–1216.
- [Sabri et al., 2008] Sabri, O., Kendziorra, K., Wolf, H., Gertz, H.-J., and Brust, P. (2008). Acetylcholine receptors in dementia and mild cogni-

- tive impairment. *European Journal of Nuclear Medicine and Molecular Imaging*, 35(1):30–45.
- [Salgado et al., 2007] Salgado, H., Bellay, T., Nichols, J. A., Bose, M., Martinolich, L., Perrotti, L., and Atzori, M. (2007). Muscarinic M₂ and M₁ Receptors Reduce GABA Release by Ca²⁺ Channel Modulation Through Activation of PI₃K/Ca²⁺-Independent and PLC/Ca²⁺-Dependent PKC. *Journal of Neurophysiology*, 98(2):952–965.
- [Sanchez-Vives and McCormick, 2000] Sanchez-Vives, M. V. and McCormick, D. A. (2000). Cellular and network mechanisms of rhythmic recurrent activity in neocortex. *Nature Neuroscience*, 3(10):1027–1034.
- [Santuy et al., 2018] Santuy, A., Rodriguez, J. R., DeFelipe, J., and Merchán-Pérez, A. (2018). Volume electron microscopy of the distribution of synapses in the neuropil of the juvenile rat somatosensory cortex. *Brain Structure and Function*, 223(1):77–90.
- [Saper et al., 2001] Saper, C. B., Chou, T. C., and Scammell, T. E. (2001). The sleep switch: hypothalamic control of sleep and wakefulness. *Trends in Neurosciences*, 24(12):726–731.
- [Saper et al., 2010] Saper, C. B., Fuller, P. M., Pedersen, N. P., Lu, J., and Scammell, T. E. (2010). Sleep State Switching. *Neuron*, 68(6):1023–1042.
- [Sarter et al., 2009] Sarter, M., Parikh, V., and Howe, W. M. (2009). Phasic acetylcholine release and the volume transmission hypothesis: time to move on. *Nature reviews. Neuroscience*, 10(5):383–390.
- [Saunders et al., 2015] Saunders, A., Granger, A. J., and Sabatini, B. L. (2015). Corelease of acetylcholine and GABA from cholinergic forebrain neurons. *eLife*, 4.
- [Saunders et al., 2018] Saunders, A., Macosko, E. Z., Wysoker, A., Goldman, M., Krienen, F. M., de Rivera, H., Bien, E., Baum, M., Bortolin, L., Wang, S., Goeva, A., Nemesh, J., Kamitaki, N., Brumbaugh, S., Kulp, D., and McCarroll, S. A. (2018). Molecular Diversity and Specializations among the Cells of the Adult Mouse Brain. *Cell*, 174(4):1015–1030.e16.
- [Schröder, 1992] Schröder, H. (1992). Immunohistochemistry of cholinergic receptors. *Anatomy and Embryology*, 186(5):407–429.
- [Schröder et al., 1989] Schröder, H., Zilles, K., Maelicke, A., and Hajós, F. (1989). Immunohisto- and cytochemical localization of cortical nicotinic cholinergic receptors in rat and man. *Brain Research*, 502(2):287–295.
- [Schultz, 2007] Schultz, W. (2007). Multiple Dopamine Functions at Different Time Courses. *Annual Review of Neuroscience*, 30(1):259–288.

- [Schwartzkroin, 1994] Schwartzkroin, P. A. (1994). Cellular electrophysiology of human epilepsy. *Epilepsy Research*, 17(3):185–192.
- [Sesack et al., 1998] Sesack, S. R., Hawrylak, V. A., Matus, C., Guido, M. A., and Levey, A. I. (1998). Dopamine Axon Varicosities in the Pre-
limbic Division of the Rat Prefrontal Cortex Exhibit Sparse Immunore-
activity for the Dopamine Transporter. *The Journal of Neuroscience*, 18(7):2697–2708.
- [Sethuramanujam et al., 2021] Sethuramanujam, S., Matsumoto, A., deRosenroll, G., Murphy-Baum, B., Grosman, C., McIntosh, J. M., Jing, M., Li, Y., Berson, D., Yonehara, K., and Awatramani, G. B. (2021). Rapid multi-directed cholinergic transmission in the central nervous system. *Nature Communications*, 12(1):1374. Number: 1 Publisher: Nature Publishing Group.
- [Shalinsky et al., 2002] Shalinsky, M. H., Magistretti, J., Ma, L., and Alonso, A. A. (2002). Muscarinic Activation of a Cation Current and Associated Current Noise in Entorhinal-Cortex Layer-II Neurons. *Journal of Neurophysiology*, 88(3):1197–1211.
- [Sharp and Barnes, 2020] Sharp, T. and Barnes, N. M. (2020). Central 5-HT receptors and their function; present and future. *Neuropharmacology*, 177:108155.
- [Shen and Yakel, 2009] Shen, J.-x. and Yakel, J. L. (2009). Nicotinic acetylcholine receptor-mediated calcium signaling in the nervous system. *Acta Pharmacologica Sinica*, 30(6):673–680.
- [Simkus and Stricker, 2002] Simkus, C. R. L. and Stricker, C. (2002). Properties of mEPSCs recorded in layer II neurones of rat barrel cortex. *The Journal of Physiology*, 545(2):509–520.
- [Smiley et al., 1997] Smiley, J. F., Morrell, F., and Mesulam, M. (1997). Cholinergic Synapses in Human Cerebral Cortex: An Ultrastructural Study in Serial Sections. *Experimental Neurology*, 144(2):361–368.
- [Sparks et al., 1998] Sparks, D. L., Beach, T. G., and Lukas, R. J. (1998). Immunohistochemical localization of nicotinic $\beta 2$ and $\alpha 4$ receptor subunits in normal human brain and individuals with Lewy body and Alzheimer’s disease: preliminary observations. *Neuroscience Letters*, 256(3):151–154.
- [Steriade, 2004] Steriade, M. (2004). Acetylcholine systems and rhythmic activities during the waking–sleep cycle. In *Progress in Brain Research*, volume 145, pages 179–196. Elsevier.

- [Steriade et al., 1993] Steriade, M., Amzica, F., and Nunez, A. (1993). Cholinergic and noradrenergic modulation of the slow (approximately 0.3 Hz) oscillation in neocortical cells. *Journal of Neurophysiology*, 70(4):1385–1400.
- [Stewart et al., 1999] Stewart, A. E., Yan, Z., Surmeier, D. J., and Foehring, R. C. (1999). Muscarine Modulates Ca^{2+} Channel Currents in Rat Sensorimotor Pyramidal Cells Via Two Distinct Pathways. *Journal of Neurophysiology*, 81(1):72–84.
- [Stiefel et al., 2009] Stiefel, K. M., Gutkin, B. S., and Sejnowski, T. J. (2009). The effects of cholinergic neuromodulation on neuronal phase-response curves of modeled cortical neurons. *Journal of Computational Neuroscience*, 26(2):289–301.
- [Sugihara et al., 2016] Sugihara, H., Chen, N., and Sur, M. (2016). Cell-specific modulation of plasticity and cortical state by cholinergic inputs to the visual cortex. *Journal of Physiology-Paris*, 110(1–2):37–43.
- [Szymusiak and McGinty, 1986] Szymusiak, R. and McGinty, D. (1986). Sleep-related neuronal discharge in the basal forebrain of cats. *Brain Research*, 370(1):82–92.
- [Takács et al., 2013] Takács, V. T., Freund, T. F., and Nyiri, G. (2013). Neuroligin 2 Is Expressed in Synapses Established by Cholinergic Cells in the Mouse Brain. *PLoS ONE*, 8(9):e72450.
- [Tasic et al., 2018] Tasic, B., Yao, Z., Graybiel, L. T., Smith, K. A., Nguyen, T. N., Bertagnoli, D., Goldy, J., Garren, E., Economo, M. N., Viswanathan, S., Penn, O., Bakken, T., Menon, V., Miller, J., Fong, O., Hirokawa, K. E., Lathia, K., Rimorin, C., Tieu, M., Larsen, R., Casper, T., Barkan, E., Kroll, M., Parry, S., Shapovalova, N. V., Hirschstein, D., Pendergraft, J., Sullivan, H. A., Kim, T. K., Szafer, A., Dee, N., Groblewski, P., Wickersham, I., Cetin, A., Harris, J. A., Levi, B. P., Sunkin, S. M., Madisen, L., Daigle, T. L., Looger, L., Bernard, A., Phillips, J., Lein, E., Hawrylycz, M., Svoboda, K., Jones, A. R., Koch, C., and Zeng, H. (2018). Shared and distinct transcriptomic cell types across neocortical areas. *Nature*, 563(7729):72–78.
- [Taylor et al., 2016] Taylor, N. E., Van Dort, C. J., Kenny, J. D., Pei, J., Guidera, J. A., Vlasov, K. Y., Lee, J. T., Boyden, E. S., Brown, E. N., and Solt, K. (2016). Optogenetic activation of dopamine neurons in the ventral tegmental area induces reanimation from general anesthesia. *Proceedings of the National Academy of Sciences*, 113(45):12826–12831.
- [Thiele et al., 2012] Thiele, A., Herrero, J. L., Distler, C., and Hoffmann, K.-P. (2012). Contribution of Cholinergic and GABAergic Mechanisms

- to Direction Tuning, Discriminability, Response Reliability, and Neuronal Rate Correlations in Macaque Middle Temporal Area. *Journal of Neuroscience*, 32(47):16602–16615.
- [Thomson, 2007] Thomson, A. M. (2007). Functional maps of neocortical local circuitry. *Frontiers in Neuroscience*, 1(1):19–42.
- [Tiesinga et al., 2001] Tiesinga, P. H., Fellous, J.-M., José, J. V., and Sejnowski, T. J. (2001). Computational model of carbachol-induced delta, theta, and gamma oscillations in the hippocampus: Model of Carbachol Oscillations in Hippocampus. *Hippocampus*, 11(3):251–274.
- [Tribollet et al., 2004] Tribollet, E., Bertrand, D., Marguerat, A., and Raggenbass, M. (2004). Comparative distribution of nicotinic receptor subtypes during development, adulthood and aging: an autoradiographic study in the rat brain. *Neuroscience*, 124(2):405–420.
- [Tritsch and Sabatini, 2012] Tritsch, N. and Sabatini, B. (2012). Dopaminergic Modulation of Synaptic Transmission in Cortex and Striatum. *Neuron*, 76(1):33–50.
- [Tsodyks and Markram, 1997] Tsodyks, M. V. and Markram, H. (1997). The neural code between neocortical pyramidal neurons depends on neurotransmitter release probability. *Proceedings of the National Academy of Sciences*, 94(2):719–723.
- [Turrini et al., 2001] Turrini, P., Casu, M., Wong, T., De Koninck, Y., Ribeiro-da Silva, A., and Cuello, A. (2001). Cholinergic nerve terminals establish classical synapses in the rat cerebral cortex: synaptic pattern and age-related atrophy. *Neuroscience*, 105(2):277–285.
- [Uchigashima et al., 2016] Uchigashima, M., Ohtsuka, T., Kobayashi, K., and Watanabe, M. (2016). Dopamine synapse is a neuroligin-2-mediated contact between dopaminergic presynaptic and GABAergic postsynaptic structures. *Proceedings of the National Academy of Sciences*, 113(15):4206–4211. Publisher: National Academy of Sciences Section: Biological Sciences.
- [Umbriaco et al., 1994] Umbriaco, D., Watkins, K. C., Descarries, L., Cozzari, C., and Hartman, B. K. (1994). Ultrastructural and morphometric features of the acetylcholine innervation in adult rat parietal cortex: an electron microscopic study in serial sections. *The Journal of Comparative Neurology*, 348(3):351–373.
- [Unal et al., 2012] Unal, C. T., Golowasch, J. P., and Zaborszky, L. (2012). Adult mouse basal forebrain harbors two distinct cholinergic populations defined by their electrophysiology. *Frontiers in Behavioral Neuroscience*, 6.

- [Urban-Ciecko et al., 2018] Urban-Ciecko, J., Jouhanneau, J.-S., Myal, S. E., Poulet, J. F., and Barth, A. L. (2018). Precisely Timed Nicotinic Activation Drives SST Inhibition in Neocortical Circuits. *Neuron*, 97(3):611–625.e5.
- [Van der Zee and Luiten, 1999] Van der Zee, E. and Luiten, P. (1999). Muscarinic acetylcholine receptors in the hippocampus, neocortex and amygdala: a review of immunocytochemical localization in relation to learning and memory. *Progress in Neurobiology*, 58(5):409–471.
- [van der Zee et al., 1992] van der Zee, E., Streefland, C., Strosberg, A., Schröder, H., and Luiten, P. (1992). Visualization of cholinergic neurons in the rat neocortex: colocalization of muscarinic and nicotinic acetylcholine receptors. *Molecular Brain Research*, 14(4):326–336.
- [Van Geit et al., 2016] Van Geit, W., Gevaert, M., Chindemi, G., Rössert, C., Courcol, J.-D., Muller, E. B., Schürmann, F., Segev, I., and Markram, H. (2016). BluePyOpt: Leveraging Open Source Software and Cloud Infrastructure to Optimise Model Parameters in Neuroscience. *Frontiers in Neuroinformatics*, 10.
- [Venter et al., 1988] Venter, J., Diporzio, U., Robinson, D., Shreeve, S., Lai, J., Kerlavage, A., Fracekjr, S., Lentres, K., and Fraser, C. (1988). Evolution of neurotransmitter receptor systems. *Progress in Neurobiology*, 30:105–169.
- [Verhoog et al., 2016] Verhoog, M. B., Obermayer, J., Kortleven, C. A., Wilbers, R., Wester, J., Baayen, J. C., De Kock, C. P. J., Meredith, R. M., and Mansvelder, H. D. (2016). Layer-specific cholinergic control of human and mouse cortical synaptic plasticity. *Nature Communications*, 7:12826.
- [Verney et al., 1984] Verney, C., Berger, B., Baulac, M., Helle, K. B., and Alvarez, C. (1984). Dopamine- β -hydroxylase-like immunoreactivity in the fetal cerebral cortex of the rat: Noradrenergic ascending pathways and terminal fields. *International Journal of Developmental Neuroscience*, 2(5):491–503.
- [Wang et al., 2006] Wang, Z., Kai, L., Day, M., Ronesi, J., Yin, H. H., Ding, J., Tkatch, T., Lovinger, D. M., and Surmeier, D. J. (2006). Dopaminergic Control of Corticostriatal Long-Term Synaptic Depression in Medium Spiny Neurons Is Mediated by Cholinergic Interneurons. *Neuron*, 50(3):443–452.
- [Wang and McCormick, 1993] Wang, Z. and McCormick, D. (1993). Control of firing mode of corticotectal and corticopontine layer V burst-

- generating neurons by norepinephrine, acetylcholine, and 1S,3R- ACPD. *The Journal of Neuroscience*, 13(5):2199–2216.
- [Wevers, 2011] Wevers, A. (2011). Localisation of pre- and postsynaptic cholinergic markers in the human brain. *Behavioural Brain Research*, 221(2):341–355.
- [Wilson and Molliver, 1991] Wilson, M. A. and Molliver, M. E. (1991). The organization of serotonergic projections to cerebral cortex in primates: Retrograde transport studies. *Neuroscience*, 44(3):555–570.
- [Xiang et al., 1998a] Xiang, Z., Huguenard, J. R., and Prince, D. A. (1998a). Cholinergic Switching Within Neocortical Inhibitory Networks. *Science*, 281(5379):985–988. Publisher: American Association for the Advancement of Science Section: Report.
- [Xiang et al., 1998b] Xiang, Z., Huguenard, J. R., and Prince, D. A. (1998b). Cholinergic Switching Within Neocortical Inhibitory Networks. *Science*, 281(5379):985–988.
- [Xu et al., 2015] Xu, M., Chung, S., Zhang, S., Zhong, P., Ma, C., Chang, W.-C., Weissbourd, B., Sakai, N., Luo, L., Nishino, S., and Dan, Y. (2015). Basal forebrain circuit for sleep-wake control. *Nature Neuroscience*, 18(11):1641–1647.
- [Yamamoto et al., 2010] Yamamoto, K., Koyanagi, Y., Koshikawa, N., and Kobayashi, M. (2010). Postsynaptic Cell Type-Dependent Cholinergic Regulation of GABAergic Synaptic Transmission in Rat Insular Cortex. *Journal of Neurophysiology*, 104(4):1933–1945.
- [Yamasaki et al., 2010] Yamasaki, M., Matsui, M., and Watanabe, M. (2010). Preferential Localization of Muscarinic M1 Receptor on Dendritic Shaft and Spine of Cortical Pyramidal Cells and Its Anatomical Evidence for Volume Transmission. *Journal of Neuroscience*, 30(12):4408–4418.
- [Zaborszky et al., 2015a] Zaborszky, L., Csordas, A., Mosca, K., Kim, J., Gielow, M. R., Vadasz, C., and Nadasdy, Z. (2015a). Neurons in the Basal Forebrain Project to the Cortex in a Complex Topographic Organization that Reflects Corticocortical Connectivity Patterns: An Experimental Study Based on Retrograde Tracing and 3D Reconstruction. *Cerebral Cortex*, 25(1):118–137.
- [Zaborszky et al., 2015b] Zaborszky, L., Csordas, A., Mosca, K., Kim, J., Gielow, M. R., Vadasz, C., and Nadasdy, Z. (2015b). Neurons in the Basal Forebrain Project to the Cortex in a Complex Topographic Organization that Reflects Corticocortical Connectivity Patterns: An Experimental Study Based on Retrograde Tracing and 3D Reconstruction. *Cerebral Cortex*, 25(1):118–137.

- [Zaborszky and Duque, 2000] Zaborszky, L. and Duque, A. (2000). Local synaptic connections of basal forebrain neurons. *Behavioural Brain Research*, 115(2):143–158.
- [Zagha and McCormick, 2014] Zagha, E. and McCormick, D. A. (2014). Neural control of brain state. *Current Opinion in Neurobiology*, 29:178–186.
- [Zeisel et al., 2018] Zeisel, A., Hochgerner, H., Lönnerberg, P., Johnsson, A., Memic, F., van der Zwan, J., Häring, M., Braun, E., Borm, L. E., La Manno, G., Codeluppi, S., Furlan, A., Lee, K., Skene, N., Harris, K. D., Hjerling-Leffler, J., Arenas, E., Ernfors, P., Marklund, U., and Linnarsson, S. (2018). Molecular Architecture of the Mouse Nervous System. *Cell*, 174(4):999–1014.e22.
- [Zhang and Séguéla, 2010] Zhang, Z. and Séguéla, P. (2010). Metabotropic Induction of Persistent Activity in Layers II/III of Anterior Cingulate Cortex. *Cerebral Cortex*, 20(12):2948–2957.
- [Zhong et al., 2020] Zhong, P., Qin, L., and Yan, Z. (2020). Dopamine Differentially Regulates Response Dynamics of Prefrontal Cortical Principal Neurons and Interneurons to Optogenetic Stimulation of Inputs from Ventral Tegmental Area. *Cerebral Cortex*, 30(8):4402–4409. Publisher: Oxford Academic.
- [Zhou and Hablitz, 1999] Zhou, F.-M. and Hablitz, J. J. (1999). Dopamine Modulation of Membrane and Synaptic Properties of Interneurons in Rat Cerebral Cortex. *Journal of Neurophysiology*, 81(3):967–976. Publisher: American Physiological Society.
- [Zoli et al., 2002] Zoli, M., Moretti, M., Zanardi, A., McIntosh, J. M., Clementi, F., and Gotti, C. (2002). Identification of the Nicotinic Receptor Subtypes Expressed on Dopaminergic Terminals in the Rat Striatum. *The Journal of Neuroscience*, 22(20):8785–8789.
- [Zoli et al., 2015] Zoli, M., Pistillo, F., and Gotti, C. (2015). Diversity of native nicotinic receptor subtypes in mammalian brain. *Neuropharmacology*, 96:302–311.
- [Zuccolo et al., 2017] Zuccolo, E., Lim, D., Kheder, D. A., Perna, A., Catarsi, P., Botta, L., Rosti, V., Riboni, L., Sancini, G., Tanzi, F., D’Angelo, E., Guerra, G., and Moccia, F. (2017). Acetylcholine induces intracellular Ca(2+) oscillations and nitric oxide release in mouse brain endothelial cells. *Cell Calcium*, 66:33–47.

CRISTINA COLANGELO

+41 786275459 ◊
cristina.colangelo11@gmail.com ◊

EDUCATION

PhD student in Neuroscience, EPFL	present
M. Sc. in Neurobiology, University of Pavia	October 2016
B. Sc. in Biological sciences, University of Milan	October 2014

SKILLS

Languages	Italian (C2), English (C1), French (C1), Spanish (B2), Romanian (B2)
Programming	Python, MATLAB
Strengths	Data analysis, Scientific programming, Unix based systems, Scientific writing
Experience	Experimental design, Human subject research, Electrophysiology

PUBLICATIONS

Cellular, synaptic and network effects of acetylcholine in the neocortex. C Colangelo, P Shichkova, D Keller, H Markram, S Ramaswamy; Frontiers in neural circuits 13, 24 <https://doi.org/10.3389/fncir.2019.00024>

Data-driven modeling of cholinergic modulation of neural microcircuits: bridging neurons, synapses and network activity. S Ramaswamy, C Colangelo and H Markram; Frontiers in Neural Circuits 12, 77 <https://doi.org/10.3389/fncir.2018.00077>

Distinct activity profiles of somatostatin-expressing interneurons in the neocortex. S Ramaswamy, C Colangelo, EB Muller; Frontiers in cellular neuroscience 11, 273 <https://doi.org/10.3389/fncel.2017.00273>

CONFERENCES

International Brain Research Organization (IBRO) World Congress, 2019	Daegu, South Korea
Computational Neuroscience (CNS) Meeting 2019	Barcelona, Spain
Young Swiss Society for Neuroscience symposium 2019	Geneva (CH)
Society for Neuroscience (SfN) Annual Meeting 2018	San Diego (CA) USA

AWARDS

Young Swiss Society for Neuroscience symposium 2019	Best presentation award
---	-------------------------

TEACHING EXPERIENCE

Physics of the Cell Alexandre Persat	EPFL-SV - 2021
In Silico Neuroscience Felix Schürmann, Armando Romani	EPFL-SV - 2020
Neuroscience: behavior and cognition Michael Herzog	EPFL-SV - 2019
In Silico Neuroscience Felix Schürmann, Eilif Muller	EPFL-SV - 2018

EXTRA-CURRICULAR ACTIVITIES

- Mental health advocacy
- Dance and performance
- Yoga and meditation